Dielectric-filled 1 to 18 ghz coaxial slotted line

Evangelos Evangelinos

DIELECTRIC-FILLED 1 TO 18 GHz COAXIAL SLOTTED LINE

By

EVANGELOS EVANGELINOS, B.Sc.(CNAA)

Graduate Society

A Thesis submitted to the Faculty of Science,
University of Durham for the degree of
Master of Science

Department of Applied Physics and Electronics,
University of Durham, U.K.

April, 1986

ABSTRACT

The slotted line has, for a number of years, been one of the most useful and necessary tools in RF and microwave measurements. It was therefore felt appropriate to attempt to design an improved version, capable of broad band operation (1 to 18 GHz) with the ability of examining modulated and unmodulated wave forms.

Initially, the relevant transmission line theory was reviewed with particular emphasis placed on the concepts that were to influence the actual design.

The unique feature of the project, was the use of semi-rigid cable, which greatly contributed to the realisation of the two main objectives, namely low cost and accuracy.

The mechanical construction proved as important as the electrical design and for this reason both topics were analysed and discussed in some detail in the text of the thesis.

The approach was justified in that on the final examination, the slotted line performed satisfactorily in comparison to more expensively purchased units, over the expected frequency range without exhibiting an anomalous behaviour.

Recommendations that would improve the slotted line even further were made in the conclusions chapter, with specific attention paid to the redesigning of the probe and the tuning mechanism.

ACKNOWLEDGEMENTS

I would like to express my thanks and appreciation to my supervisor Dr. B.L.J. Kulesza for his continuous enthusiasm, interest and advice throughout this project. More importantly, Dr. Kulesza has taught me the fundamental concepts of research, and for this I am grateful.

My thanks must also extend to the technical staff of the Department for their co-operation, and in particular to Mr. P.J.E. Richardson whose quality of work contributed to the successful realisation of the project.

Finally, I am deeply grateful to my mother for her support and understanding during the years it took to achieve my ambitions.

CONTENTS

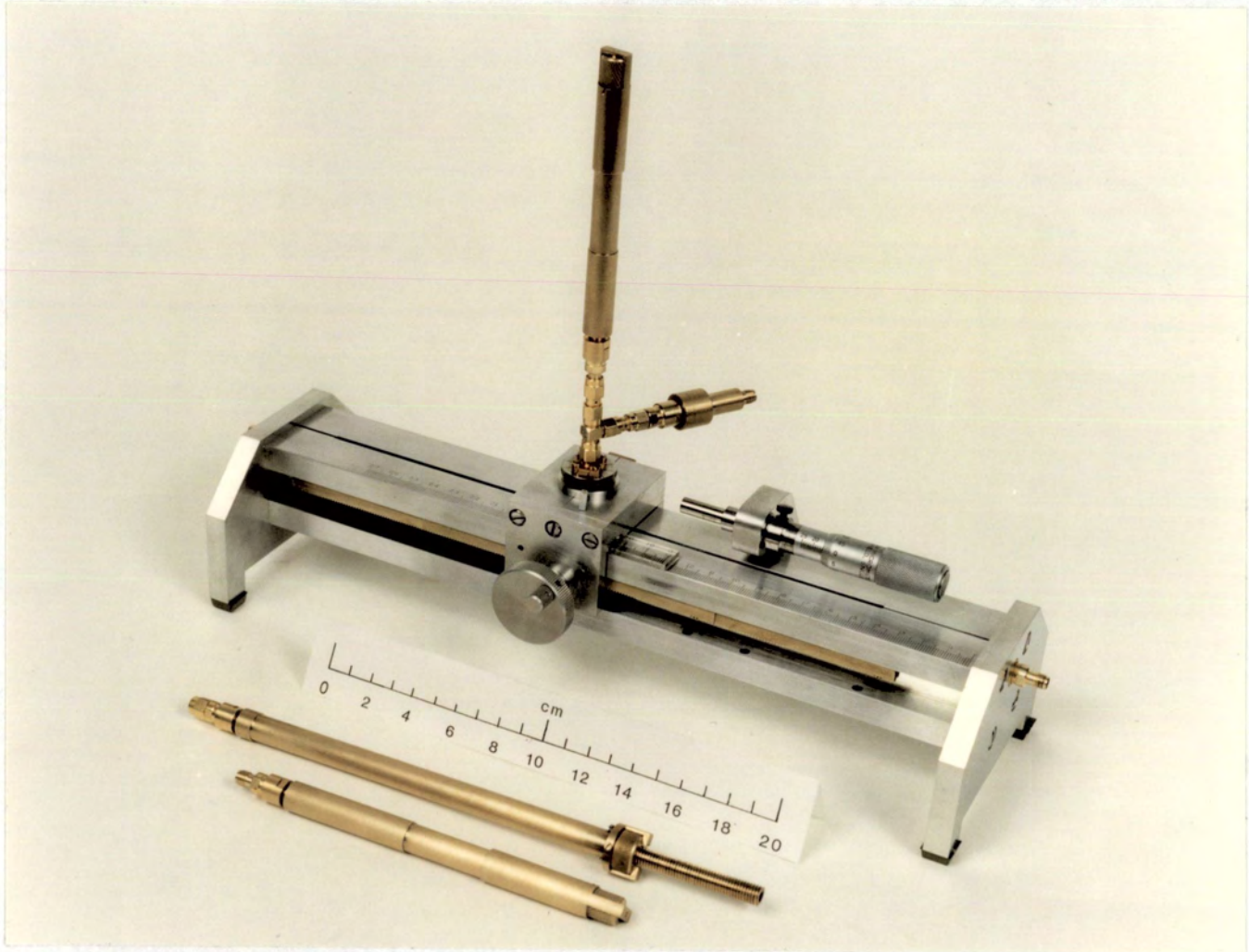

PHOTOGRAPH 1 Complete Slotted Line with Accessories

CHAPTER 1

INTRODUCTION

1.1 GENERAL PRINCIPLES OF A SLOTTED LINE

One of the most unique and informative measurements that can be carried out on a transmission line, is the measurement of a standing wave ratio. What makes it so important in high frequency work is the fact that from simple measurements on the standing wave the secondary parameters of a transmission line may be determined. Using the Voltage minimum position and VSWR, quantities such as the impedance of a load terminating the line, the impedance presented at the input line terminals, the characteristic impedance, the voltage breakdown level of the line and many more may be calculated.

There are classical and modern ways of measuring VSWR, some being direct others indirect. An example of an indirect VSWR measurement is the reflectometer method using the directional coupler. The ratio can then be obtained from the equations relating the incident and reflected voltages or power levels. On the other hand, the slotted line allows direct VSWR measurements since it is designed to couple to the electric field inside the transmission line and thus record the intensities at the maxima and minima of the standing wave. It also has the advantage over some methods in that it gives the positions of the voltage maxima and especially and more importantly the positions of the minima.

Slotted lines have been regarded as one of the most useful and principal components of microwave equipment for very many years. Their versatility and measurement accuracy has enabled the microwave engineer to use them in conjunction with powerful and more sophisticated electronic instruments (e.g. spectrum analyser) at all levels of research.

If well designed, a slotted line allows a wide range of secondary parameters such as reflection coefficient its magnitude and its phase, attenuation or insertion loss, wavelength, complex terminations to be accurately determined over a wide range of frequencies. Precision lines, however, are found to be increasingly costly, mainly due to the mechanical close tolerances required to achieve a high degree of accuracy in electrical performance. For this reason and for the fact that no microwave test bench is complete without such a useful measuring aid, it was felt that an attempt should be made to design a low cost, yet precise coaxial slotted line which would cover a range of frequencies from 1 to 18 GHz.

The design described in this thesis was intended for a broad band operation, and allow the output to be fed to either a VSWR meter, an amplifier, or a spectrum analyser for harmonic analysis. It was felt that it would be possible to construct such a slotted line which would provide an adequate output level without appreciably disturbing the electric field patterns.

A section of transmission line, coaxial or waveguide, where the standing waves are to be investigated, normally contains a longitudinal slot at least one-half wavelength long. The slot is usually placed parallel to the lines of energy flow and is narrow enough not to disturb the field pattern. A probe is then inserted into the slot,

which responds to the fields inside the transmission line, picking up a small fraction of the flowing energy. By a suitably designed r-f line the probe output is then connected to a detector which converts radio or microwave frequency into direct current. If the input is AM-modulated with LF, greater sensitivity is obtained by feeding the envelope detector output into a high gain LF amplifier with a meter already calibrated to give VSWR readings directly. The design of the slotted line described in this thesis was based on these principles.

Measurements on a slotted line at different positions are made by allowing the probe carriage to travel the length of the slot. For precision slotted lines rack and pinion or screw drive arrangements are normally required to provide accurate readings, as well as enabling the probe to travel while maintaining an almost perfect translational symmetry. The position of the probe is read by using a millimetre scale and a vernier set against a reference point.

1.2 MODERN METHODS OF DESIGN

The project described here was undertaken being aware that a variety of slotted lines were available with some of them being capable of similar broad band operations. Coaxial airline, parallel plate, and waveguide are the usual types of transmission line incorporated in such designs. Examining their advantages and disadvantages and manufacturers' claims it was justified for having pursued the proposed type of slotted line.

With the continuous improvement in the quality of connectors

the upper limit of operation of coaxial systems had risen to about 18 GHz. However, careful design is still required to ensure that unwanted coaxial modes, other than the principal, are not present. Other than the principal modes of excitation are generated when a departure from axial symmetry occurs, say due to the presence of the slot,. Also, using various types of supports such as beads, rods etc..., to rest the inner conductor, means that some reflections will occur. Even then it is still difficult to guarantee absolutely central positioning of the inner conductor. Furthermore, care must also be taken not to allow the slot dimensions to alter the characteristic impedance of the coaxial line by any apreciable amount.

A parallel plate slotted line has eliminated some of the above problems encountered in coaxial air lines. For example, the natural slot between two parallel plates provides an easy access to the electric field. However, an abrupt transition between the parallel plates and the coaxial line at the connecting end results in standing waves being created due to the discontinuity. Furthermore, as reported [6] their operation is limited at about 8 GHz. Waveguide slotted lines, on the other hand, can be built to operate anywhere in the range up to 140 GHz, but only over limited frequency bands. Since the waveguides are used at wavelengths much smaller than those used in coaxial lines, their dimensions become smaller and the problem of tolerances can become very important. Probe penetration, slot width, and slot-end reflections will cause difficulties which have to be considered and overcome.

Realising the limitations and requirements of the different types of slotted line, became apparent that if a coaxial cable filled with a dielectric was to be used as the slotted line section, some of the

length and support problems found in air lines may be eliminated. Also the fact that such cable could be purchased at a fairly low price meant that the main objectives of creating an inexpensive and relatively accurate slotted line could be realised.

1.3 THE PROJECT

The main feature of the design has been the use of a semi-rigid cable (Radiall RG401/U) as the slotted section. The largest available size was chosen, having an outside 6.4 mm diameter, with inner and outer conductors made of coppered steel and copper, respectively. The cable was PTFE-filled which not only provided the insulation and concentricity of the conductors, but it also reduced the required overall length of the device by a factor of $1/\sqrt{2.1}$ where 2.1 is the permittivity $\acute{\epsilon}$. It has a nominal characteristic impedance of 50 Ω and a nominal capacitance of 96 pF/m. It is a fairly low loss cable rated at less than 1 dB/m at 10 GHz.

Although the cable apparently offered excellent electrical characteristics the manufacturer was not able to supply absolutely straight lengths which may affect the slotted line performance. The resulting reflections which would be set up can give erroneous readings, and to eliminate such errors it was decided to encapsulate the slotted section in a clamp, in order to keep it straight. As a consequence a natural platform was created, rigid enough to allow the probe carriage to be mounted directly on it. In slotting the cable meant that not only a strip of conductor was removed but also some dielectric had to be taken out to form a trough for the probe. Because of the small size of the line a change in impedance was feared and therefore

the slot width was kept at a minimum. This in turn dictated the size of the probe which was reduced in size accordingly. Radiall SMA connectors were used throughout the design, and even the probe was obtained by slightly altering the outline of an SMA flange receptacle. Fitting the stub tuners with SMA connectors, direct tuning of the probe was achieved.

Most of the required components, parts and accessories were constructed in the workshop with the exception of the micrometer head, thumbwheel, rack and pinion, and of course the connectors which were purchased. The various components, mechanical details and subsequent behaviour of the design, are discussed in the appropriate chapters.

In Chapter 2 the basic theoretical background is reviewed. Coaxial line primary parameters such as R, L, G and C may be found from the equivalent circuit for the transmission line. The manner in which electromagnetic energy propagates is examined, and secondary parameters such as attenuation and phase of the propagation constant, are discussed together with the interaction of incident and reflected waves creating standing waves.

Chapter 3 is concerned with the electrical requirements which must be obeyed if the performance objectives are to be met. The effect of the slot in the cable was examined and the analysis of the transmission line involving the probe and the tuning systems was carried out.

The mechanical design of the slotted line, probe carriage, tuners, and crystal detector dictated by electrical considerations are discussed in Chapter 4. An attempt is being made to highlight the relevant electrical requirements that influenced the final design.

In Chapter 5 the performance of the slotted line and its accessories is examined by carrying out a number of tests, results of which are presented. Detailed descriptions and procedures of the tests are fully explained.

Finally in Chapter 6 an assessment of the slotted line based on the performance achieved is made. Interpretation of the results obtained in Chapter 5, together with suggestions for possible improvements are proposed.

CHAPTER 2

THEORETICAL BACKGROUND

2.1 INTRODUCTION

The purpose of this chapter is to review the theory relevant to the design and subsequent testing of the slotted line.

The transmission line theory is a rather broad subject and the emphasis has been placed in seeking the equations that were of practical importance and used throughout the project. Equations, for example, that relate the primary constants or the characteristic impedance to the dimensions of the semi-rigid cable are of interest not only in assessing the cable, but in designing coaxial sections with impedances compatible to that of the main transmission line.

A basic equation such as the one for the attenuation constant α written in terms of the input and output power, was used extensively during the electrical measurements to establish the power loss characteristics. Relationships between the wavelength λ and the phase velocity υ_p were similarly useful especially in the design of the tuning stubs. Components such as the plungers being frequency sensitive depend on being of correct lengths.

Another set of useful relationships are those relating the voltage standing wave ratio S_v to the reflection coefficient ρ and the load impedance Z_L. These are of particular importance because their values are a measure of the mismatches and subsequent power losses in the system. Through every step of the design the equations were applied to ensure that the slotted line and its accessories were

perfectly matched, unwanted reflections were kept at a minimum and that the attenuation through the whole system was kept as low as possible.

Similarly during test procedures these equations were used to obtain the residual VSWR, S_R, response of the slotted line as well as assess the quality of different types of termination such as a fixed short circuit, all three of the stub tuners and a number of characteristic impedance terminations.

Finally, quantities such as γ, Z_o, VSWR, ρ etc., are the very parameters that the slotted line is used to measure and if full use of them is to be made, one should be familiar with the topics discussed in this chapter.

2.2 PRIMARY CONSTANTS OF THE SLOTTED LINE SECTION

One of the most commonly used means of transmission is via coaxial line or cable. As all such transmission lines, it consists of a conducting medium, inner solid and outer shell concentric conductors and a dielectric medium which occupies the space between them. In a particular case of the space being air, dielectric spacers are normally used to support the inner conductor. Electric and magnetic fields will exist in both air or dielectric and the principal advantage of a coaxial line design is that these fields are entirely confined to the space between the conductors and do not therefore radiate.

In defining the primary constants it is necessary to develop an equivalent circuit representing the transmission line. Such a circuit, is shown in Fig. 1 and it contains all four elements, resistance, conductance, inductance and capacitance, R, G, L and C

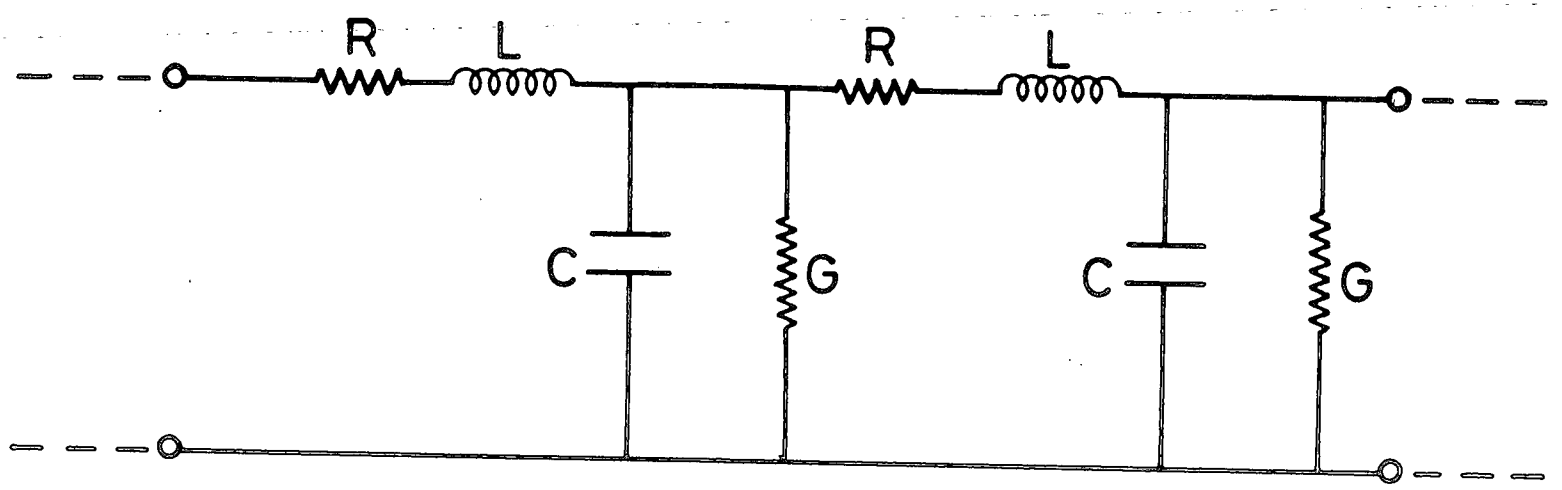

FIG. 1. Distribution of Impedance and Admittance Along a Transmission Line.

which do not, however, represent lumped components but are the values per unit length distributed uniformly along the line [2]. Therefore, a small unit length δx will have a series impedance $(R + j\omega L)$ and a shunt admittance $(G + j\omega C)$ per unit length. The primary constant R is the total resistance (a.c., d.c.) of the line per unit length. At high frequencies the total a.c. resistance per unit length is given as [7].

$$R_{a.c.} = \frac{1}{2\pi} \left(\frac{\omega\mu\rho}{2}\right)^{\frac{1}{2}} \times \left(\frac{1}{a} + \frac{1}{b}\right) \left(\frac{\Omega}{m}\right) \qquad (2.1)$$

where

μ = is the conductor permeability

ρ = conductor resistivity

and, a, b = radius of inner and outer conductor, respectively.

This formula, however applies only to a coaxial line having a homogeneous screen of the same material as the inner conductor. In the case of the semi-rigid cable employed in our project as the slotted section the conductors were made of different materials thus yielding different resistivity constants. This can be taken care of by slightly altering eqn. 2.1 which then becomes

$$R_{a.c.} = \frac{1}{2\pi} \left[\frac{\omega\mu}{2}\right]^{1/2} \times \left[\frac{(\rho_1)1/2}{a} + \frac{(\rho_2)1/2}{b}\right] \left(\frac{\Omega}{m}\right) \qquad (2.2)$$

where ρ_1, ρ_2 = inner and outer conductor resistivities.

From the above formula, it can be seen that the resistance is due to the conductor forming material and depends upon its cross-sectional shape and conductivity.

The inductance per unit length is the result of the magnetic field established around the conductors as current flows through them and is effectively in series with the line resistance. It is substantially dependent upon the total flux in the dielectric space and, to a lesser extent, upon the flux linkages within the conductors. For a coaxial line the inductance is given by [4]

$$L = \frac{\mu_d}{2\pi} \ln \frac{b}{a} + \frac{\mu_c}{8\pi} \left[\frac{4r^4}{(r^2-b^2)^2} \ln \frac{r}{b} - \frac{2r^2}{r^2-b^2} \right] \left(\frac{H}{m} \right) \qquad (2.3)$$

where μ_c = the conductor permeability

μ_d = the dielectric permeability

r = the radius to the external surface of the outer conductor.

For the semi-rigid cable to be used in our slotted line an inductance of 0.25 μH/m was calculated using $Z_o = \sqrt{L/C}$. It is obvious from eqn.2.3 that the value of inductance depends on the dimensions of the line, and on the magnetic permeability of the dielectric medium.

Capacitance between the two conductors will also be present. They can be thought of as the plates of a capacitor, with a voltage existing across them. The capacitance per unit length C, will depend on the line configuration and relative permitivity of the dielectric, and can be expressed as [4]

$$C = \frac{2\pi\varepsilon}{\log_e \frac{b}{a}} \quad (F/m) \qquad (2.4)$$

where ε = dielectric constant of the material.

For the semi-rigid cable a capacitance of 96 pF/m was specified by the manufacturer.

Finally, due to the imperfections of the dielectric medium some leakage current will flow between the conductors. This conduction, or leakage path, may be represented by a shunt resistance or, more conveniently by a conductance G between the conductor whose value can be calculated from the following equation [7]

$$G = \omega C \tan \delta \quad (S/m) \qquad (2.5)$$

where δ = the loss angle

Because the loss angle, δ, also may vary with frequency [7] it is important to use the particular value which corresponds to the frequency of operation.

2.3 THE CHARACTERISTIC IMPEDANCE

Secondary parameters of a line, the characteristic impedance Z_o, attenuation and phase, depend and are expressed in terms of the

distributed primary constants. The characteristic impedance Z_o, defined as the voltage to current ratio at any point along the matched line, is given by

$$Z_o = \sqrt{\frac{R+j\omega L}{G+j\omega C}} \qquad (\Omega) \qquad (2.6)$$

In general, eqn. 2.6 gives a complex result, however, there are two special cases of line where Z_o has a purely resistive value. Firstly, in the case of a lossless line, where $R \doteq 0$ and $G \doteq 0$ results in

$$Z_o = \sqrt{\frac{L}{C}} \qquad (\Omega) \qquad (2.7)$$

an expression which is independent of frequency. The second case results from the condition $\frac{L}{R} = \frac{C}{G}$ or $LG = RC$. Using this relationship equation 2.6 reduces again to eqn. 2.7. In practice, this is not an easy condition to obtain, however, it may be achieved sometimes by altering the conductor sizes and/or changing the dielectric material. At radio and microwave frequencies the lines are virtually lossless and eqn. 2.7 applies. Actual lines and cables do exhibit some loss even at high frequencies. Usually, $\omega L >> R$ and G is so small that it may be neglected [4] resulting in

$$Z_o = \sqrt{\frac{Z}{Y}} \cong \sqrt{\frac{R+j\omega L}{j\omega C}} = \sqrt{\frac{L}{C} + \frac{R}{j\omega C}}$$

$$\therefore \quad Z_o \cong \sqrt{\frac{L}{C}} \times \sqrt{1 - j\frac{R}{\omega L}}$$

Using binomial expansion, and since normally $\frac{R}{\omega L} << 1$ leads to

$$Z_o \cong \sqrt{\frac{L}{C}} \times \left(1 - j\frac{R}{2\omega L}\right)$$

or

$$Z_o \cong \sqrt{\frac{L}{C}} \times \sqrt{1 + \left(\frac{R}{2\omega L}\right)^2} \angle -\arctan \frac{R}{2\omega L} \qquad (2.8)$$

Examining eqn. 2.8 it can be seen that Z_o can be considered to be slightly capacitive while maintaining approximately a magnitude of nearly $\sqrt{\frac{L}{C}}$.

Now, since L and C can also be determined from the geometry and dimensions of the line cross-section, Z_o can be expressed in terms of these quantities. For a coaxial line the corresponding formula for Z_o can be developed as follows: [11]

$$Z_o = \sqrt{\frac{L}{C}} = \frac{1}{2\pi} \sqrt{\frac{\mu}{\varepsilon}} \times \log_e \frac{b}{a}$$

$$= \frac{120\pi}{2\pi} \sqrt{\frac{\mu_r}{\varepsilon_r}} \times 2.303 \log_{10} \frac{b}{a}$$

$$\therefore \quad Z_o = 138 \sqrt{\frac{\mu_r}{\varepsilon_r}} \log_{10} \frac{b}{a} \qquad (\Omega) \qquad (2.9)$$

where $\varepsilon_r = \frac{\varepsilon}{\varepsilon_o}$ relative permittivity of the dielectric medium

$\mu_r = \frac{\mu}{\mu_o}$ relative permeability of the dielectric medium

2.4 PROPAGATION CONSTANT AND WAVE TRANSMISSION

The purpose of a coaxial line is to carry energy from the source to the load. The efficiency with which it performs this function at RF and microwave frequencies is dependent on the purity of the mode in which it propagates the electromagnetic-wave energy.

The dominant mode is the one in which both electric and magnetic field components of the wave are entirely transverse to the direction of propagation (see Fig.2). Such a wave is known as a transverse electromagnetic wave (TEM). This mode has the advantage of having no low-frequency cut off in comparison to higher-mode lines.

One of the main interests in coaxial line performance is the manner in which power is attenuated during transmission. It has been

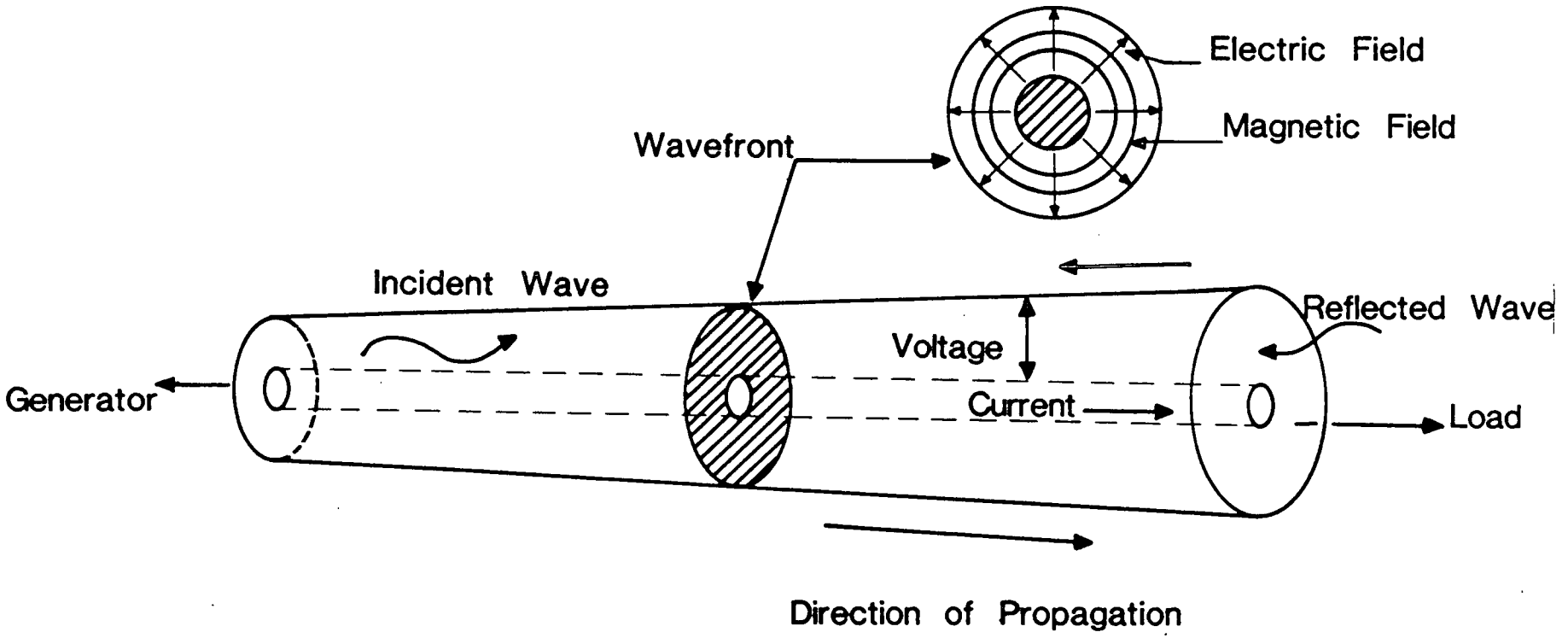

FIG. 2. T.E.M. – Mode Field Pattern in a Coaxial Transmission.

shown that the line contains impedance Z and admittance Y distributed along its entire length. The quantity $\sqrt{ZY}$ dictates how the voltages and currents vary along the line; it governs the way in which the waves are propagated. It is known as the propagation constant γ and is given by [7]

$$\gamma = \sqrt{ZY} = \sqrt{(R+j\omega L)(G+j\omega C)} \qquad (2.10)$$

The real part of the solution of the above equation, known as the attenuation factor or coefficient, α, determines the way in which the waves are attenuated as they travel along the line. The imaginary part is known as the phase shift constant and indicates the change in the angle of the propagating waves. It is a complex quantity expressed as

$$\gamma = \alpha + j\beta \qquad (2.11)$$

The attenuation constant α in dB can be written as the logarithm of the ratio of powers [1]

$$\alpha = 10 \log_{10} \left(\frac{P_1}{P_2} \right) \qquad (2.12)$$

where

P_1 = initial value of power

P_2 = final value of power

The value of α depends on the conductor and dielectric losses in R and G respectively. By solving eqn. 2.10 a relationship can be obtained for α which is stated below [2]

$$\alpha \cong \left[\frac{1}{2} R\sqrt{C/L} + \frac{1}{2} G\sqrt{L/C}\right]\left[1 - \frac{1}{2}\left(\frac{R}{2\omega L} - \frac{G}{2\omega C}\right)^2\right] \qquad (2.13)$$

When considering the case of the high frequency low loss coaxial line, it becomes apparent that the terms $\frac{R}{2\omega L}$ and $\frac{G}{2\omega C}$ are extremely small and can therefore be neglected. This will give the following "high frequency approximation " [1] for a low loss case, i.e.

$$\alpha \cong \frac{1}{2}\left(\frac{R}{Z_o}\right) + \frac{1}{2}\left(GZ_o\right) \qquad (2.14)$$

The above equation indicates that in practical lines the attenuation factor increases with frequency since R and G increase with frequency due to the skin effect and changes in dielectric loss respectively. Manufacturers data for the semi-rigid cable used quotes a nominal attenuation of less than 1 dB/m at 10 GHz.

The phase factor, β, of eqn. 2.11 can be obtained by expanding eqn. 2.10 and equating β to its imaginary part. This will yield

[2]

$$\beta \cong \omega\sqrt{LC}\left[1 + \frac{1}{2}(R/2\omega L - G/2\omega C)^2\right] \qquad (2.15)$$

As for the attenuation factor, α, a similar "high frequency approximation" can be obtained for β in the case of low loss coaxial line. Thus,

$$\beta \cong \omega\sqrt{LC} \qquad \text{in radians/m} \qquad (2.16)$$

The phase shift constant, β, can also be expressed in terms of wavelength λ and phase velocity v_p as follows:

$$\beta = \frac{2\pi}{\lambda} = \frac{2\pi f}{v_p} \qquad (\text{rad}/_{\text{m}}) \qquad (2.17)$$

from which we have the phase velocity of a signal propagating through a coaxial line at a given frequency [2] i.e.

$$v_p = \frac{\omega}{\beta} \qquad (2.18)$$

On substituting for β , one can express the phase velocity in terms of the line parameters in the case of low loss high frequency lines, i.e.

$$v_p = \frac{1}{\sqrt{LC}} \tag{2.19}$$

The phase velocity of the voltage wave in a line is the velocity of the electromagnetic wave in the medium between the line conductors. Therefore, for a nondissipative medium [1]

$$v_p = \frac{1}{\sqrt{\mu\varepsilon}} \tag{2.20}$$

where

μ = magnetic permeability of the medium

ε = electric dielectric constant of the medium

For any other medium [1], and this applies in our case,

$$v_p = \frac{c}{\sqrt{\mu_r \varepsilon_r}} \tag{2.21}$$

or

$$v_p = \frac{c}{\sqrt{\varepsilon_r}} \tag{2.22}$$

where

c = velocity of electromagnetic wave in vacuum or air

since $\mu_r = 1$ for the most commonly used dielectric materials.

The semi-rigid cable uses PTFE as the dielectric medium, with ε_r of 2.1, giving a velocity ratio $\frac{v_p}{c}$ of 0.7.

2.5 REFLECTIONS AND STANDING WAVES

The performance and behaviour of a transmission line can be explained in terms of the electromagnetic waves propagating along the line from the source to the load and back since at the load end some, or all of it, may be reflected.

A wave is known as the incident or a reflected depending on whether it is travelling from the source to the load or is reflected from the load towards the source, respectively. There is also a fixed amplitude and phase relationship between them. At any point x along the transmission line, measured from the source to the load the voltage V_x is given as

$$V_x = V_{ix} + V_{rx} \tag{2.23}$$

where

V_{ix} = incident voltage at point x

V_{rx} = reflected voltage at point x

V_{ix} and V_{rx} can in turn be obtained from the following equations:-

$$V_{ix} = \left[\frac{V_s + I_s Z_o}{2}\right] e^{-\gamma x} \tag{2.24}$$

$$V_{rx} = \left[\frac{V_s - I_s Z_o}{2}\right] e^{+\gamma x} \tag{2.25}$$

where

V_s = voltage at the source end

I_s = current at the source end

The incident and reflected waves interact, and the result is a composite and stationary wave known as a standing wave.

The maximum amplitude of such wave occurs when both incident and reflected waves are in phase. The minimum amplitude occurs when the two waves are 180^o out of phase. As a consequence the successive maxima and minima along the line are spaced respectively half a wave length apart. The magnitude and phase of the reflected wave at the load end, depends on the load impednace (Z_L). In the case of the matched load (i.e.$Z_L = Z_o$) the incident wave will be totally absorbed, without creating any reflections. But, if the load is lossless (i.e. $Z_L = 0$, or $Z_L = jX_L$) then the incident wave will be completely reflected with a resulting phase change. The magnitude and phase of the reflected voltage or current wave (V_r or I_r), relative to the

incident wave (V_i or I_i), at the load is known as the reflection coefficient ρ. The voltage reflection coefficient ρ_v can be evaluated from [17]

$$\rho_v = \left| \frac{V_r}{V_i} \right| e^{j\phi} \tag{2.26}$$

whilst the current reflection coefficient ρ_i is expressed as:

$$\rho_i = -\left| \frac{I_r}{I_i} \right| e^{j\phi} \tag{2.27}$$

Similarly, both voltage and current reflection coefficients can be expressed in terms of the characteristic impedance Z_o and the terminating load Z_L, as follows [17]

$$\rho_v = \frac{Z_L - Z_o}{Z_L + Z_o} \tag{2.28}$$

$$\rho_i = \frac{Z_o - Z_L}{Z_1 + Z_o} \tag{2.29}$$

One of the most important quantities of a lossless transmission line is the standing wave ratio of voltage or current along the line. It is defined as the ratio of the amplitude of a standing wave at an anti-node to the amplitude at a node. In other words it is the ratio of maximum to minimum voltage (or current) and is stated as

$$S_\nu = \frac{V_{max}}{V_{min}} \tag{2.30}$$

where

S_ν = voltage standing wave ratio or VSWR

V_{max} = voltage at a maximum or anti-node

V_{min} = voltage at a minimum or node

Since the creation of a standing wave depends on reflection, equations relating VSWR and the reflection coefficient ρ can be obtained.

Since at a maximum

$$V_{max} = |V_i| + |V_r| = |V_i|\left[1 + |\rho_\nu|\right] \tag{2.31}$$

and at a minimum

$$V_{min} = |V_i| - |V_r| = |V_i|\left[1 - |\rho_\nu|\right] \tag{2.32}$$

the ratio results in

$$S_\nu = \text{VSWR} = \frac{1 + |\rho_\nu|}{1 - |\rho_\nu|} \tag{2.33}$$

VSWR can also be expressed in decibels

$$S_\nu \text{ (dB)} = 20 \log_{10} \left[\frac{V_{max}}{V_{min}} \right] \tag{2.34}$$

From the above equations it can be observed that the standing wave ratio or S_ν is a real quantity unlike the reflection coefficient ρ_ν which can be complex. The minimum value of S_ν is 1.0 in the case of a matched load with $\rho = 0$ and the maximum value of S_ν is obtained when the line is terminated in a pure reactance, short or open circuit, i.e. for these conditions, $|\rho| = 1.0$.

CHAPTER 3

THE ELECTRICAL CIRCUIT OF THE SLOTTED LINE

3.1 GENERAL OBJECTIVES

A diode detector and a probe assembly are used to measure the standing wave in a slotted transmission line without disturbing significantly the field pattern. Such an arrangement was briefly outlined in chapter 1. In this chapter, a number of objectives will be defined which, if fulfilled, will ultimately produce a slotted line having the required electrical performance.

These objectives can generally be defined as follows:

(i) cross-sectional uniformity. It is critical for a slotted line to have a uniform cross-section throughout its entire length. If this is not so, the measurement of the electric field intensity will not accurately represent the characteristics of the waves as they exist outside the slotted section.

(ii) minimisation of reflections and hence standing waves. Care should be taken to ensure that such unwanted phenomena do not appear in the final design. These are usually constructional problems, i.e. a wrongly placed slot, or mismatches occurring from not having correctly attached connectors etc etc...

(iii) minimal disturbance of the electric field due to probe penetration. In a successful design the probe should protrude into the slotted section as little as possible and

sensitive detecting arrangement is needed which will respond adequately to the small amounts of power picked up by the probe. Also a reliable tuning system is required to increase the sensitivity of the detector.

(v) finally, the slotted line should operate satisfactorily over the frequency range it was designed for, i.e. a flat response over the required band from 1 - 18 GHz.

3.2 SLOT AND ASSOCIATED PROBLEMS

A slot along the length of the outer coaxial conductor is the only suitable means of gaining access into the transmission line. Positioning the slot is very important as its presence should not disturb the flow of the current. In coaxial lines carrying TEM the current flow is everywhere parallel to the axis of the transmission line. Therefore, in principle a longitudinal slot should not alter the field appreciably, since there will be no current crossing it. It will, however, change the characteristic impedance slightly and also introduce a finite but usually negligible loss. Such change can be readily understood when considering that the characteristic impedance is also determined by the line capacitance per unit length in a lossless line. This capacitance per unit length will slightly decrease in the vicinity of the slot. A formula for calculating the magnitude of the impedance change is given by [6]

$$\frac{\Delta Z_o}{Z_o} = \frac{1}{4\pi^2} \times \frac{w^2}{b^2 - a^2} \qquad (3.1)$$

where

ΔZ_o = change in characteristic impedance

w = width of the slot

b,a = radii of outer and inner conductors respectively.

The above formula applies to a coaxial cable with an infinitely thick outer conductor. For a conductor wall of finite thickness the magnitude of impedance change will be only marginally higher. The prominent effect of such impedance discontinuity is, that at the beginning and at the end of the slot small reflections will be set up. The reflection coefficients absolute value is given by [12]

$$|\Delta\rho_v| = \frac{1}{2} \times \frac{\Delta Z_o}{Z_o} \tag{3.2}$$

where

$|\Delta\rho_v|$ = value of reflection coefficient due to impedance change

The above mentioned reflections caused by impedance and slot discontinuities are indistinguishable from usually more moderate reflections, caused by the load, and hence erroneous results will be obtained. Abruptly-ended slots create slightly different fields in the slotted and unslotted sections. Such discontinuities may be represented as a small reactance shunting the line. These undesirable effects can be greatly reduced by gradually decreasing the width of the slot in steps comparable to the wavelength. Since these local waves attenuate exponentially with distance and become negligible

very quickly, it is good practice in measurements not to use the portions of the slot close to the ends.

Another property of the slotted line, is the creation of new modes. The slot waves, as they are known, exist because of the changes in the boundary conditions of the transmission line. Even though they are more prominent in slotted waveguides, they sometimes exist in coaxial lines and have a disturbing effect on the standing wave measurements. The probe and carriage divides the slot in two sections and as they move along the line the sections vary allowing at some point a resonance to be set up, if the slot wave is excited. Radiation into free space usually dampens the slot resonance and the resultant Q is very low. For a coaxial line Q can be approximately obtained from [12]

$$Q \simeq \frac{\lambda_c^2}{2\pi^2 ab} \tag{3.3}$$

where

λ_c = cut off wavelength

a = mean circumference of coaxial line

b = distance between inner and outer conductors.

The cut off wave length for the slot wave resonance can be approximately derived from the relationship deduced in [12] i.e.

$$\cot\left(\frac{\pi a}{\lambda_c}\right) = \frac{2b}{\lambda_c}\left[2\,\ell n\left(\frac{0.372b\,\lambda_c}{w^2}\right) + \frac{2}{1-\left(\frac{2b}{\lambda_c}\right)^2} + \frac{2\pi t}{w}\right] \qquad (3.4)$$

where

t = thickness of outer conductor wall

w = slot width

Consideration of distortion due to the slot inside the transmission line, leads to a conclusion that it should be made as small as possible. A narrow one, can have an almost negligible effect on the line properties, allowing the slotted section to behave as a uniform, low loss transmission line, supporting only one propagating mode.

3.3 PROBE ASSEMBLY

There is a need for some arrangement to couple to the fields inside the coaxial line (or waveguide) and deliver the output to the indicating instrument. Basically, there are two types of coupling recognised. One is known as the PROBE which responds to the electric field in the line; the other is the LOOP which responds to the magnetic field. Fig. 3 shows a schematic representation of the electric field probe, and it is this kind of probe that was used in the slotted line assembly.

Because it can be made very small in size, the field in the coaxial cable is not disturbed sufficiently to cause erroneous readings. Since it responds to the electric field alone it is more advantageous than the loop which due to its self-inductance responds, to some extent, to both electric and magnetic fields.

Difficulties, however, will arise from using a sampling probe. These arise because the probe extracts a very small amount of power, and to a lesser degree, because of the mechanical inaccuracies in the construction of the various parts of the sampling unit. The distortion of the standing wave due to power absorption by the probe can be easily analysed if two assumptions are made.

The first is that the line connecting the probe to the indicating instrument as seen from the probe, presents an impedance independent of input level. Since the signal to the detector diode is very weak, at microwave frequencies the detecting system appears as a non-varying load. This means that in setting-up an equivalent circuit there is no need for introducing non-linear elements. The second assumption requires that the probe dimensions are small in comparison with the wavelength, and it does not move transversely to the slot. This can become valid if sufficient care is undertaken in mechanical design. On these basis, the sampling probe can be shown as an admittance shunting the transmission line. An equivalent circuit representing the generator, probe and load components is outlined in Fig. 4. The probe admittance consists of a resistive and reactive part. The resistive component G_p represents the power absorbed by the probe; the reactive component B_p represents the reflection caused by the probe and is a function of the probe tuning.

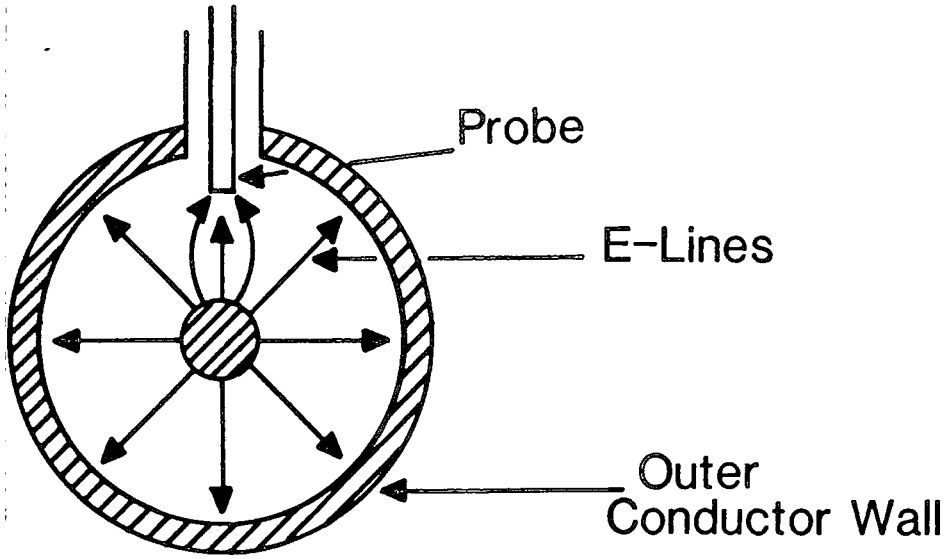

FIG. 3. Schematic Representation of the Probe Coupling to the Electric Field in a Coaxial Line.

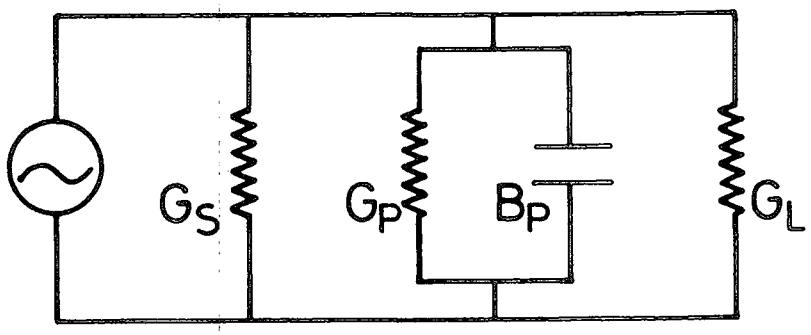

FIG. 4. Equivalent Circuit Representing the Interaction Between the Generator, Probe and the Load Admittance.

If the power absorbed by the probe is expressed in terms of probe position, generator and load admittances, certain observations can be made of the effects on the standing wave pattern.

The case of the generator matching to the transmission line will only be considered in this chapter, (i.e. $Y_g = G_g = 1$). Also for ease of analysis the load will be taken to be real, since the standing wave pattern is similar for either real or complex loads. The only difference lies in the fact that it will be shifted along the line in the latter case. If the load is complex then the distance d_L will not be from the probe to the load, but from the probe to the point on the line where the load is real and has a magnitude equal to G_L. If the power indicated by the probe is considered to be equal to the power absorbed, the following approximate equation [12] can be used to calculate the power absorbed, i.e.

$$P_p \simeq \frac{G_p(1+G_L^2\tan^2\theta)^2}{\left[1+G_L+G_p+G_L(1+G_L+G_pG_L)\tan^2\theta\right]^2 + \left[B_p+(1-G_L^2)\tan\theta+B_pG_L^2\tan\theta\right]^2} \qquad (3.5)$$

where

P_p = power absorbed by the probe

$$\theta = \frac{2\pi d_L}{\lambda}$$

When the generator and load impedances both equal Z_o, the standing wave ratio is unity which will not be the case when the load is replaced by, say, a short circuit or an open circuit. When carrying out measurements like for example wavelength, the probe should be positioned at voltage minima, so as not to disturb the field pattern. The reason being, that voltage maxima can be affected by the presence of the probe, since it absorbs power and places a reactance across the line. This causes magnitude and positional changes. Arbitrary loads will cause both maxima and minima to be shifted from their true locations. Shifts of this nature can be predicted analytically by considering the circuit of Fig. 4. First, assuming that $G_L = 0$, i.e. the load is an open circuit, will result in reducing eqn. 3.5 to

$$P_p \simeq \frac{G_p}{(1+G_p)^2 + (B_p+\tan\theta)^2} \qquad (3.6)$$

The nodes of the standing wave will occur when $\tan\theta = \infty$. At these points the power P_p will be minimum - almost zero - and their locations are not affected by G_p or B_p. Therefore, the nodes will occur at the same points they would have done if the probe size was negligibly small. On the other hand the antinodes, which are the voltage maxima will not appear when the condition is $\tan\theta = 0$ but when $\tan\theta = -B_p$. As a result the standing wave pattern will become distorted because of the introduced shift. The shift in the location of the antinodes is related to the positions where the maxima should actually occur, when using an infinitesimal probe, B_p can be evaluated

by employing the following procedure; readings of P_p are obtained from either side of the minimum at distances of $\lambda/8$, at which point tan θ = +1 and -1, respectively. The ratio of the two readings will then be [12]

$$\frac{P_{p_1}}{P_{p_2}} = \frac{(1+G_p)^2 + (B_p-1)^2}{(1+G_p)^2 + (B_p+1)^2} \tag{3.7}$$

where

P_{p_1} = probe power reading at tan θ= +1

P_{p_2} = probe power reading at tan θ= -1

The above equation can be further reduced to

$$\frac{P_{p_1}}{P_{p_2}} = 1 - 2B_p \tag{3.8}$$

if G_p and B_p are considered to be very small.

If the load is other than open circuit then the position of the maxima and minima, as well as the value of the VSWR will be altered. Positional shifts can be calculated from eqn. 3.5. For small B_p and G_p and for $G_L \leq 1$ differentiating eqn. 3.5 w.r.t. tanθ will yield [6]

$$\frac{\delta_{min}}{\lambda} = \frac{G_L^2 B_P}{(1+G_L)^2} \qquad (3.9)$$

$$\frac{\delta_{max}}{\lambda} = \frac{B_P}{(1+G_L)^2} \qquad (3.10)$$

where

δ_{min} = shift in the position of a minimum

δ_{max} = shift in the position of a maximum

if $G_L \geq 1$ then

$$\frac{\delta_{max}}{\lambda} = \frac{G_L^2 B_P}{(1+G_L)^2} \qquad (3.11)$$

$$\frac{\delta_{min}}{\lambda} = \frac{B_P}{(1+G_L)^2} \qquad (3.12)$$

or instead, G_L can be replaced by $\frac{1}{G_L}$ in eqn. 3.9 and eqn. 3.10

Due to the presence of G_P the true standing-wave ratio S_t will be altered. The ratio of the measured standing-wave ratio S_m to the true SWR S_t is given as [6,12]

$$\frac{S_m}{S_t} = \frac{1 + G_L + G_L G_P}{1 + G_L + G_P} \qquad (3.13)$$

(assuming $B_P = 0$)

where

G_L = load admittance

G_P = probe admittance

Eqn.3.13 demonstrates how large probe depth (increasing Gp) can alter the SWR ratio and hence impedance measurements. For best results the location of the minimum should be used, since it results in less error. When the generator and load impedances are matched, the value of the probe conductance G_P is numerically equal to the amount of power diverted to the probe circuit, and for this reason it is sometimes called the "coupling coefficient". Tuning the probe with a reactive tuner, for maximum output, will reduce the probe succeptance B_P to zero.

3.4 DETECTOR CIRCUIT

The diagram of Fig. 5 shows a schematic representation of the probe and its equivalent circuit looking into the detecting system. The transmission line voltage acts on the probe through C_1 which is the capacitance between the probe and the opposite side of the transmission line. The capacitance between the probe and the slot is indicated by C_2 and is greater than C_1 . For maximum output the tuner is adjusted so that C_2 and L resonate at the operating frequency. However, erratic changes will be observed in the defected

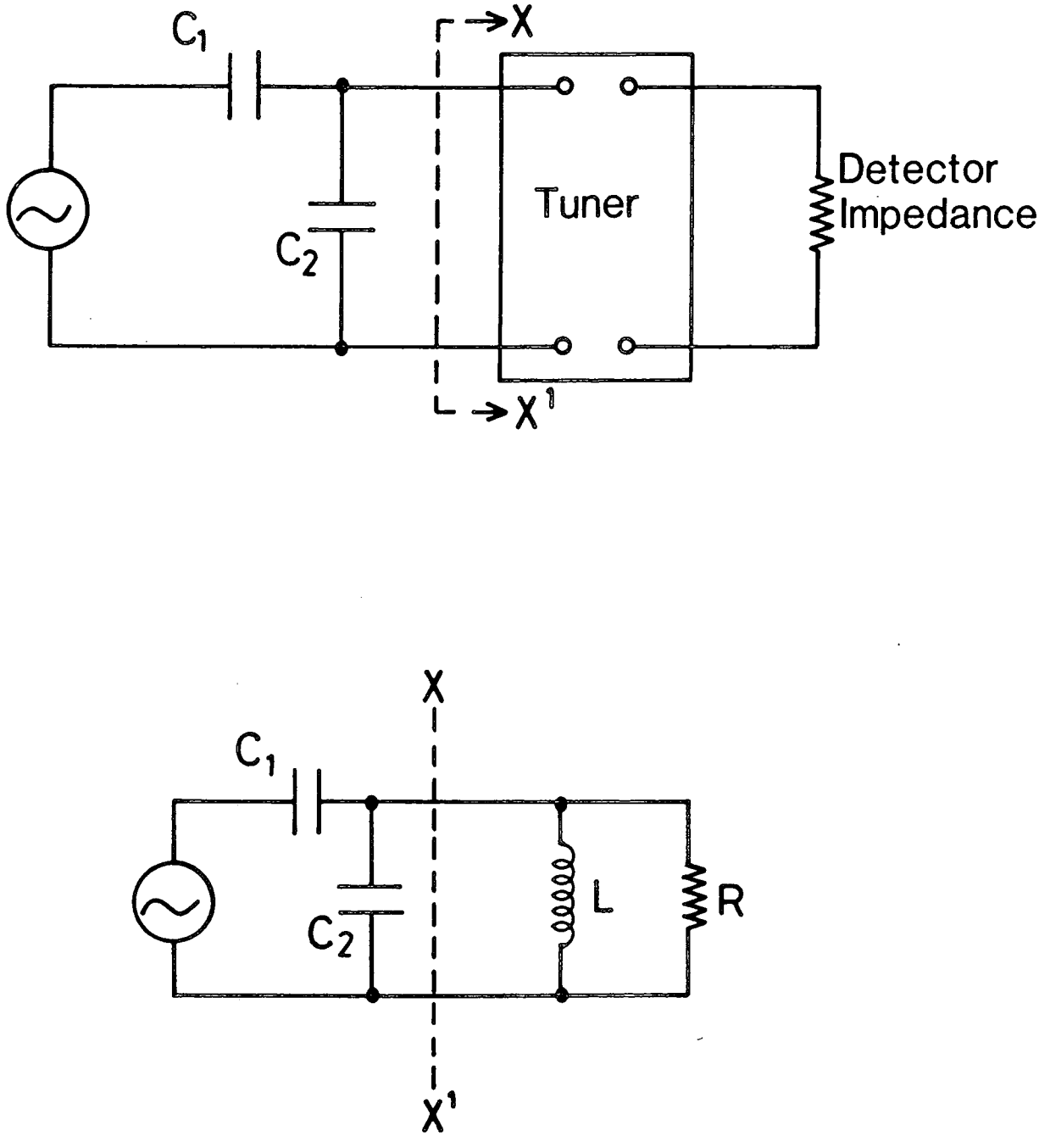

FIG. 5. Schematic Representation of the Probe Circuit and its Equivalent Circuit

output if C_2 does not remain constant as the probe moves along the slot. This can be eliminated by detuning the probe mechanism by a large factor.

Tuning for maximum output can create restrictions in the construction of the device, because not only the coupling capacitance must be constant, but the capacitance of the probe to its surroundings must remain the same as well. This additional requirement on the accuracy of construction is difficult to meet in practice since even the smallest transverse displacement can make an appreciable change in C_2 . To counteract such defects a skirt can be made to protrude into the slot to shield the probe from its environs. A circular resonant trap ensures that the probe shield is electrically connected to the transmission line. This is illustrated in Fig. 6.

Finally, the sensitivity of the detecting system should be kept as high as possible in order to minimise the various possible errors caused by the probe and slot problems. It is necessary to determine the response law of the diode in the expected signal level range, just prior to use. Specifically, the adjustment of the r-f tuning mechanism can result in the change of the r-f source impedance as seen by the detector, which can change the output.

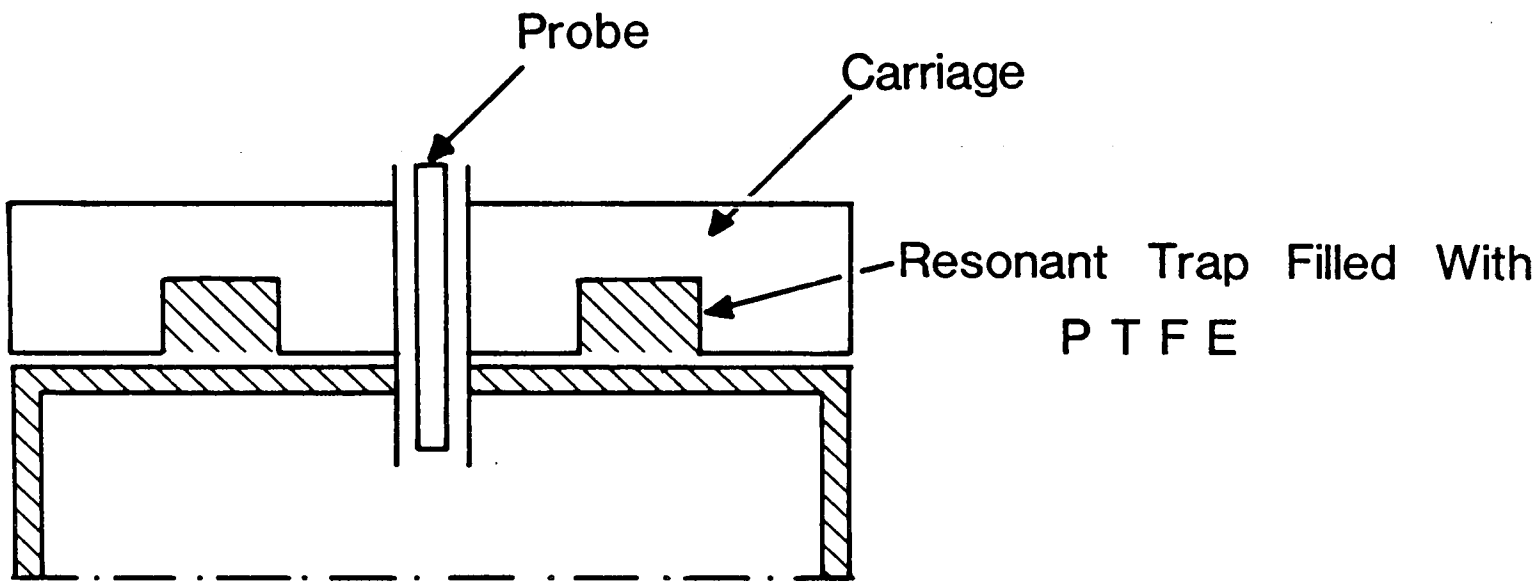

FIG.6. Use of the Resonance Trap for Connecting the Probe Line to the Transmission Line.

CHAPTER 4

ELECTRO-MECHANICAL DESIGN

4.1 THE SLOTTED LINE

In chapter 1 the method for investigating the nature of the standing-wave pattern inside the transmission line was briefly discussed. This section is mainly concerned with the practical aspects of obtaining the information needed to evaluate the load, and impedance along the line. It was assumed in particular, that it was possible to investigate the fields without disturbing their distribution, and hence record their magnitudes.

In a successful design two main requirements must be observed; uniformity and concentricity. Therefore, during the construction every possible care was taken to ensure that the cross-sections of the clamp, semi-rigid cable and the probe assembly were perpendicular w.r.t. the line, and thus displaying perfect symmetry. Precautions were also taken to avoid the shape of the cross-sectional area being altered in any way as the probe travels along the length of the slot. Departure from symmetry and uniformity can create reflections and a change of probe penetration will result in variation of the probe admittance. It became obvious that in order to satisfy the above requirements a good mechanical design was of the utmost importance. The method of construction had to be such that close tolerances could be maintained on all critical dimensions.

The slotted section of transmission line was obtained from a length of Radiall RG401/U semi-rigid, PTFE-filled cable. Of the three

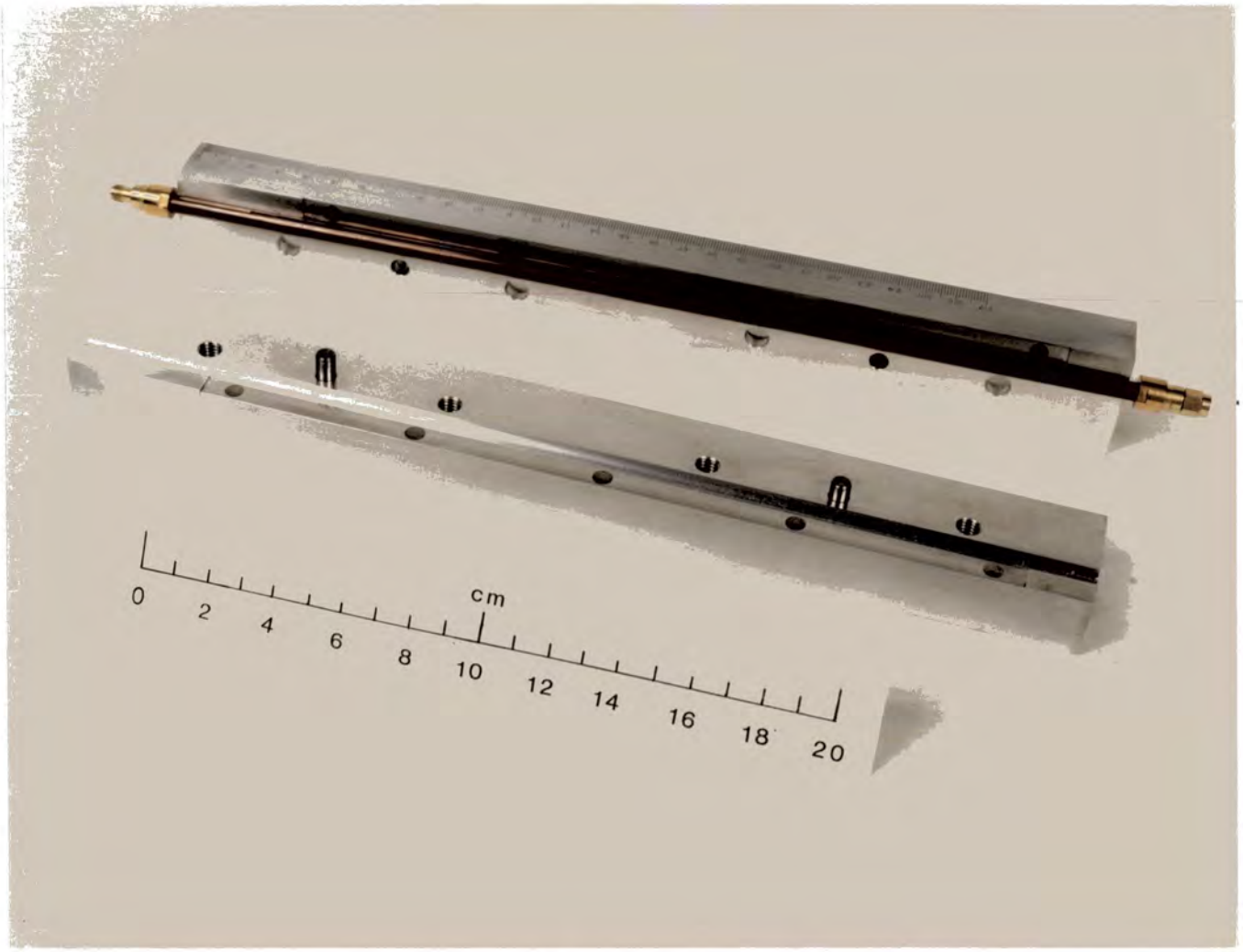

PHOTOGRAPH 2 Opened Clamp Showing the Positioning of the Slotted Semi – Rigid Cable

standard diameter sizes available, the one with 6.35 mm dia. was chosen as it was realised that the effect of the slot on SWR would be less in the largest diameter cable. It also became apparent from the beginning that the purchased cable lengths were not rigid enough to slot it, and mount the probe carriage directly on it.

These problems were overcome mechanically by clamping the cable in a vice type arrangement which ensured its uniformity along the entire length of the slot. It also provided the base on which the probe carriage would be mounted, ensuring a fixed reference for the longitudinal movement of the probe at a constant depth.

The clamp was machined from Duralumin chosen because of its strength, rigidity and the ease with which it can be milled. Its low weight and resistance to corrosion made it ideal for this application. It consisted of two halves with semi-circular grooves along their lengths, so that when they were brought together, the cable was held firmly in position. A cross-sectional view of the clamp supporting the slotted cable is shown in Fig. 7. All surfaces were machined precisely to given specifications. Its length was decided to be 322 mm allowing a carriage movement of approximately 250 mm, which was found to be adequate for locating two voltage minima at the lowest frequency of 1 GHz. The guide grooves at the sides of the clamp were necessary for the firm mounting of the probe carriage. Sufficient clamp width and height were therefore required to allow them to be machined into each half of the clamp and also sturdy bolts to be screwed into it for joining the two halves. A semi-circular groove was placed in each half with diameter slightly smaller than that of the cable. With the cable gripped between the grooves, the top of its outer conductor was 8 mm from the top surface of the clamp. For

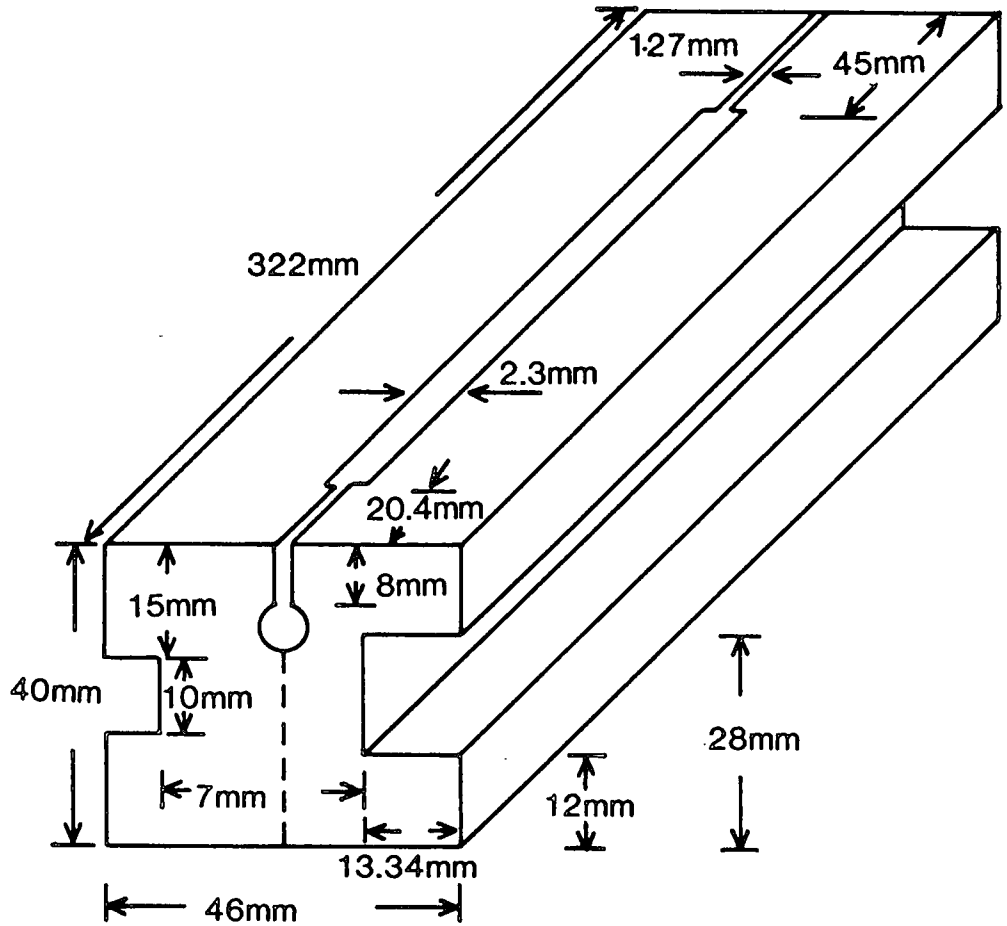

FIG. 7 The Slotted Line Clamp.

effective construction a tolerance in dimensions of ±0.01 mm was specified and achieved.

Two end plates were milled to serve as means of standing the instrument on the bench. Each plate had four holes drilled and tapped to allow fastening to the main body. (see Fig.8). Once positioned and held within the clamp the cable was then slotted so as to ensure complete symmetry of the slot to its surroundings. It was milled out using a slitting saw to obtain the required depth and width. (Fig.9) The depth was such that the inner conductor was not completely stripped of dielectric, but instead a fine layer of PTFE was left around it. To eliminate any unwanted reflections that may occur due to the slight impedance change, the slot was not abruptly ended, but instead a reduction at its ends to half the depth and width was introduced for about 5.5 mm ($\lambda/4$ of average frequency).

A millimeter scale was also engraved on the top surface of the clamp to be used in conjunction with a vernier mounted on the probe carriage. This allowed the position of the probe to be accurately determined to within 0.05 mm. The zero on the scale corresponded to the probe being at the start of the slot (load end) and provided a reference point for measurements.

The side plates were joined together by a metal rod on which a micrometer was mounted. This was used to allow a greater degree of accuracy in the probe positioning measurements at the higher frequencies (4 - 18 GHz). Directly beneath one of the guide slots a rack was placed. A helical type was chosen to provide the smooth and uniform movement of the carriage, by minimising the back lash. The slotted line input and output were fitted with Radiall SMA connectors (R125056, R125226). If properly assembled these connectors

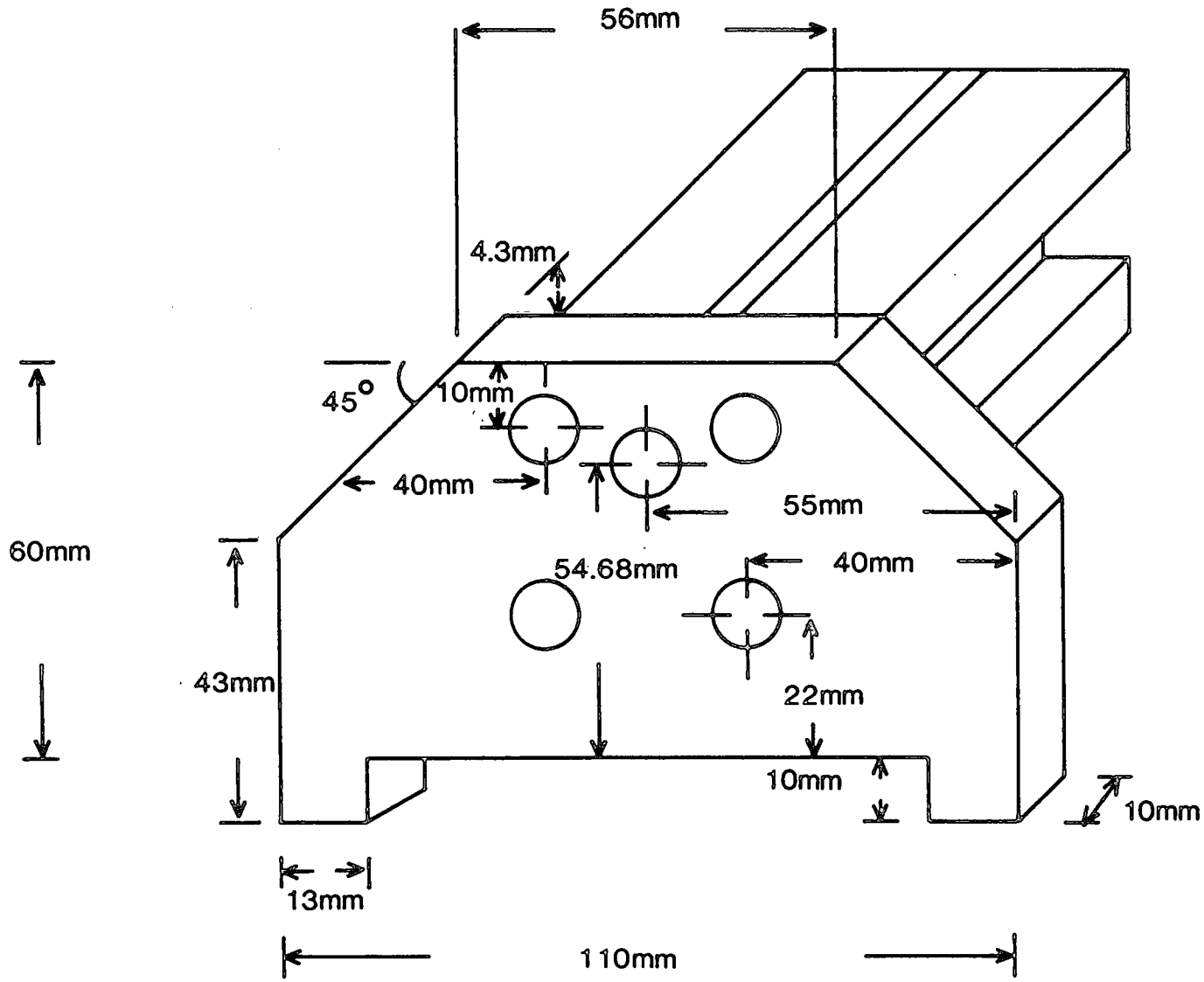

FIG. 8. Design Details of the Slotted Line End Plates.

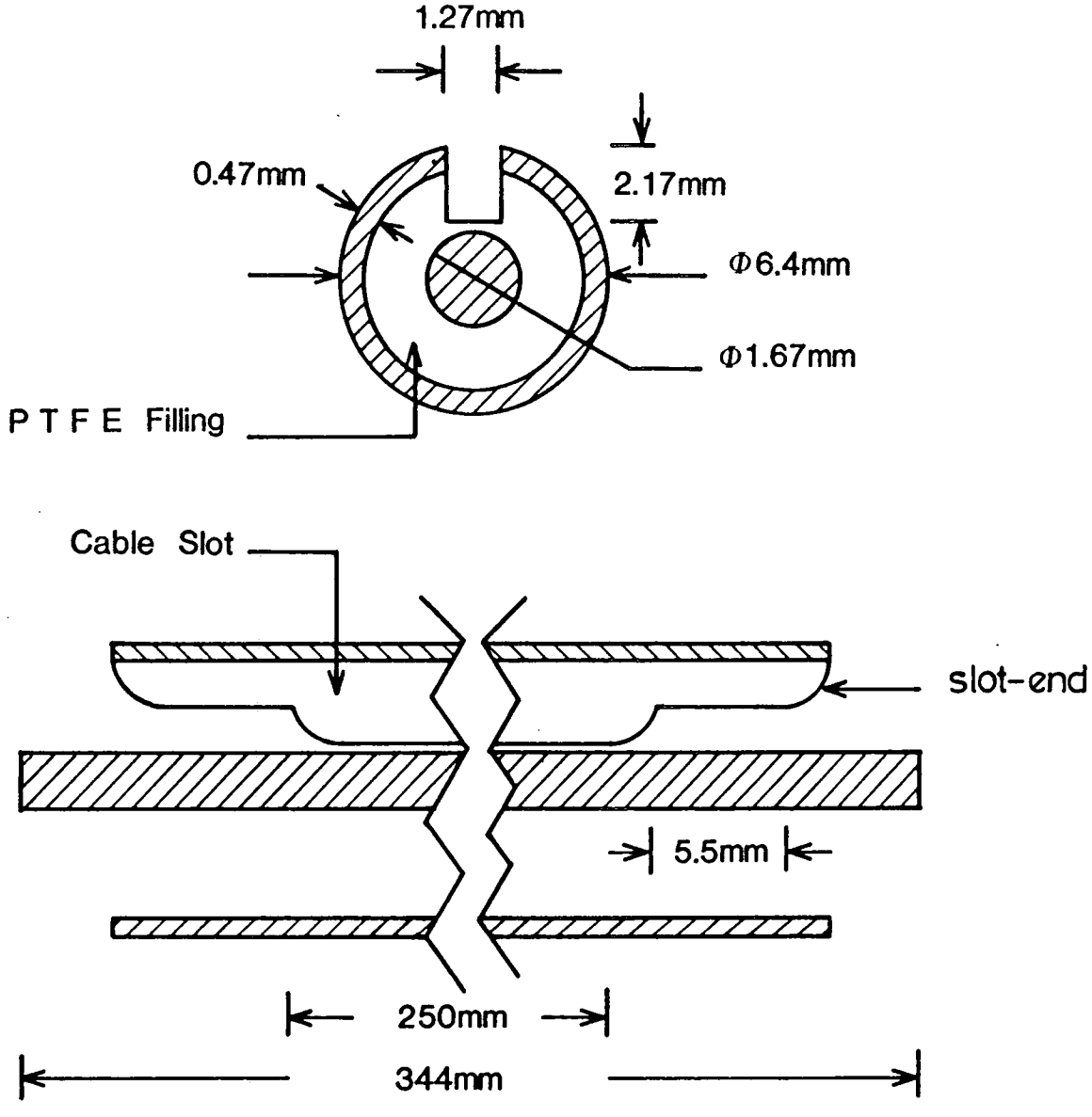

FIG.9. Cross Section of the Slotted Semi-Rigid Cable.

should provide satisfactory performance up to 18 GHz.

4.2 THE PROBE CARRIAGE

In the early stages of design it became clear that the probe and its carriage were to be the most important, and critical, parts of the slotted line. Indeed, for satisfactory detection performance a great deal depended on the behaviour of these mechanisms.

In designing the probe carriage the aim was to firstly define a path as accurately as possible for the probe, and secondly to ensure that it was shielded from its surroundings until it actually protruded in the cable slot.

The probe shield seen in Fig. 10 as a rectangular extension of the under carriage formed an integral part of the probe carriage, and its lower surface was level with the inner wall of the outer conductor. The probe itself ran through a hole within the shield and in so doing the possibility of slot waves being excited through lack of symmetry was reduced. In an attempt to supress any reflections that might occur at the shield's ends, it was made half a wave-length long at the average operating frequency of 9.5 GHz.

No part of the carriage actually touched either the top or sides of the clamp. A clearance was maintained on both sides of the shielding skirt as well as beneath the carriage. It was found that a clearance of 0.31 mm was easier to maintain with a close tolerance of one or two hundredths of a millimeter, then assuring consistent but free-sliding contact everywhere, between the carriage, skirt and the clamp. Besides, avoiding physical contact meant that the electrical requirements did not depend on minute irregularities which might have

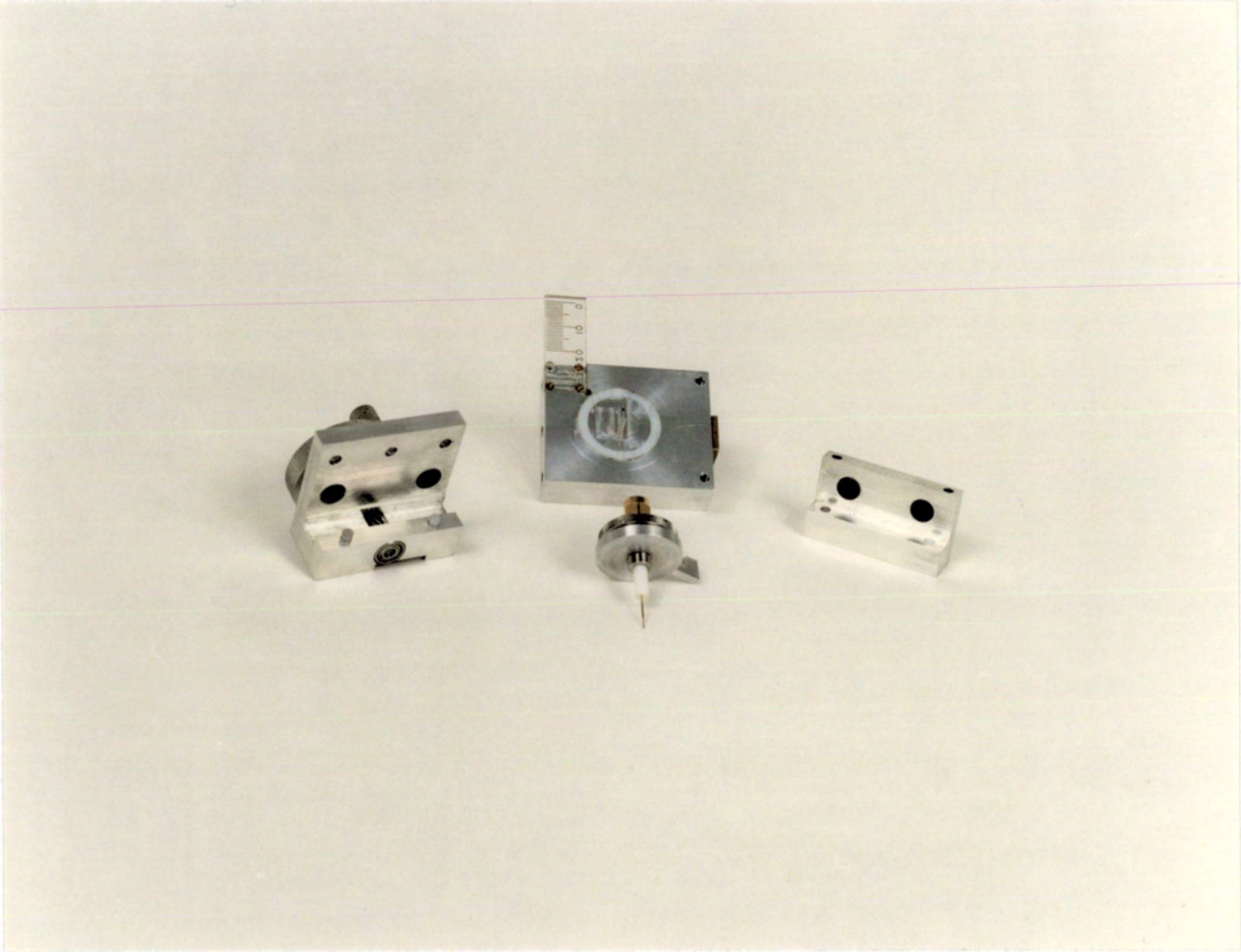

PHOTOGRAPH 3 Dismantled Probe and Carriage Assembly

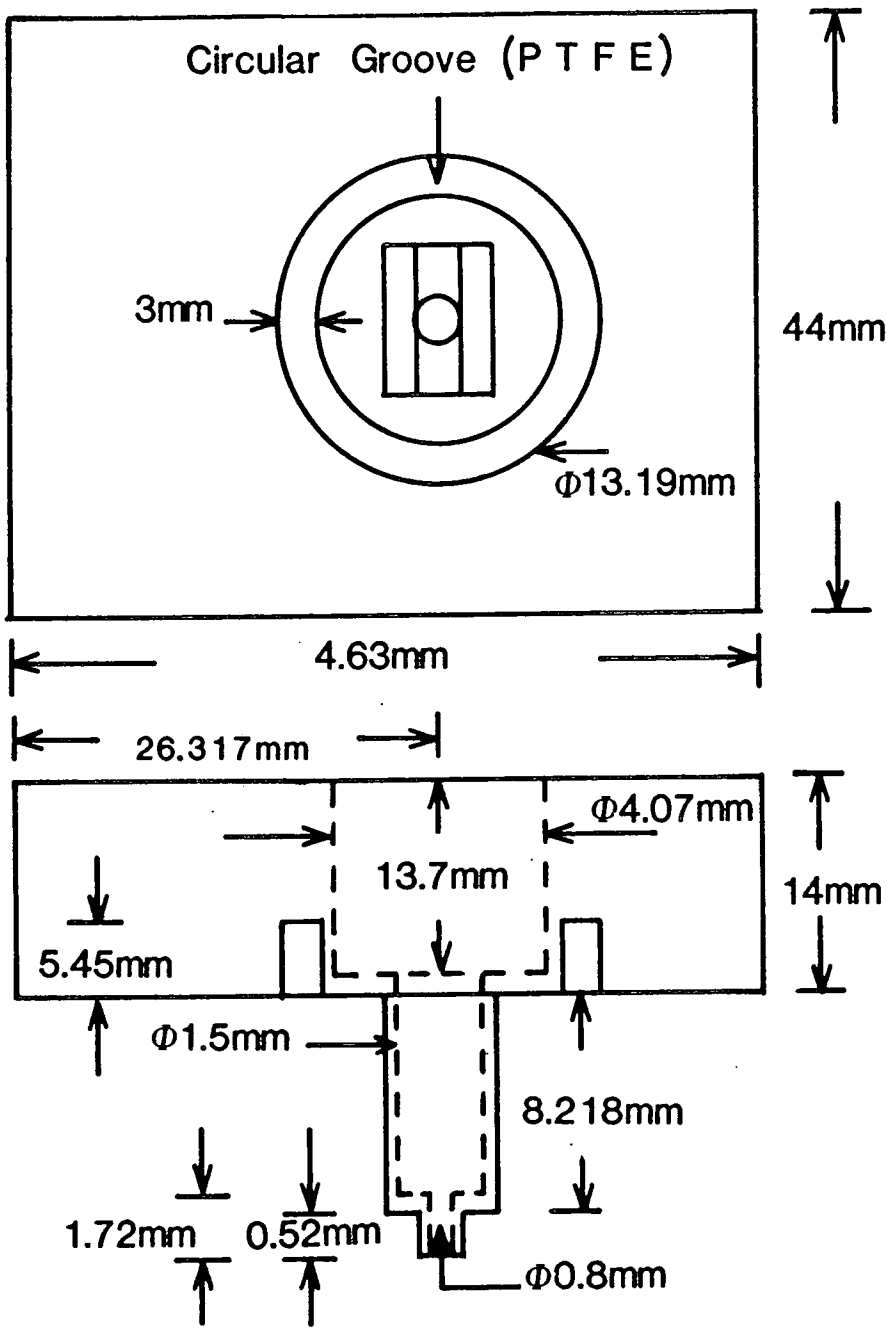

FIG.10. Under and Side View of the Undercarriage.

upset the electrical symmetry of the whole system. Unavoidably, the narrow gap on either side of the shield was slightly excited by the waves in the slot. This excitation could be considered to arise from the current that tends to flow across the gap. Normally, the current flowing through the probe is predominant and greatly exceeds the shield current. The impedances corresponding to the two gaps can be thought of as being connected in series with the probe whose amount of absorbed power will be affected if these impedances were to vary. Design precautions were taken to eliminate such effects. This was achieved by extending the gap between the shield and the clamp into the space underneath the carriage. In so doing, a type of transmission line was created which when terminated in an open circuit about $\lambda/4$ from the gap resulted in avery low impedance being created. The open-circuit condition was obtained by a quarter-wave circular trap machined in the under carriage. The groove was filled with PTFE mainly to save space having a depth equal to $(\lambda/4)\sqrt{1/\varepsilon_r}$ with λ being the wavelength of the average frequency of 9.5 GHz. The distance from the groove to the bottom of the shield should be approximately a quarter of a wavelength. This was not possible because the length of the skirt was much greater than $\lambda/4$, but it was assumed not to be critical and the impedance of the gap was made very small. It was accepted that the wavelength concerned was that of free space.

The carriage (Fig.11) was made from Duralumin and it consisted of three parts, which, when assembled ensured that it ran in fixed relationship with respect to the clamp surface so that constant coupling was maintained. Both side plates were held on to the main body with five screws placed at easy access locations. A thumb wheel was also placed on the front side plate so that the carriage was able

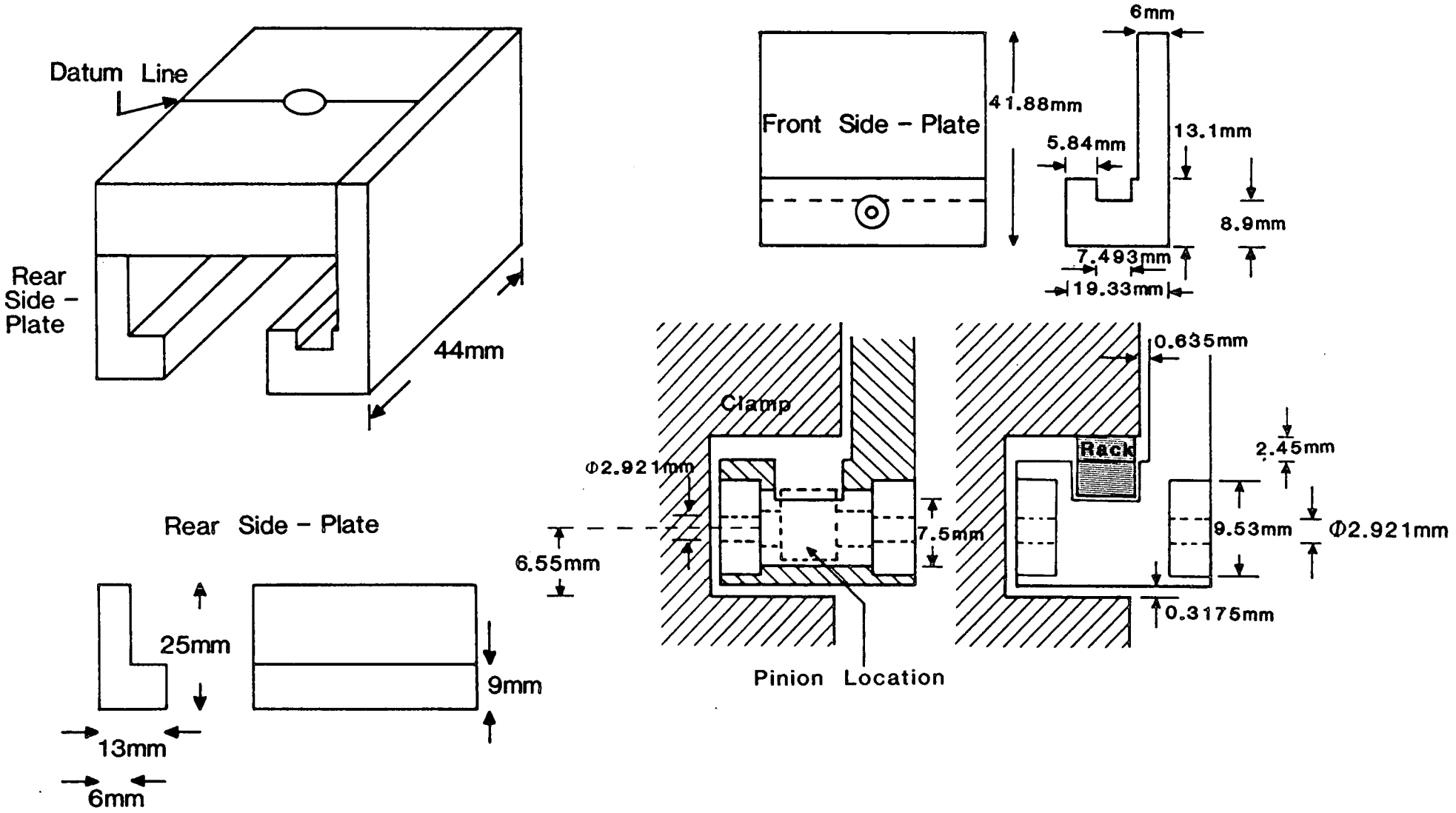

FIG. 11 Cross-Sectional View of the Carriage Side Plate.

to traverse the length of the clamp. It ran on two floating ball races with a spring leaf arrangement fitted directly behind them. That exerted a force on the pinion pushing it upwards towards the rack ensuring good contact during movement. This eliminated backlash between the rack and pinion which had at first proved to be troublesome. The pinion was mounted on two ball races and it meshed directly with the rack. A teflon sleeve insulated the thumbwheel from the carriage.

The idea of using a Radiall flange receptacle as a probe was considered to be very convenient, because not only did its shape allow to be easily formed into the required outline, it also provided direct access to the output monitoring equipment. The receptacle was the R125449 one, complete with a male SMA connector and a captive contact. It covered the required frequency range and produced a VSWR of 1.05 + 0.003f (GHz). The probe was inserted from the carriage top and was made long enough to allow its tip to protrude sufficiently into the cable slot. The probe end was turned down to 0.35 mm diameter which was adequately small so not to introduce unwanted reflections. It was turned on a lathe, machined in 1 mm stages so that the tool forces did not deflect the probe and cut into the metal.

The probe and carriage mechanism were at first designed in a slightly different manner. The probe was shaped as shown in Fig. 12 with some of the dielectric sleeve completely removed. A horizontal hole drilled through the main carriage body and rear sideplate housed a Radiall R125415 SMA female flange receptacle, with an attachment soldered on making contact with the exposed section of the probe. The detector module was then simply attached to the output connector of the receptacle. This of course allows power, or direct spectral

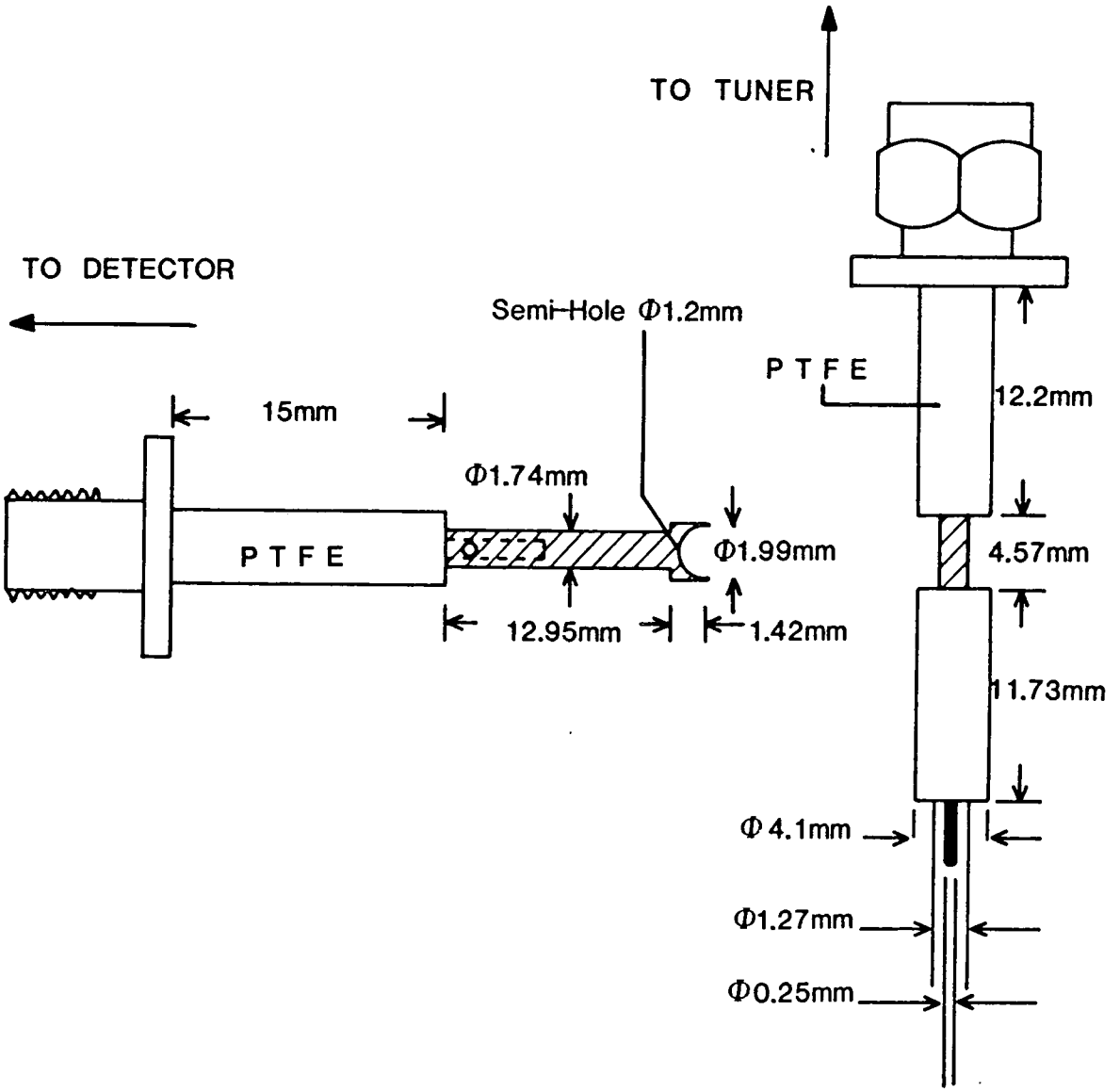

FIG. 12. A Connection Between the Probe and the Detector Module.

measurements, to be carried out by simply removing the module, while maintaining access to the probe pick-up. At a later stage however, during the course of modifications, the horizontal path was closed and the diode holder was connected to the probe output via a standard tee-junction. (R125780 F-F/m).

Another facility that was incorporated in the design was that of adjustable probe penetration and it was achieved by constructing a mechanism upon which the probe was mounted prior to being inserted in the carriage. It consisted basically of a hollow screw (Fig.13) located on the carriage top. The adjuster was made from stainless steel, as was the screw cut insert set in the top surface of the carriage. The strength and resilience of stainless steel ensured that the thread did not stretch when the locking nut was tightened. The thread pitch was 0.5 mm yielding a 0.5 mm vertical movement per one revolution of the adjuster. The top of the screw head was graduated into 10 divisions and there was also a corresponding datum line engraved on the carriage top. This arrangement ensured an effective 1.65 mm vertical probe travel accurately adjusted to within 0.05 mm.

The isolation between the clamp and the carriage was achieved with the aid of eight pads placed at the undercarriage and sideplates. Apart from maintaining electrical isolation they also contributed to eliminating mechanical"play" which could have been a major cause of erratic readings. Two pads were placed on each of the inner surfaces of the carriage sides and two more on each of the upper surfaces of the carriage side runners. Small adjusting screws made of nylon were also placed behind each pad which could be tightened depending on the degree of pad wear.

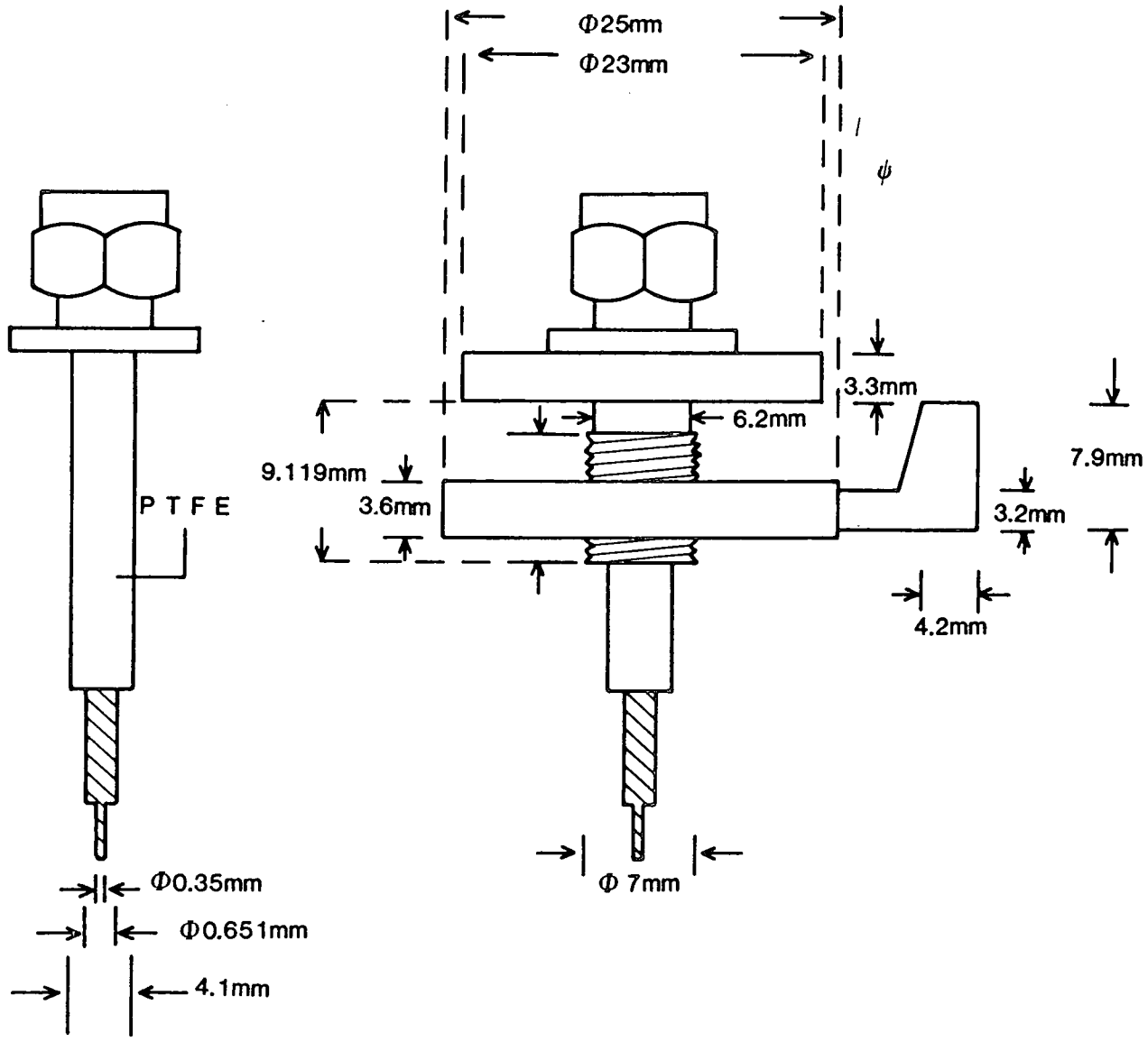

FIG.13. (a) Outline of Probe (b) The Probe Depth Adjustor Mechanism.

Finally, a perspex vernier was mounted on the carriage in such a way, that it aligned with the scale engraved on the clamp. Twenty graduations were marked in the space of nineteen millimetres giving a read-out accuracy of 0.05mm.

4.3 THE STUB TUNER

4.3.1 General Principles of Non-Contacting Plungers

One important provision which must be made for proper slotted line operation, is that the probe susceptance B_p must be kept to a minimum value for various coupling coefficients and for different frequencies.

A tuning device is therefore needed to ensure that maximum power transfer, from the probe to the detector module input, is obtained for all operating conditions. Such devices, consist simply of a section of transmission line, within which a sliding short circuit is placed, whose correct positioning will optimise the detector output.

The main advantage in employing a coaxial stub is that large tuning ratios of up to 3:1 or more, can be achieved, as opposed to a tuning range of less than 2:1 for say, a waveguide section. The reason for this being, that a coaxial line has a principal TEM mode which allows operation at frequencies much lower than those required for propagation of the higher order TE or TM modes. Such a wide tuning ratio can be achieved by introducing a short circuit at the end of the coaxial section which will "tune" a specific frequency within the range of the stub.

Before discussing the design of stub tuners a brief mention will be given of the different types of plungers that exist. [3]

PHOTOGRAPH 4 Dismantled Tuner and Detector Module Assembly

There are basically, two distinct categories, depending on whether they are contacting or non-contacting. The simplest form of a contactking short circuit is a metal ring with spring fingers that make contact between the inner and outer conductors [15] . While a plunger of this type can prove satisfactory for applications requiring few tuning operations, it can cause serious problems in the slotted line assembly. Because the tuning device will be subjected to thousands of tuning operations, mechanical wear will almost certainly be unavoidable. This will cause uneven electrical contact, which is certain to produce erratic performance, change of frequency calibration and tuning "noise".

Non-contacting plungers on the other hand, offer none of the disadvantages, but, they are fairly difficult to construct. The plungers designed for tuning the slotted line probe are non-contacting in as much that their front sections do not make physical contact with the walls of the coaxial line. By eliminating this type of contact, the resonant properties of the plunger were maintained and with no irregular changes in impedance, frequency deviation and power loss were avoided. A small section at the back of the plunger did however make contact with the line conductors so that the plunger was kept concentric within close tolerance limits.

Two different variations of non-contacting plungers were at first considered; one was the high-low impedance type, [13] the other was the capacity-coupled design. The former is fairly simple to construct and it consists of three, one quarter wavelength long metal rings, whose dimensions comply with the high-low impedance requirements.

Two of these plungers were designed to cover the entire frequency band from 1-18 GHz. The first one operated from 1-10 GHz and the

second from 9-18 GHz. Although these two plungers and their respective stubs did tune the probe over the entire frequency range, it was felt that better performance could be achieved by the use of the capacity-coupled type. For best results it was decided to have three different sized plungers with their respective stubs, so that the frequency range could be covered in three wide band steps of 3:1, 3:1 and 2:1 tuning ratios respectively.

Designing such plungers [9], calls for a number of factors to be considered. The electrical length should be kept as short as is practically possible, so that the internal power loss at the high frequency end of the tuning range is reduced. Also, the rear cavity leakage loss should be less than the internal loss by some reasonable factor of about 10:1. It is therefore good practice to choose the value of the gap-impedance ratio m so that the rear cavity leakage reduced to 1/10 the value of the internal leakage resistance at the low frequency end of the tuning range.

4.3.2 Design of Capacity-Coupled Plungers

A cross-section of a capacity-coupled plunger is shown in Fig.14a and Fig. 14b. For the first two, operating on 3:1 ratio the design length ℓ is such that the electrical length θ varies from 40 to 120 degrees. For the other, being of a 2:1 tuning ratio, the length ℓ of the sections is such that θ varies from 45 to 90 degrees. These may be considered as optimum design ranges.

Eqn. 4.1 gives an approximation of the plunger resistance of the wavelength λ_ℓ at the lowest frequency of the tuning range [9]

$$r_{p\ell} \simeq \frac{231 \times 10^{-6}}{\sqrt{\lambda_\ell}} \left[1 + 0.72 d_\ell\right] \qquad (4.1)$$

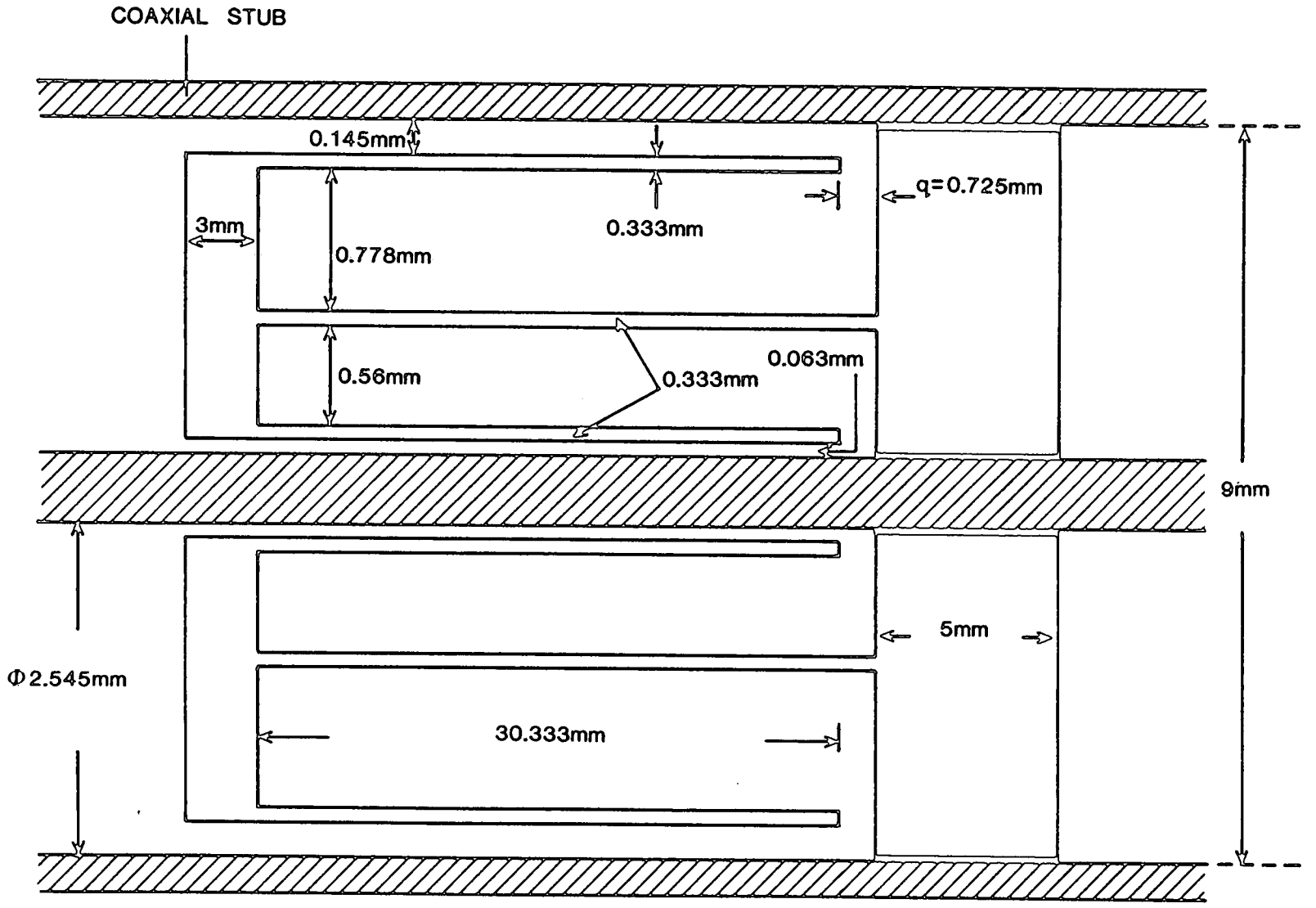

FIG. 14a Capacitively - Coupled Plunger for the 1 to3 GHz Stub Tuner.

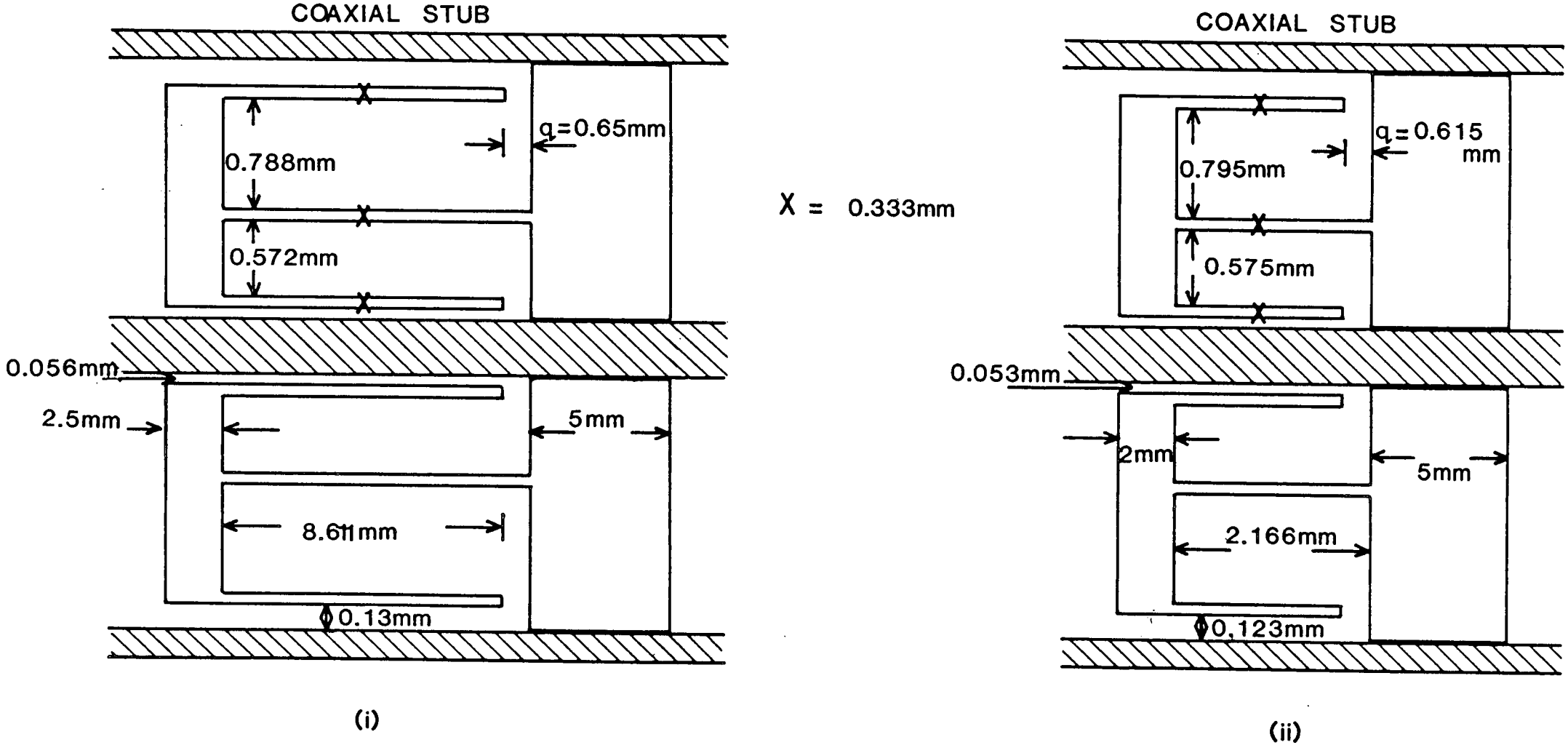

FIG. 14 (b) Capacitively Coupled Plungers for (i) 3 to 9 GHz Stub Tuner (ii) 9 to 18 GHz Stub Tuner.

where

$r_{p\ell}$ = plunger resistance of lowest frequency

d_ℓ is a dimensional parameter defined as

$$d_\ell = \frac{\ell}{\ell n(b/a)} \left(\frac{1}{a} + \frac{1}{b} \right) \tag{4.2}$$

The value of the gap-impedance ratio m necessary to make the leakage resistance equal or less than 1/10 of the internal resistance can be obtained from the following equations derived in [9].

For a 2:1 tuning ratio

$$m \simeq 0.5 + 14.5 \left[\frac{1+0.72d_\ell}{\sqrt{\lambda_\ell}} \right]^{-1/4} \tag{4.3}$$

and for a 3:1 tuning ratio

$$m \simeq 0.71 + 17.32 \left[\frac{1+0.72d_\ell}{\sqrt{\lambda_\ell}} \right]^{-1/4} \tag{4.4}$$

The three plungers were designed to operate from 1 - 3 GHz, 3 - 9 GHz and 9 - 18 GHz respectively. Consequently, the wavelengths varied from 30 - 10 cm, 10 - 3.333 cm and 3.333 - 1.667 cm.

For the 3:1 tuning ratio with $\theta = 40^{o}$ or $\lambda/9$, where λ is the longest wavelength, the length of the plungers are

$$\ell_1 = \frac{30}{9} = 3.333 \text{ cm} \quad \text{for the first range}$$

$$\ell_2 = \frac{10}{9} = 1.111 \text{ cm} \quad \text{for the second range}$$

and for the 2:1 tuning ratio with $\theta = 45^{o}$ or $\lambda/8$, where λ is the longest wavelength, the length of the plunger is

$$\ell_3 = \frac{3.333}{8} = 0.417 \text{ cm} \quad \text{for the third range}$$

Solving eqn. 4.2 yields values for d_{ℓ_1}, d_{ℓ_2}, and d_{ℓ_3}, which are the geometrical parameters for the first, second and third plunger respectively. Similarly values for m_1, m_2, and m_3 can be obtained by solving eqn. 4.3 and eqn. 4.4.

The coaxial line stubs have a characteristic impedance of 50 Ω Therefore, the impedance of the gaps (Fig. 14) between the plungers and the inner and outer conductors should not be greater than $Z_g = Z_o/(2m)$.

The gap spacing t, which is considered to be much smaller than the mean circumference r is related to Z_g and r as follows: ref.[9]

$$Z_g = \frac{\eta t}{r} \qquad (4.5)$$

where η = intrinsic impedance $\left(\sqrt{\mu_0/\varepsilon_0}\right)$

The gap spacings denoted as t_a and t_b refer to the spacings between the plunger and the inner and outer conductor respectively.

For the three different short-circuiting plungers the spacings were found to be from eqn. 4.5

Plunger 1	$t_{a1} = 0.06$ mm,	$t_{b1} = 0.145$ mm
Plunger 2	$t_{a2} = 0.559$ mm,	$t_{b2} = 0.13$ mm
Plunger 3	$t_{a3} = 0.06$ mm,	$t_{b3} = 0.147$ mm

Although the above derived values may be considered as the optimum design dimensions, it was decided that t_{a3} and t_{b3} respectively should be reduced even further. Even though that would make the parameter m_3 larger, it was felt that this was acceptable since the plunger in question operated on a relatively narrow tuning range of 2:1. The gap dimensions rested finally on what was mechanically achievable, bearing in mind the close tolerance requirements previously discussed. There were found to be

$$t_{a3} = 0.053 \text{ mm}, \quad t_{b3} = 0.123 \text{ mm}$$

The gap q between the folded sections and the rear part of the plungers was made approximately equal to five times the largest gap spacing for each stub. The folded sections were made as thin as was mechanically possible, with the actual dimensions given in Fig. 14a and Fig. 14b. The stub tuners were made of brass, chosen not only for its fairly high conductivity coefficient but mainly because machining can produce a very smooth, mirror like, surface.

4.3.3 Tapered Tuning Stubs

The stubs were designed to behave as 50Ω coaxial line lengths with inner and outer conductor diameters of 3.91 mm and 9.0 mm respectively. For resonant free operation the stub mean circumferance $\pi(a+b)$ should be less, or at least equal to one wavelength of the maximum frequency of 18 GHz. This however, would require a much smaller plunger design which mechanically would be an almost impossible task. Furthermore, since the chosen dimensions did allow successful operation up to 18 GHz the above condition was not obeyed.

The use of SMA connectors neccessitated the introduction of tapers to gradually reduce the stub dimensions to the required diameters while avoiding reflections and impedance changes. The formula given below applies to the general case of joining two lines of different impedance values, and the reflection coefficient introduced by the taper is obtained from [8,15]

$$\rho = \frac{\ell}{\pi} \left| \frac{\sin 2\pi\ell / \lambda}{4\ell / \lambda} \right| \ell n \frac{Z_{o2}}{Z_{o1}} \qquad (4.6)$$

where

ℓ = taper length

Z_{o1}, Z_{o2} = characteristic impedances of the two lines to be joined

The plot of Fig. 15 may be used to obtain a ratio of ℓ/λ such that the lowest possible reflection can be achieved; this was made use of in deriving the taper lengths for the three stubs.

However, eqn. 4.6 suggests that if Z_{o2} and Z_{o1} were to be equal, and provided the lines were filled with the same dielectric medium say air, then $\rho \to 0$ irrespective of the taper length. This condition was taken advantage of when designing the taper for the 1 - 3 GHz stub. The coaxial lengths on either side of the very short taper (5 mm) were both designed to give a characteristic impedance of 50 Ω (air dielectric). Taper dimensions for all three tuners are given in Fig. 16a, Fig. 16b and Fig. 16c.

4.3.4 Movement Mechanisms of Plungers

Two distinctly different mechanisms were used for the movement of the plungers. For the lowest frequency tuner the short circuit was attached to a hollow, threaded brass rod as shown in Fig. 17. This rod did not come into contact with neither the inner nor the outer conductor, and was sufficiently long to permit full vertical movement of the plunger. The inner conductor was secured by fitting a metal plug at the top of the stub and was held in place by a metal pin running horizontally through it and the conductors. To overcome the problem of the pin preventing the free run of the threaded rod

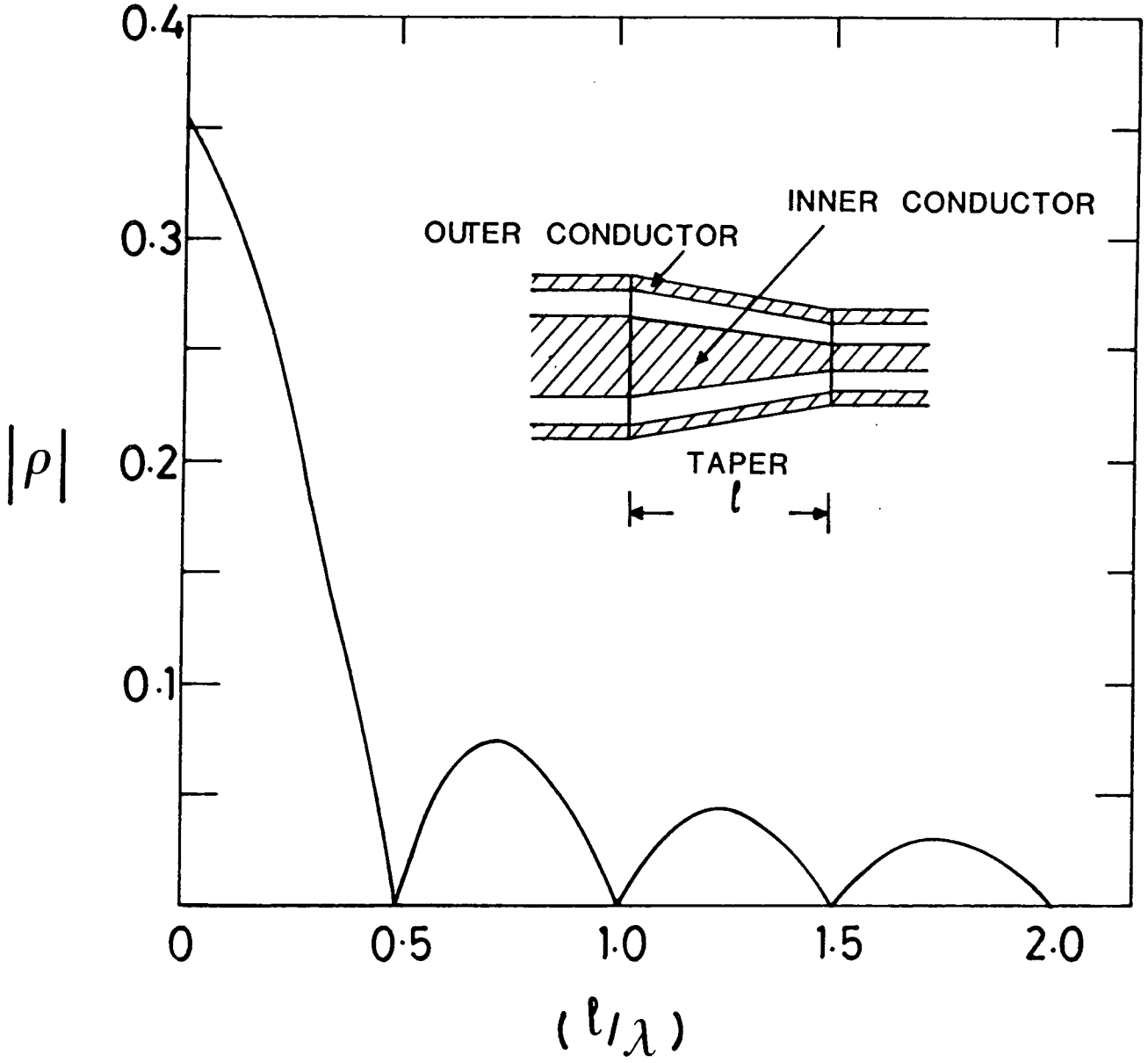

FIG. 15. Variations of the Reflection Coefficient $|\rho|$ with Taper Length $\left[\frac{Z_{02}}{Z_{01}} = 2\right]$

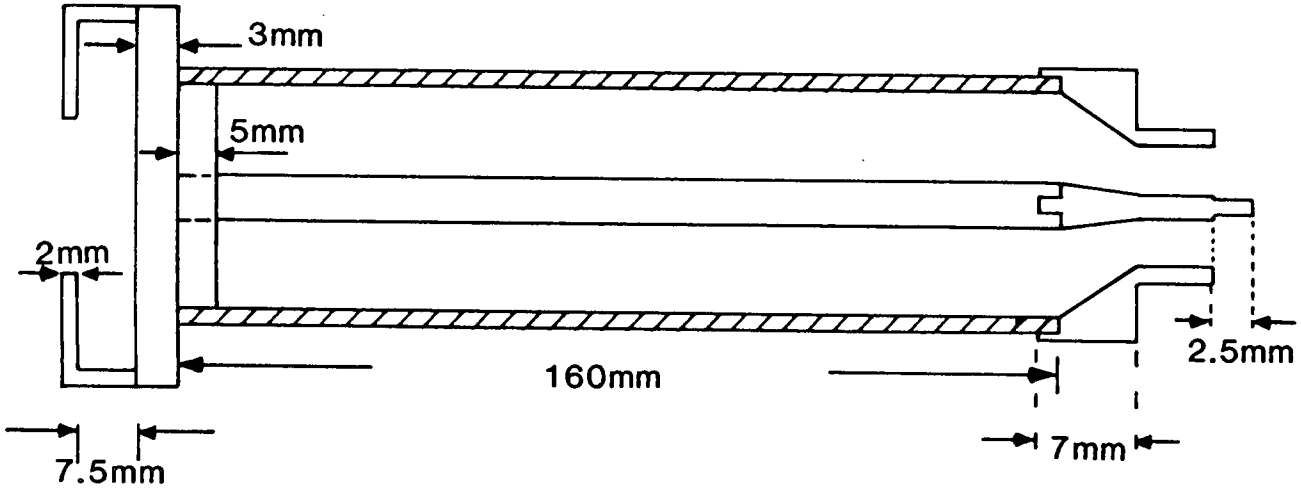

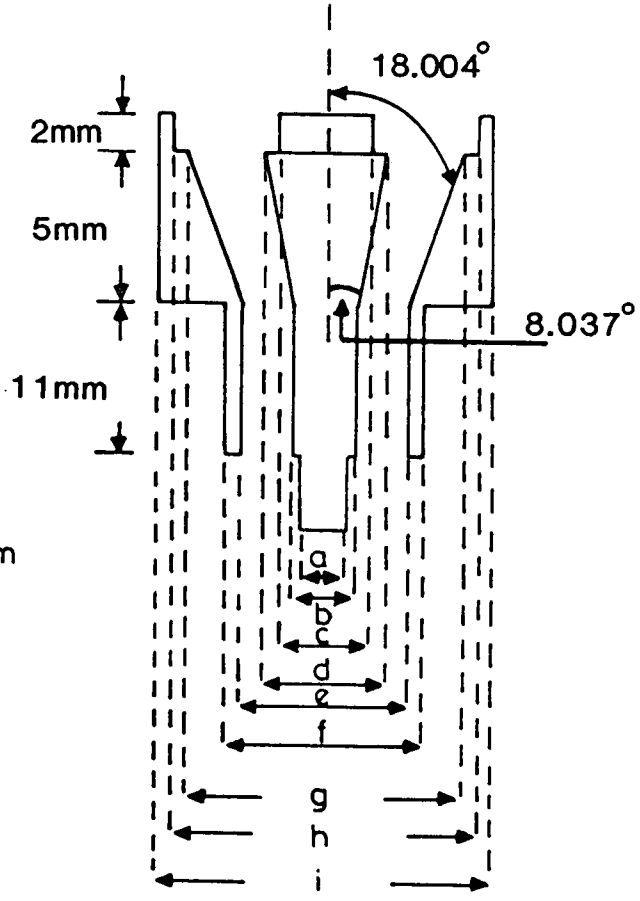

a = 1·62 mm
b = 2·5
c = 2·794
d = 3·91
e = 5·75
f = 6·37
g = 9·0
h = 11·0
i = 12·0

FIG. 16(a) 1 to 3GHz Tapered Stub Tuner.

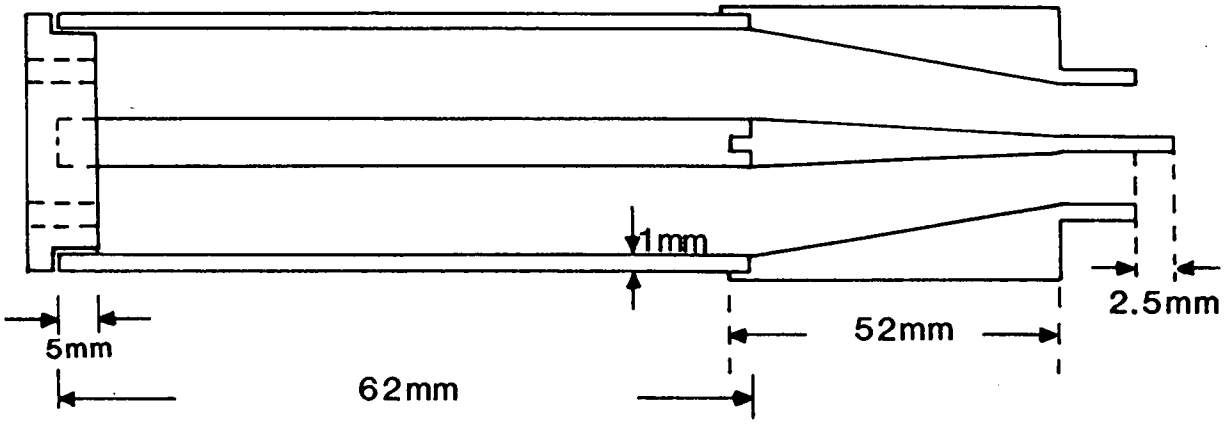

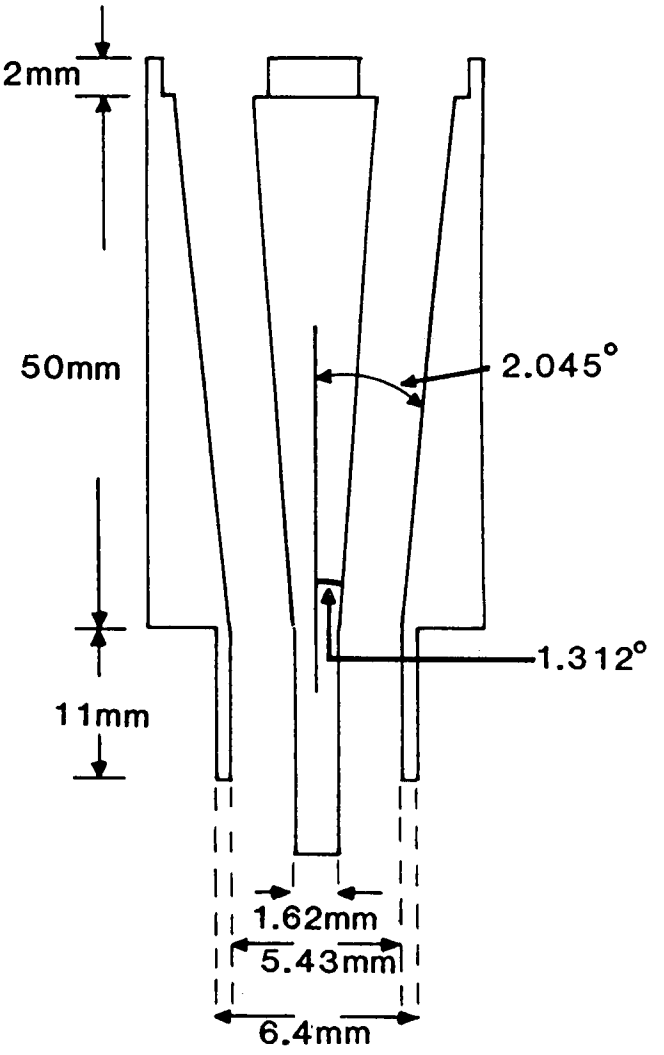

FIG. 16.(b) 3 to 9 GHz Tapered Stub Tuner.

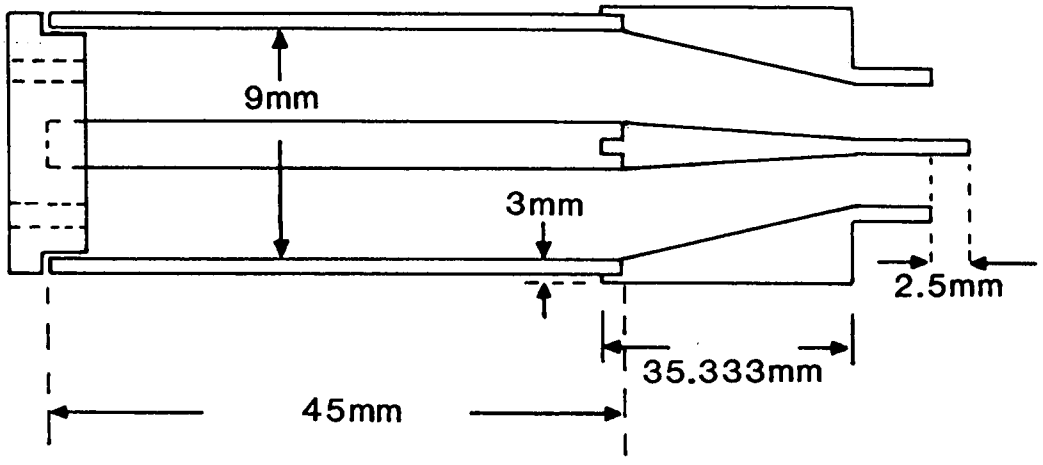

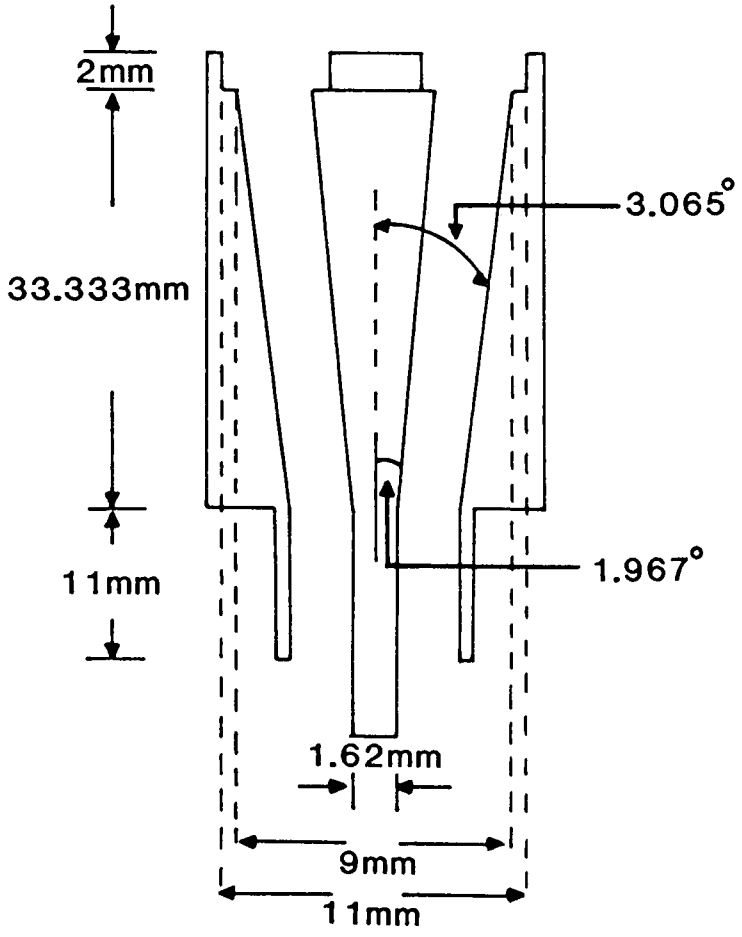

FIG. 16 (c) 9 to 18 GHz Tapered Stub Tuner

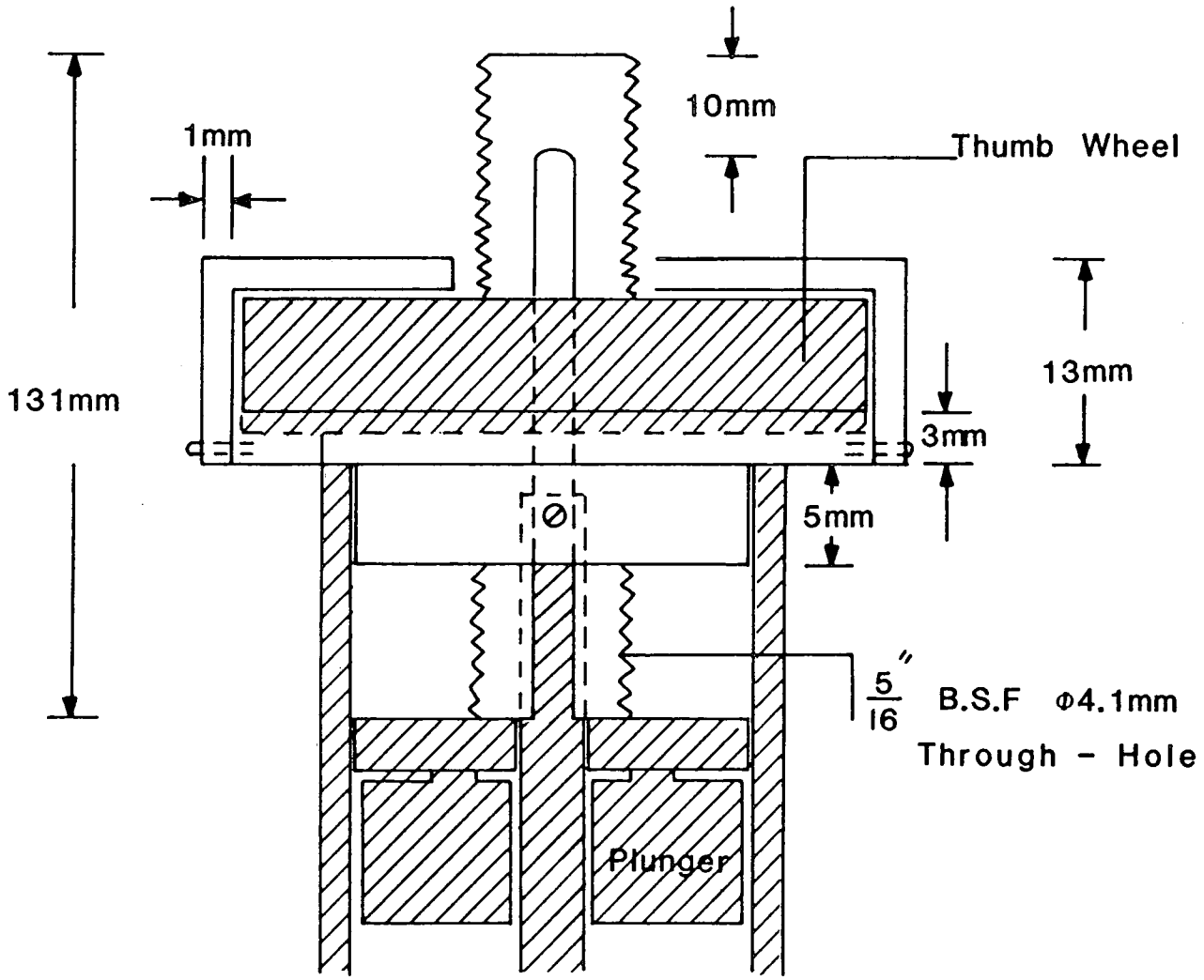

FIG. 17. Movement Mechanism of the 1to3GHz Plunger.

the latter was slotted lengthwise on either side enabling it to clear the pin. The short circuit movement was achieved by simply turning a thumb-wheel firmly secured by a collar which was part of the metal plug.

For the other two tuners a different arrangement was used, shown in Fig. 18. As before, the inner conductor was held rigid by fitting a tapped metal plug at the top of the stub. It was then hollowed out providing sufficient clearing for a threaded rod to be allowed to move within it. The top end of the rod was attached to a knurled thumbwheel which, when turned, raised and lowered the rod accordingly. The plunger was in turn attached, via two thin rods to a metal plug. This plug was made to move with the thumbwheel as follows. A long thin cap was machined so that its top end formed a collar. This was then placed over the thumbwheel and was fastened to the plunger plug with two screws. So, when the knob was turned the cap and subsequently the short circuit were forced to stay with it as the threaded rod moved in and out of the inner conductor.

4.4 THE DETECTOR MODULE

The power absorbed by the probe will ultimately cause a deflection of a meter or a scope trace. One way of achieving this is by converting the microwave signal to d-c, or low frequency, which can then be measured by conventional methods. Non-linear elements such as diodes can be used as rectifiers or frequency convertors, and the whole detecting arrangement need only consists of a crystal detector, followed by a narrow-band amplifier tuned to the modulating frequency.

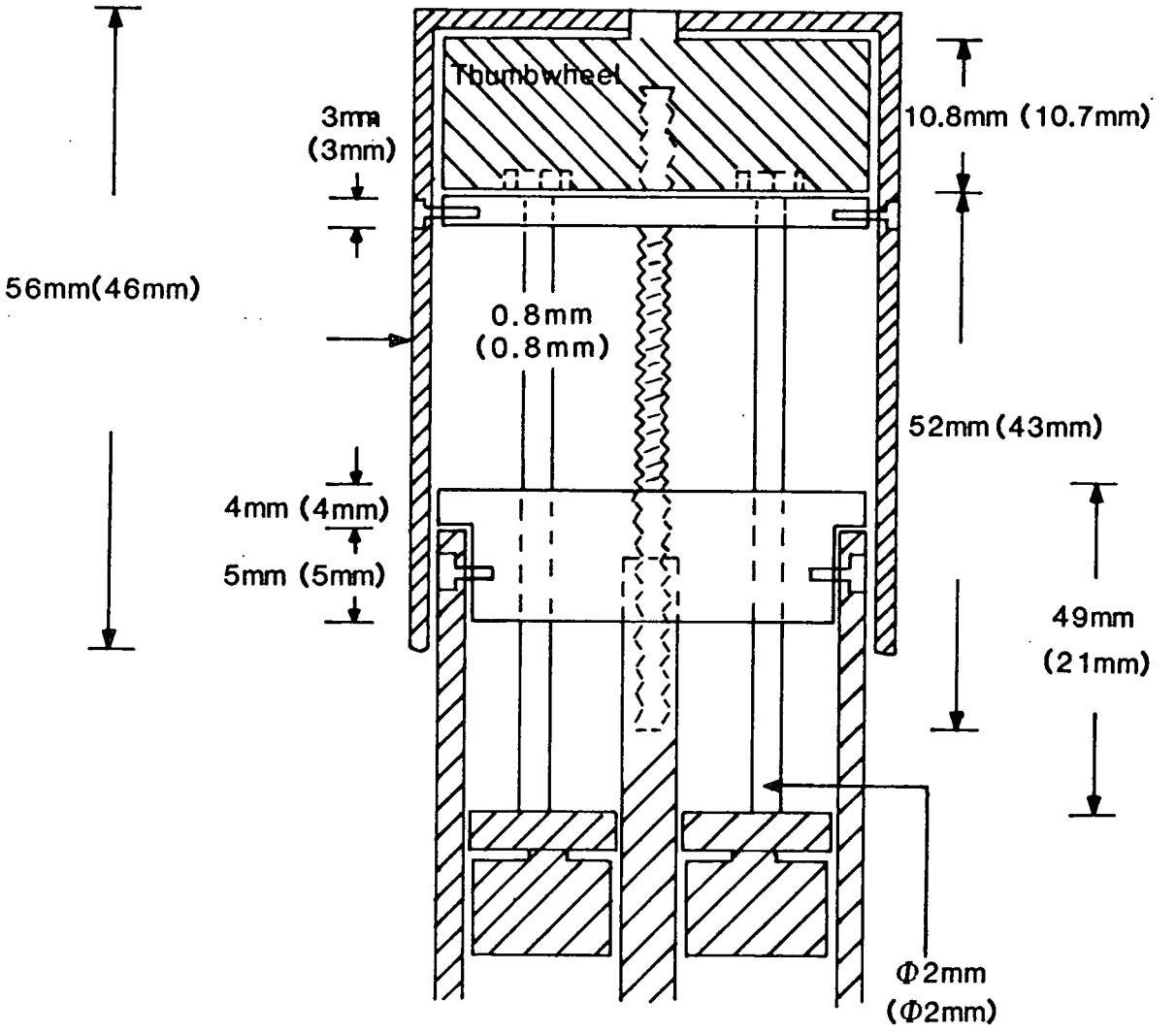

FIG.18. Movement Mechanism of the 3 to 9 GHz and (9 to 18 GHz) Plungers.

The modern crystal detector is the most sensitive and the simplest of all rectifying devices. It consists of a fine wire carefully pointed and brought to contact with the semi-conductor which is usually silicon or germanium. By controlling the pressure against the semi-conductor, the area of contact is adjusted to the desired value. This determines the resistance of the barrier contact, its capacity, as well as the power handling ability of the device. When a high frequency signal is applied to the diode a d-c current will appear in the load circuit. The magnitude of the current depends upon the device characteristics such as r-f source impedance and the d.c. load impedance. The diode can be simply considered as a current generator with a certain dynamic impedance.

For the slotted line application, a J-band detector diode (DC 1535) was purchased from M.E.D.L. A silicon Schottky barrier type was chosen mainly for its mechanical and electrical ruggedness, highest output voltage, and best tangential sensitivity. It provides a high burn out level (200 mW CW, 400 mW peak) and has the additional advantage of producing a low video resistance (200 Ω at 150 μA). Considering low level detector performance, this type of device realises an operational sensitivity of about -48 dbm under unbiased conditions. The diode outline and approximate dimensions are shown in the diagram of Fig. 19.

The diode was incorporated to the slotted line as a self-contained unit able to be removed when unmodulated waveforms had to be examined. For this purpose a crystal holder was designed to accommodate the detector. Its main function was to introduce the terminals of the rectifying diode into the microwave circuit, ensuring that all r-f power is absorbed by the crystal without escaping through the

output terminals.

The design of the holder was influenced mostly by the diode outline and the dimensions of the input connector. Theoretically for the module to operate properly a return path has to exist for the microwave frequencies (1 -18 GHz), while modulating frequency - usually 1 KHz - is allowed to pass through the diode. (Fig. 20). This was achieved by placing a capacitor in shunt between the diode and the holder's wall and the return path was completed by the stub tuner being connected in parallel with the module. The capacitance per unit length was obtained from

$$\frac{C}{\ell} = \frac{24.2 \times \varepsilon_r}{\log \frac{b}{a}} \qquad \left[F/m \right] \qquad (4.7)$$

where the symbols have their previously defined meanings.

The capacitance was obtained mechanically as follows: a tight-fitting, 7.0 mm wide metal ring was placed over the diode body, effectively increasing its diameter to 9.0 mm. A narrow gap of approximately 0.0254 mm was created between the module wall and the outer surface of the metal ring. A thin film of mica was then inserted in the circular gap and the by-pass capacitance was obtained according to eqn. (4.7).

The impedance at high frequencies (GHz) as well as at low frequencies (KHz) can be calculated from the following relationship

$$X = \frac{1}{2\pi f C} \quad (\Omega) \qquad (4.8)$$

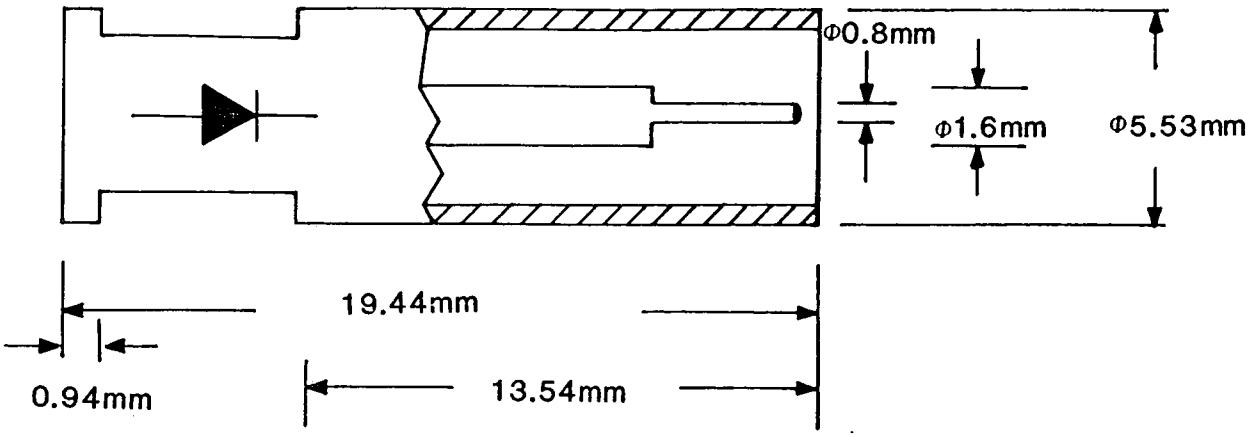

FIG.19 Detector Diode Outline.

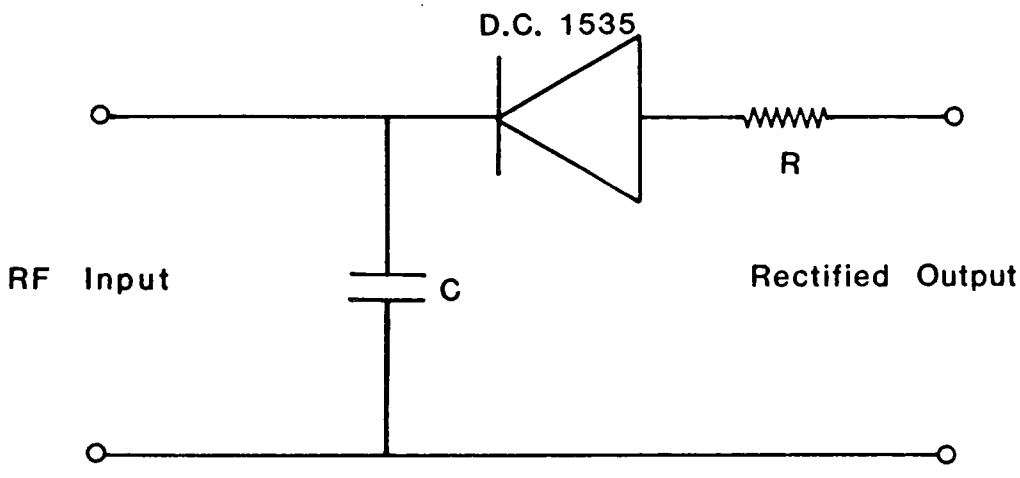

FIG.20 Circuit Diagram of the Detector Module.

It can be seen that at microwaves, the gap is presenting an almost negligible impedance - i.e. a near short-circuit condition - while at low frequencies the impedance is extremely high, resembling an open circuit.

A cross-section of the detector module including relevant dimensions is presented in Fig. 21. It was machined out of brass and it consisted of two cylindrical parts with the adjoined ends threaded. When the two halves were brought together, the metal ring and the mica film were held firmly into position w.r.t. the rectifying crystal. A Radiall SMA connector (R125056) was fitted at the holder input, while its output was turned down to dimensions similar to those of an SMA-Jack connector carrying the detected signal to the measuring instrument.

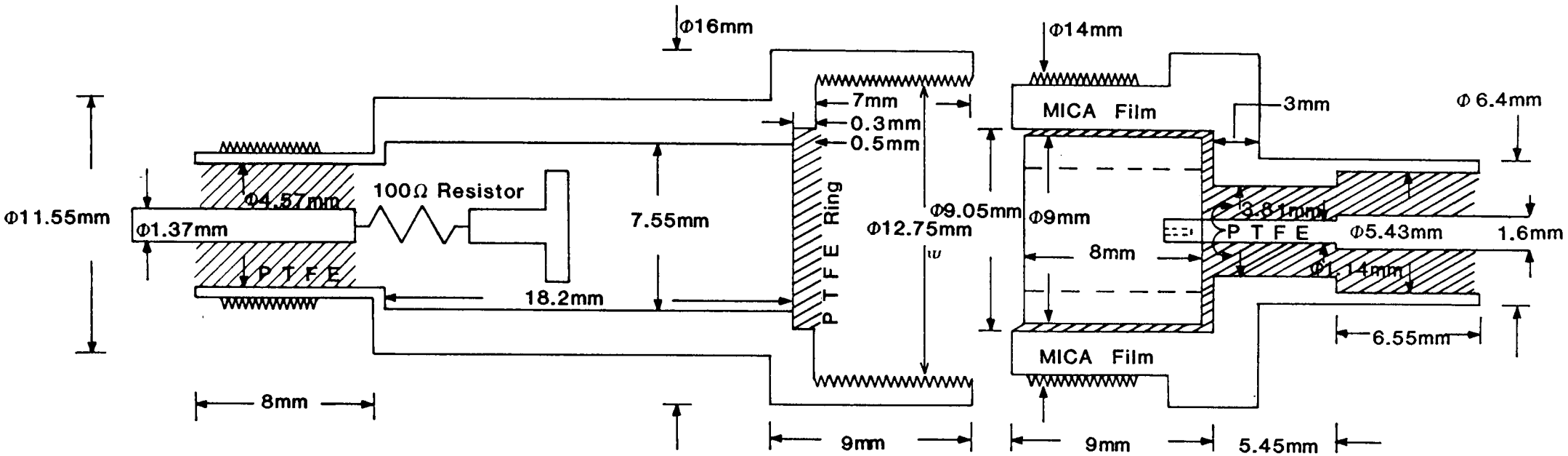

FIG. 21 Cross - Sectional View of the Detector Module.

CHAPTER 5

ELECTRICAL MEASUREMENTS AND PERFORMANCE

5.1 WAVELENGTH CORRECTION FACTOR

On completion of the slotted line design and construction, various tests were carried out to establish the quality of its performance.

Wavelength, was the first quality to be measured. Since the cable was slotted and a trough cut out for the probe measured meant that it was no longer completely dielectric filled. On investigation it was confirmed that as a consequence the relationship $f = c/(\lambda\sqrt{\varepsilon_r})$ no longer applied unless a correction factor was introduced. This factor was determined approximately using the precision of high quality instrumentation. The frequency of the generator was accurately set to the desired value by calibrating it against the spectrum analyser. The slotted line was then connected to the source output via a 6dB attenuator so that any possible mismatches were eliminated. With the line terminated in a short circuit a number of standing wave minima were located along it and their positions recorded. Having measured the wavelength at the set frequency, simple substitution yielded the value for the correction factor, x_c, from the following relationship

$$f = \frac{c}{\lambda'\sqrt{\varepsilon_r}} \quad x_c$$

where $\lambda = \frac{\lambda'}{x_c}$

OR

$$x_c = \frac{f\,\lambda'}{c}\sqrt{\varepsilon}_r \qquad (5.1)$$

where

λ' = slotted line wavelength

ε_r = relative permittivity of cable dielectric (PTFE)

For better accuracy it was decided to carry out the above measurements initially at low frequency since the corresponding wavelength would then be large enough to minimise errors in establishing precisely the minima positions along the line. The frequency of 2GHz was chosen, and the procedure was repeated at least three times so that the average reading could be obtained. Measurements were then made at selected frequencies up to 18 GHz. It was found that the value of $x_c = 1.050$ approximately applied over the range. By combining x_c, $\sqrt{\varepsilon_r}$, and c, eqn. 5.1 can be given as

$$f = \frac{2.174 \times 10^8}{\lambda'} \quad \text{(Hz)} \qquad (5.2)$$

for λ' in metres.

5.2 RESIDUAL VSWR (S_R) OF THE SLOTTED LINE

Another important parameter measured was the residual VSWR of the line. This is the standing wave ratio when the slotted line is terminated in a matched impedance. Although it is impossible to completely eliminate residual VSWR, it can be, with some care, reduced to acceptable values. It is mainly caused by changes in the characteristic impedance. These in turn may be due to the slot position and dimensional variations which, unless compensated, can create standing waves along its length.

Connector reflections is another source of residual VSWR. These can, however, be drastically reduced by carefully selecting the type of connectors to be used by ensuring that they are of low loss and of high quality. It is generally accepted that the above-mentioned imperfections could introduce a residual VSWR which may be considered as a single lumped discontinuity, since the reflections that are predominant in causing it are of fixed phase.

Ideally it should be determined by terminating the line in a perfect, reflectionless, matching load. Such perfect termination does not, however, exist since even the best quality low loss load will produce some reflections. This can be overcome by employing a measurement technique which requires the slotted line to be terminated in a sliding load instead. In doing so the reflections caused by the load may be distinguished from those caused by the line. It is important to bear in mind that any discontinuities in the load connector will be combined with the residual VSWR, since only the VSWR of the load is isolated from the rest of the system. Although a variable load was not available the use of a three-stub tuner

produced similar effects.

With the three-stub tuner terminating the line, (Fig.22) the probe was tuned and its position adjusted to obtain a maximum output on the VSWR meter. This indicated that both reflections caused by the load and the line were added and in-phase creating the highest obtainable VSWR, S_{max}. Having measured this, the probe was placed at the maximum of the standing wave pattern and the stubs were adjusted to obtain this time a minimum reading on the meter. This now indicated that the load and line discontinuities were now out of phase resulting in a low VSWR value, S_{min}. The maximum and minimum reflection coefficients, ρ_{max} and ρ_{min}, were calculated from the following relationships [10]

$$\rho_{max} = \frac{S_{max} - 1}{S_{min} + 1} \tag{5.3}$$

$$\rho_{min} = \frac{S_{min} - 1}{S_{max} + 1} \tag{5.4}$$

Where ρ_{max} and ρ_{min} reflection coefficients are defined in terms of the load reflection coefficients, ρ_L and ρ_D, [10] i.e.

$$\rho_{max} = \rho_L + \rho_D \tag{5.5}$$

$$\rho_{min} = \rho_L - \rho_D \tag{5.6}$$

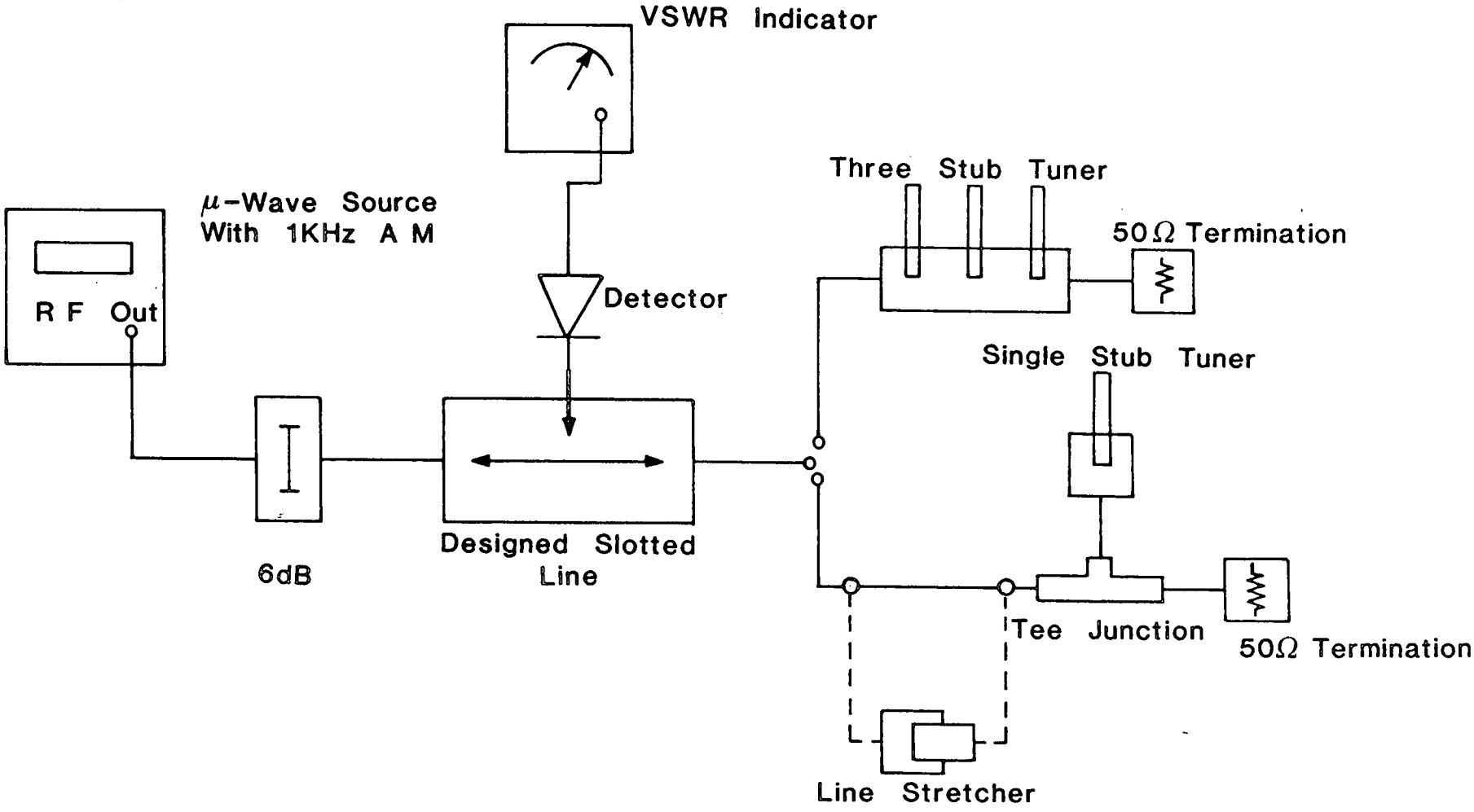

FIG. 22. Block Diagram of the Test Setup for Residual VSWR (S_R) of the Slotted Line.

resulting in

$$\rho_L = \frac{\rho_{max} + \rho_{min}}{2} \tag{5.7}$$

$$\rho_D = \frac{\rho_{max} - \rho_{min}}{2} \tag{5.8}$$

on the assumption that $\rho_L >> \rho_D$

The above method was used at frequencies of up to 12 GHz. Beyond this frequency, because of the inability of the three-stub tuner to operate consistently a slightly different approach had to be employed. The slotted line was terminated in a 50 Ω load via a tee-junction (see Fig.22). A single stub tuner was connected to the third part of the tee, and was adjusted to produce the smallest possible VSWR, S_{min}. Having done this a line stretcher was inserted between the line and the junction and was varied until a previously defined maximum was made a minimum. The value of the VSWR was then recorded and the residual VSWR, S_R, of the line, was obtained from [5]

$$S_R = 1 + \frac{[S_{min} - 1]}{2} \tag{5.9}$$

The residual VSWR, S_R, of the line was plotted against frequency and the graph is shown in Fig. 23. The values varied from 1.02 to 1.25 depending on the frequency. It should be noted, of course, that since two variables had to be adjusted during the course of the measurements, i.e. probe position and stub tuning, it was at times very difficult to accurately obtain the maximum standing wave value. This could partially explain the discrepancies observed in the graph where the residual VSWR does not seem to increase with frequency. Another explanation could be that at some frequencies the fixed discontinuities interact in such a manner that they either add or subtract and in so doing enhance or diminish the effect. The connectors used, also have a residual VSWR which varies with frequency according to the graph of Fig. 24.

Similarly, the fixed, matched, terminations not been reflectionless, produced a maximum residual VSWR of almost 1.2.

5.3 LINE ATTENUATION AND POWER LOSS CHARACTERISTICS

The semi-rigid cable had a specified attenuation of 30 db/100 ft at 10 GHz. Consequently, the amoung of power lost in the slotted line was investigated, and the attenuation A calculated from the relationship

$$A(dB) = 10 \log_{10} \frac{P_1}{P_2} \qquad (5.10)$$

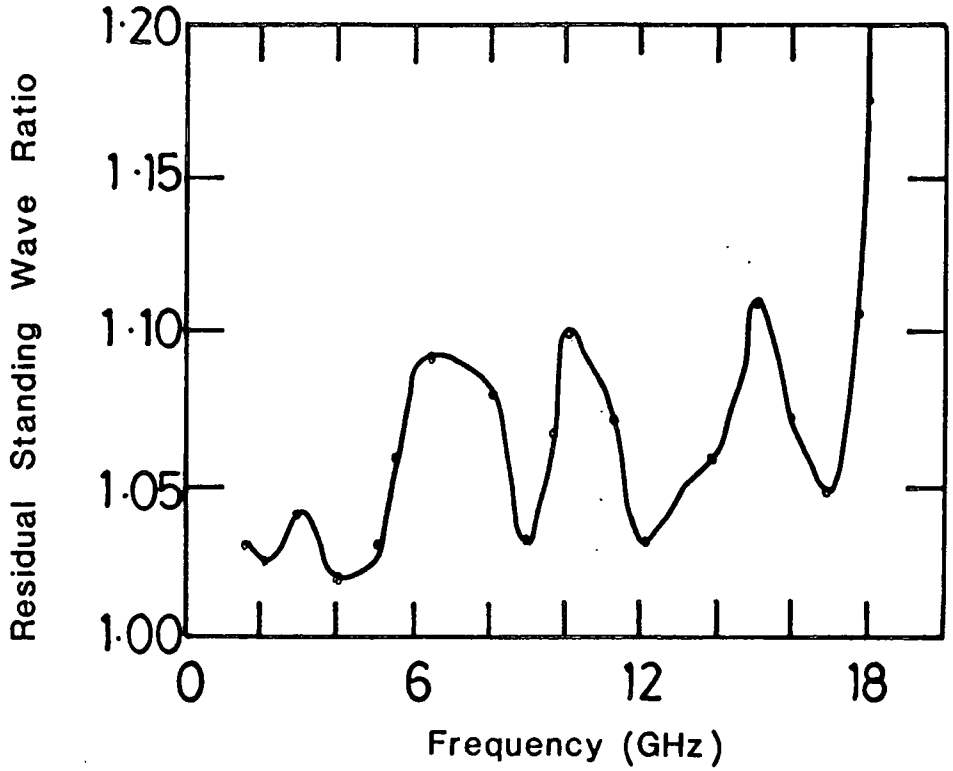

FIG.23. Residual VSWR (S_R) Variations of the Slotted Line with Frequency.

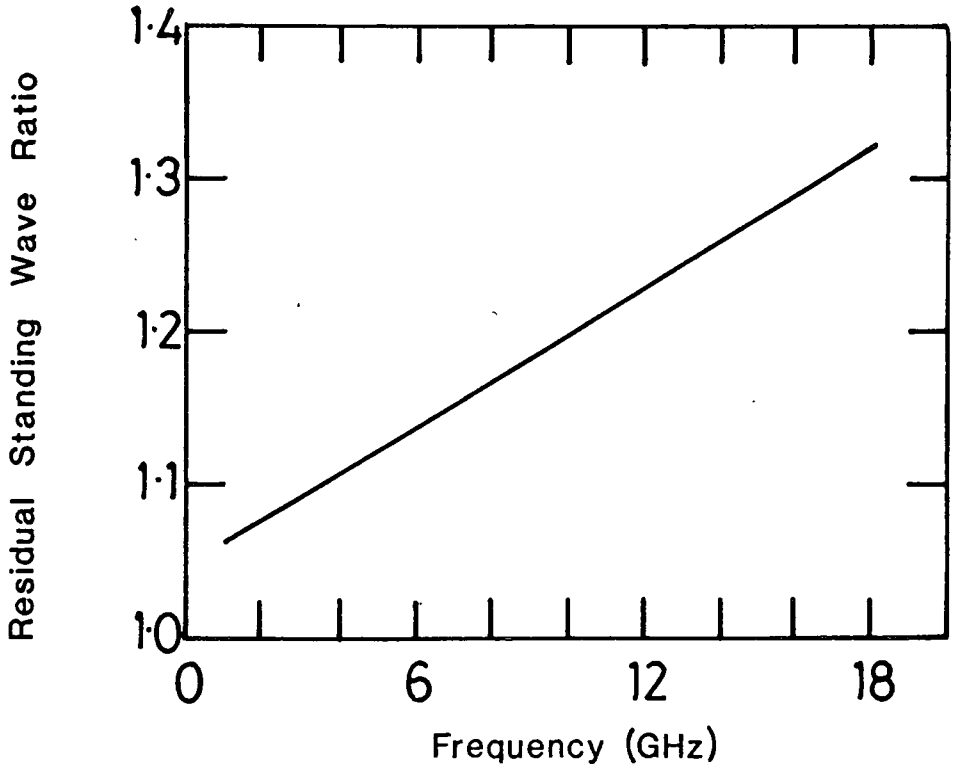

FIG.24. Specified Residual VSWR (S_R) of the SMA Conector.

where

P_1 = input power to the slotted line

P_2 = output power from the slotted line

The decrease in the level between the input and the output, expressed as a relative value in decibels was plotted against frequency shown in the graph of Fig. 25. The readings obtained were a combination of the cable loss and the loss of the two Radiall connectors. Slot radiation was another contributing factor becoming more prominent at the higher frequencies.

The rate at which a signal was attenuated, travelling through the slotted line was next examined. The attenuation constant of the slotted line under test was obtained for the frequencies between 1 and 12 GHz only, a limit dictated by the slotted line that was available for the measurement. The following method, based on transmission line theory, was used.

The attenuation constant α as mentioned in chapter 2 is a function of R, L, G and C and is usually quoted per unit length. It can be either related to the power loss of the line, or the reflection coefficients at its terminals i.e. [17]

$$\alpha = \frac{1}{2\ell} \ln \frac{P_1}{P_2} \quad \text{nepers /unit length} \tag{5.11}$$

or

$$\alpha = \frac{1}{2\ell} \ln \left| \frac{\rho_2(\ell)}{\rho_1(0)} \right| \quad \text{nepers/unit length} \tag{5.12}$$

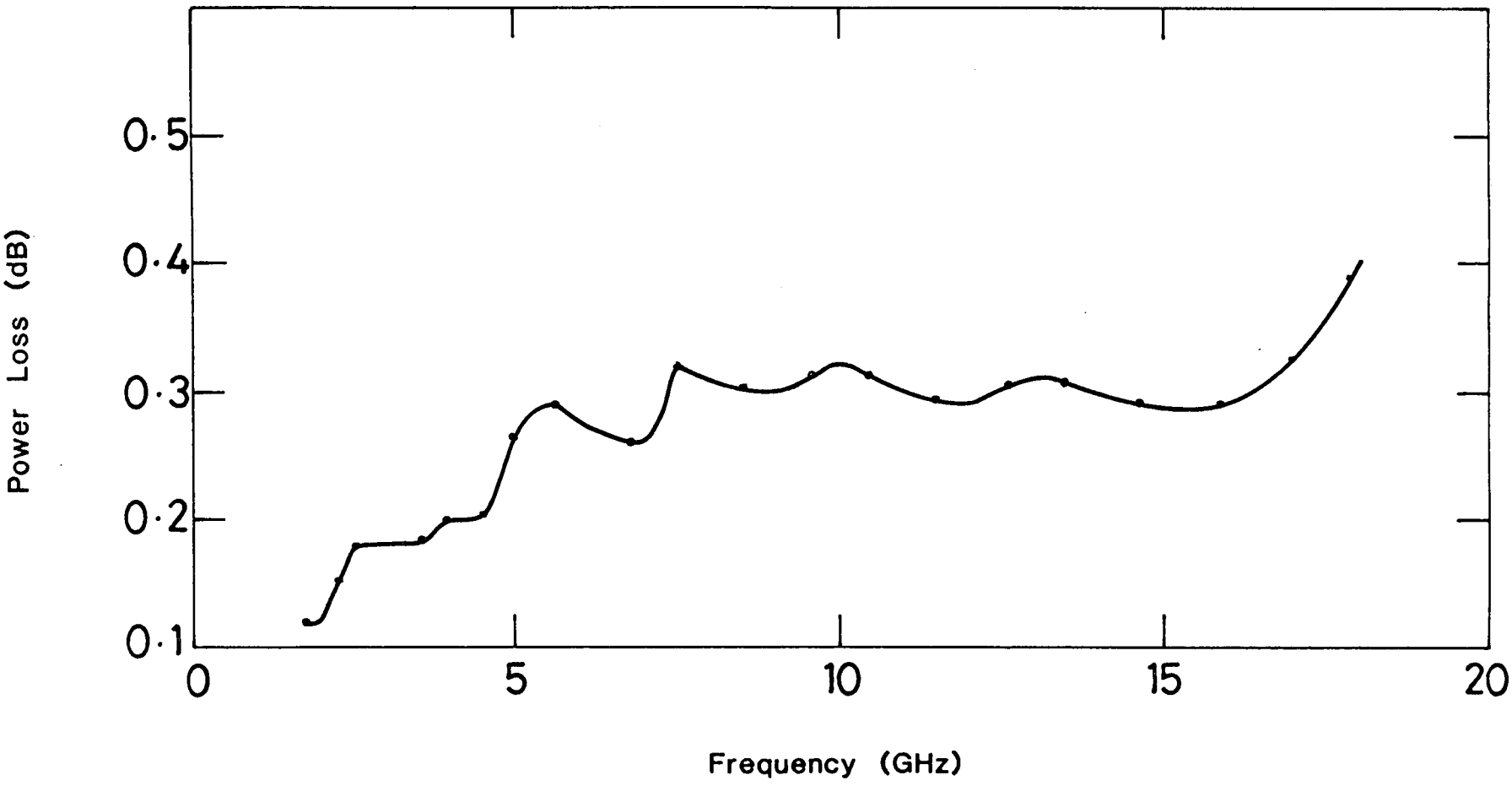

FIG. 25. Power Loss Variations of the Slotted Line with Frequency.

where

ℓ = length of the line.

It can also be expressed as a function of the VSWR i.e.

$$\alpha = \frac{1}{2\ell} \ln \left[\frac{S_2 - 1}{S_2 + 1} \right] \left[\frac{S_1 + 1}{S_1 - 1} \right] \tag{5.13}$$

where

S_1 = input VSWR at $\ell = 0$

S_2 = output VSWR at length ℓ

the above can be further simplified by terminating the line with a short circuit.(See Fig.26). This will theoretically make $S_2 \to \infty$ yielding

$$\alpha = \frac{1}{2\ell} \ln \left[\frac{S_1 + 1}{S_1 - 1} \right] \tag{5.14}$$

The variation of attenuation constant, α, with frequency is shown in Fig.27. The length ℓ of the slotted line was 36.7 cm and α was expressed in dB/m.

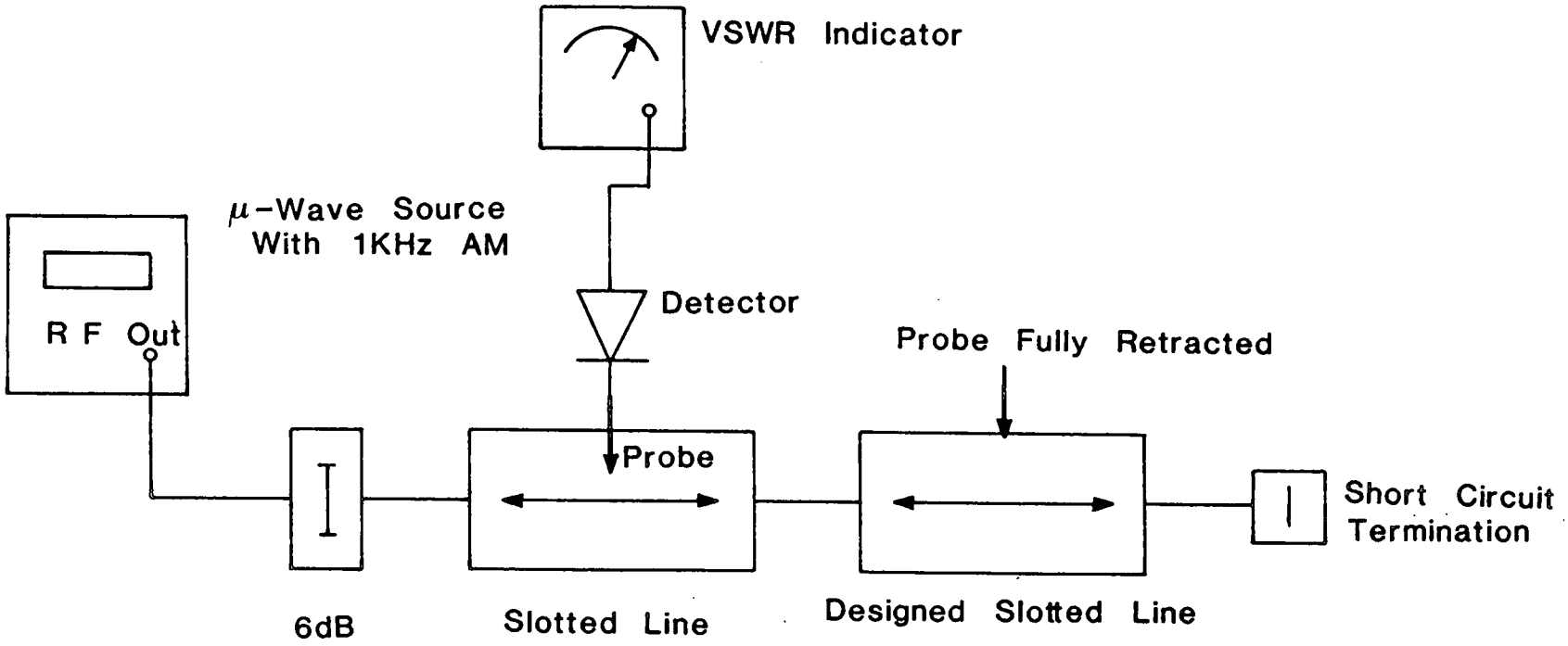

FIG. 26. Block Diagram of Equipment Setup for the Attenuation Constant (α)

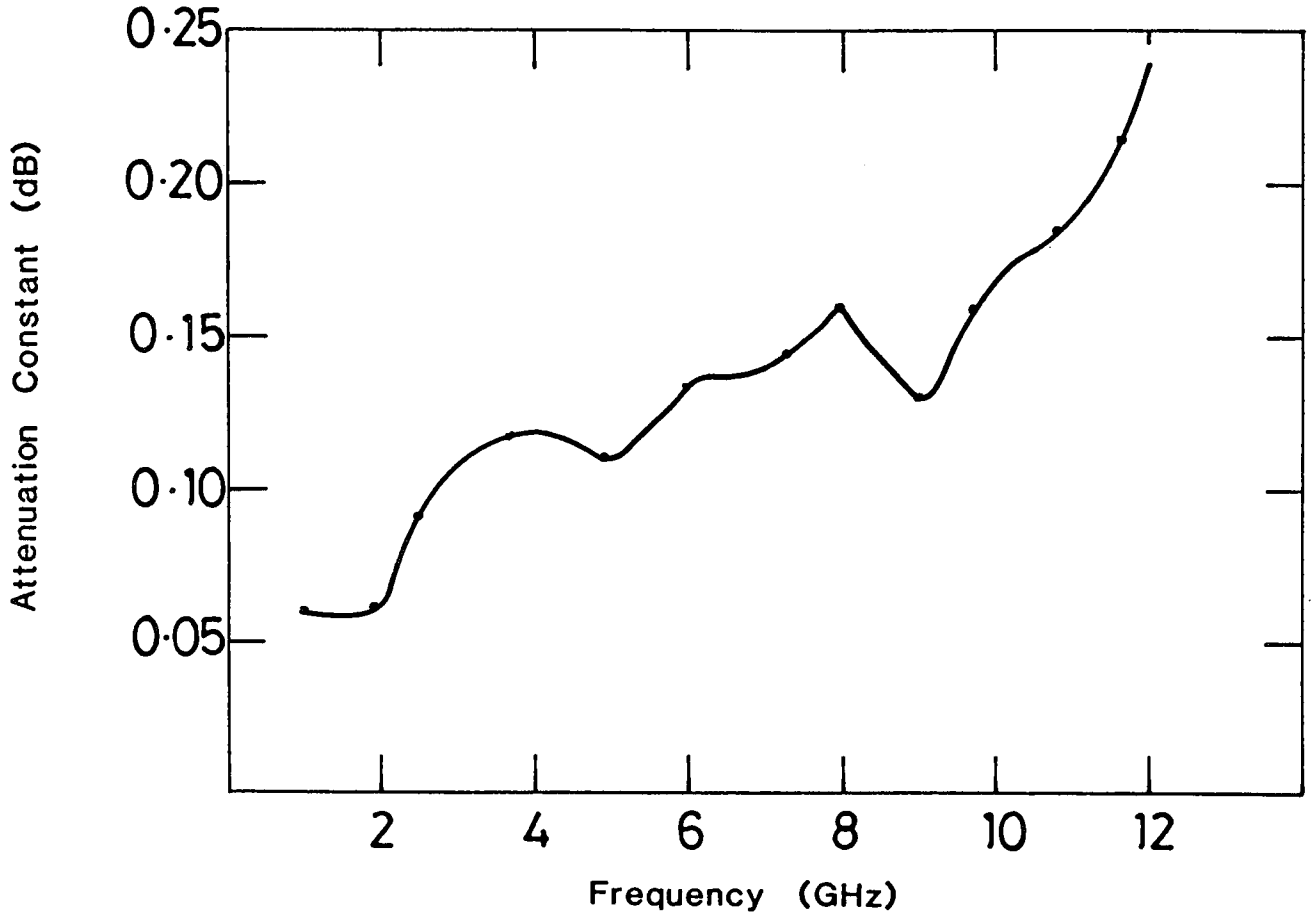

FIG. 27. Variations of the Attenuation Constant (α) of the Slotted Line with Frequency.

Tests were also carried out to determine if any irregularities in conductor concentricity, or in slot machining were present. In particular there was concern that when the slot was cut out some very small particles of the outer conductor copper shielding might have been embedded in the remaining dielectric, thus causing erroneous probe pick-up.

For the tests the type of termination was not important, and neither was the drive level nor the actual values of the electric field intensity along the line. What was important however, was that these arbitrary values, when plotted against slotted line position produced a uniform pattern. The graphs in Fig. 28, Fig. 29 and Fig.30 show the variation of maxima and minima along the line for the chosen frequencies of 4, 6 and 12 GHz respectively, while the line was terminated in 50 Ω

It should be noted that at 4 GHz the results were obtained before some minor modifications were carried out on the carriage and clamp. These involved altering the outline of the undercarriage which in consequence narrowed the clamp slot, to avoid radiation of the input signal. These modifications did not have a direct effect on the cable, and the previous results were therefore still valid. At 4 GHz intermediate readings were taken in addition to the readings at maxima and minima. This also applied to the results obtained at 12 GHz but since a lot more maxima and minima were present, purely for clarity only three sections of the slotted line were used for the measurements. At 6 GHz only the maxima and minima readings were noted. A gradual decrease in level was observed, becoming more apparent at the higher frequencies. It was not assumed to be the result of conductor non-

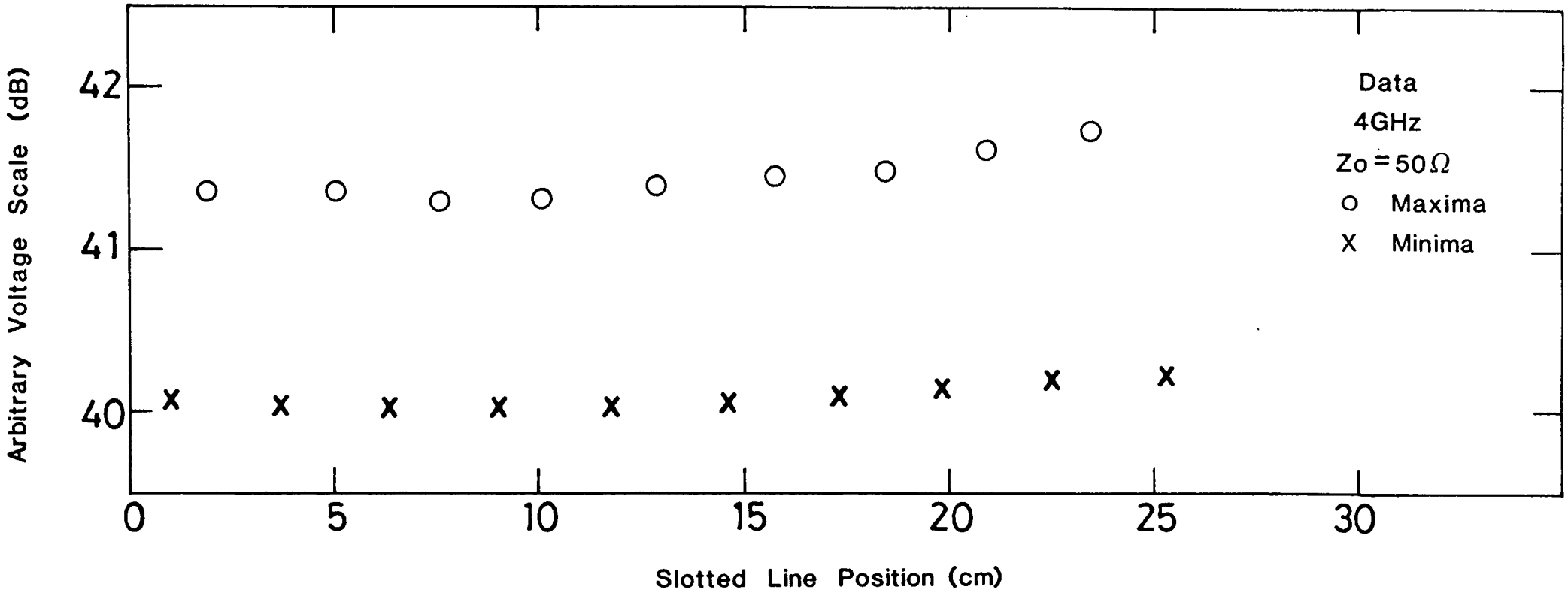

FIG.28. Variations of Maxima and Minima Along the Slotted Line.

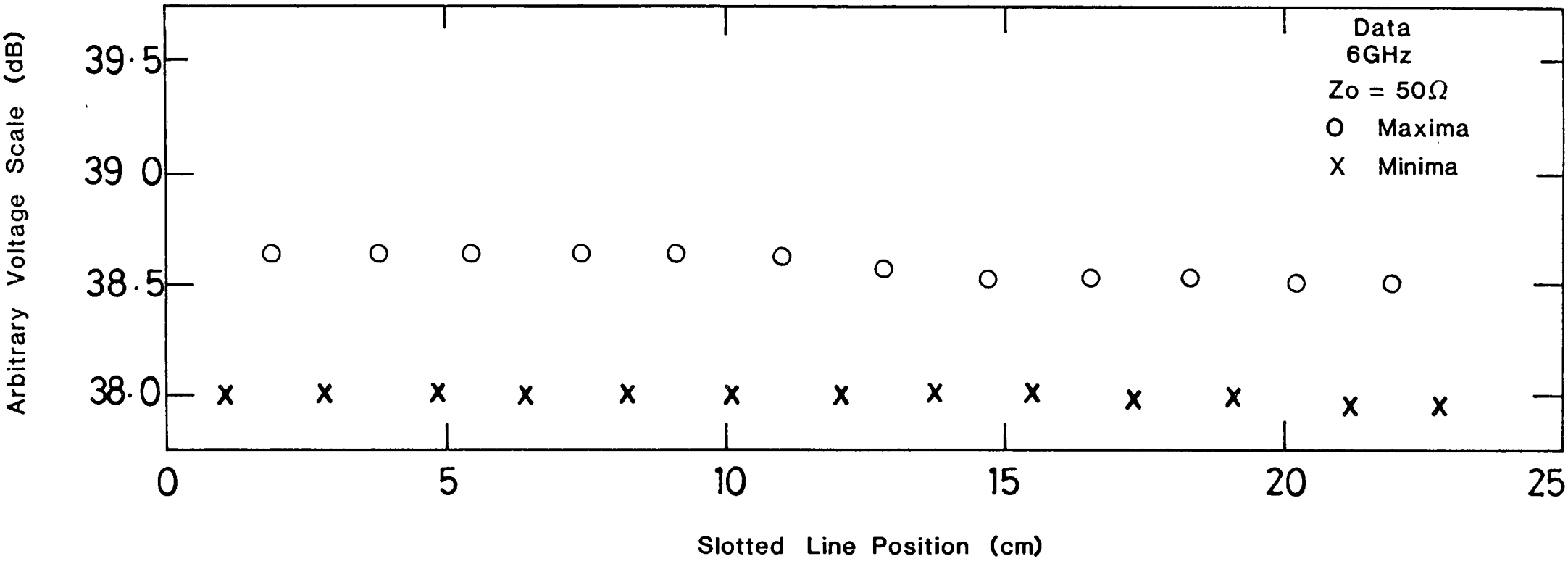

FIG. 29. Variations of Maxima and Minima Along the Slotted Line .

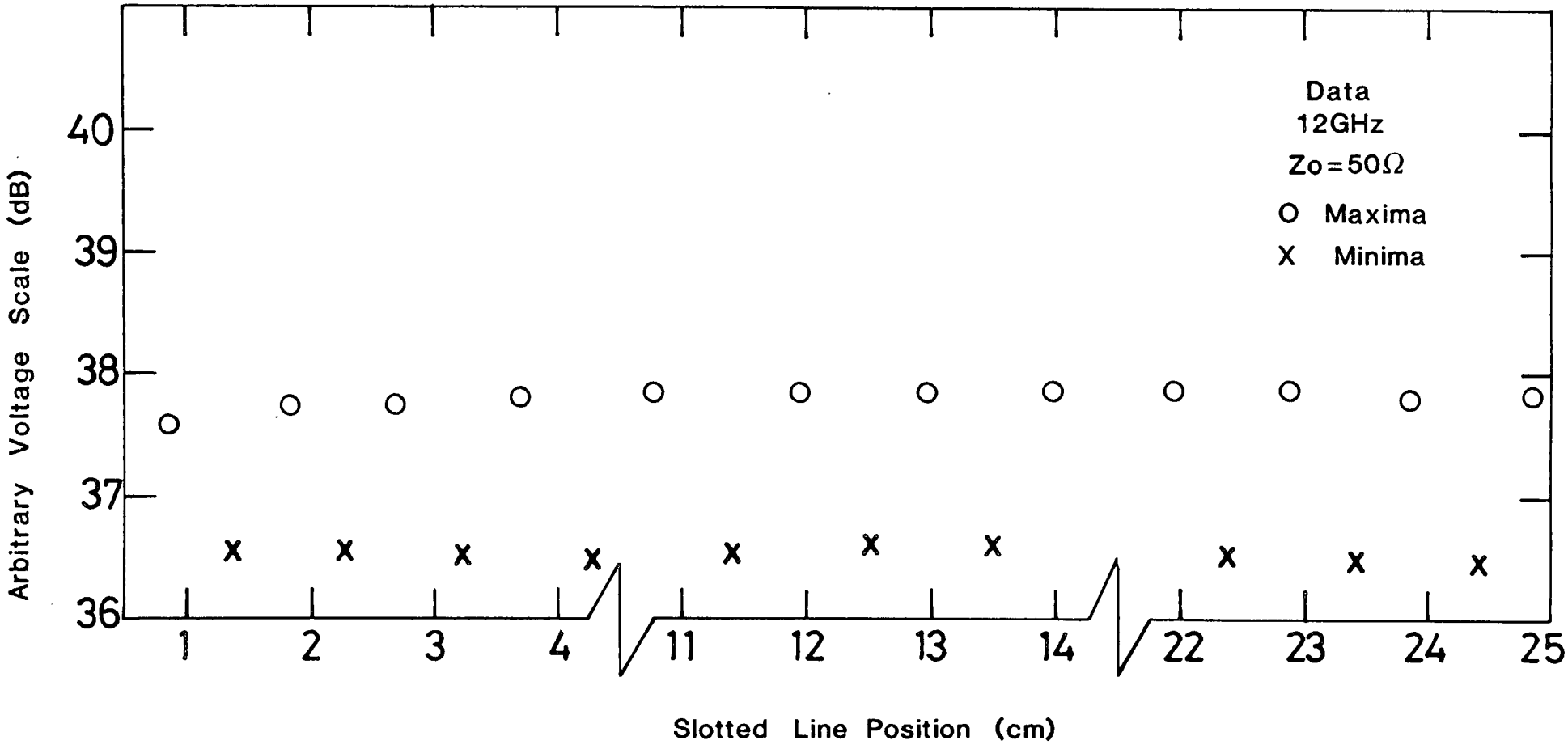

FIG. 30 Variations of Maxima and Minima with Slotted Line Position.

uniformity, but rather caused by the cable losses. This was confirmed by feeding the input signal to the output connector, and repeating the test which produced similar level variations.

The above procedure was repeated with the line terminated in a short-circuit. The reason being that the minima would now be more sensitive to any existing irregularities. The results obtained at 2 GHz and 4 GHz are shown in Fig. 31 and Fig. 32 respectively.

For comparison purposes a graph with the line open-circuited is also included. (Fig. 33).

5.4 PROBE COUPLING COEFFICIENT

The probe coupling was examined by determining the amount of power absorbed from the line. It was an important test, because it gave a direct assessment of the carriage and probe assembly designs.

For the measurement, the detector module was removed and the slotted line operated on unmodulated CW. The power at the output of the slotted line was recorded and then compared with that obtained at the probe. During the measurements (Fig.34) the slotted line was terminated in its characteristic impedance thus eliminating reflections that might have upset the true power levels. The degree of coupling (dB) was obtained from the relationship

$$k_p = 10 \log_{10} \frac{P_p}{P_L} \qquad (5.16)$$

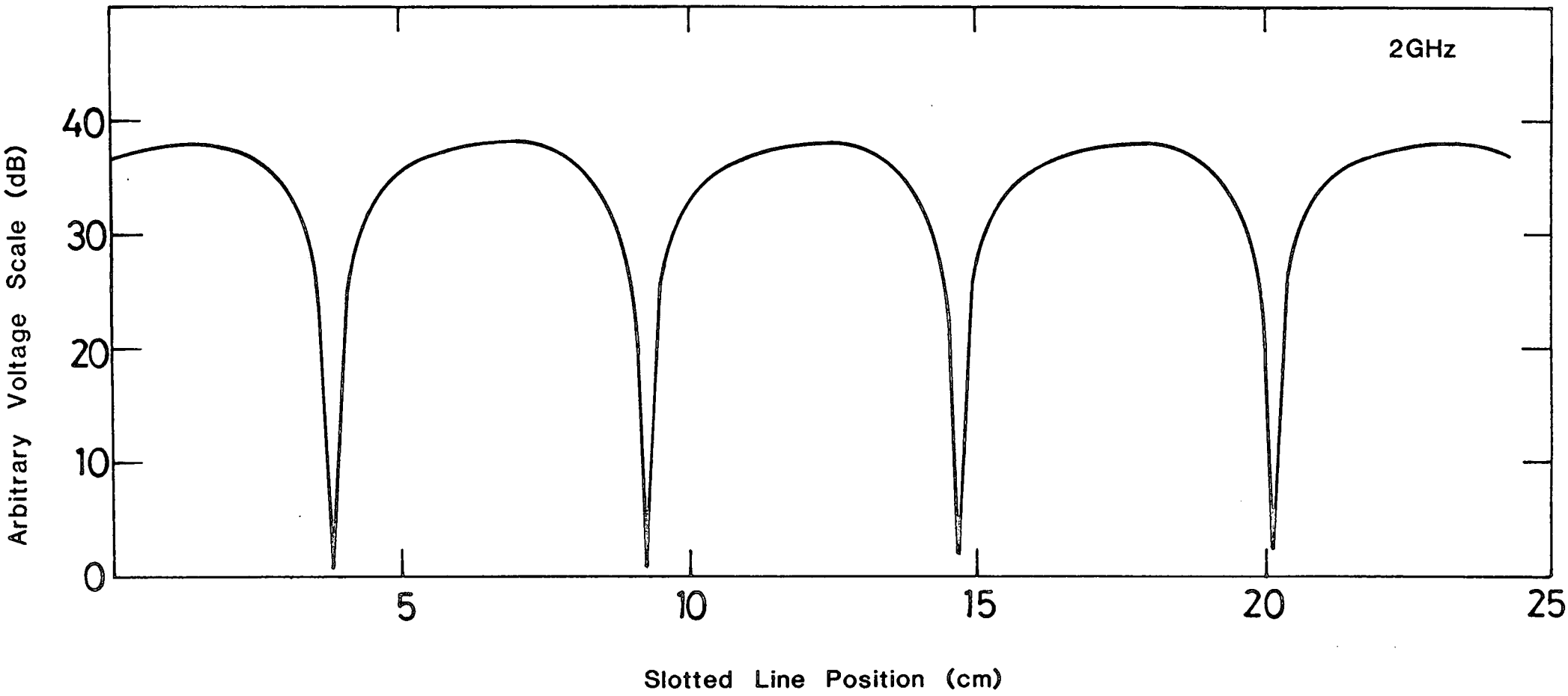

FIG. 31 Standing Wave Along the Short Circuted Slotted Line.

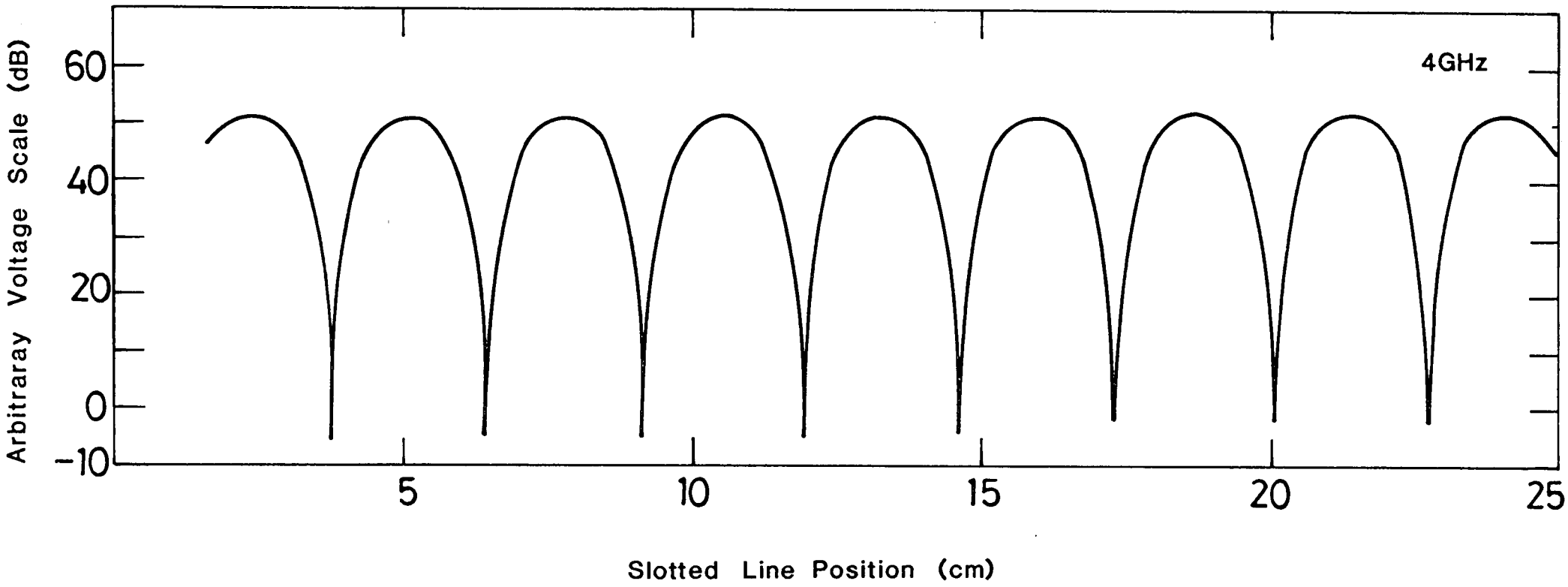

FIG. 32 Standing Wave Along the Short Circuited Slotted Line.

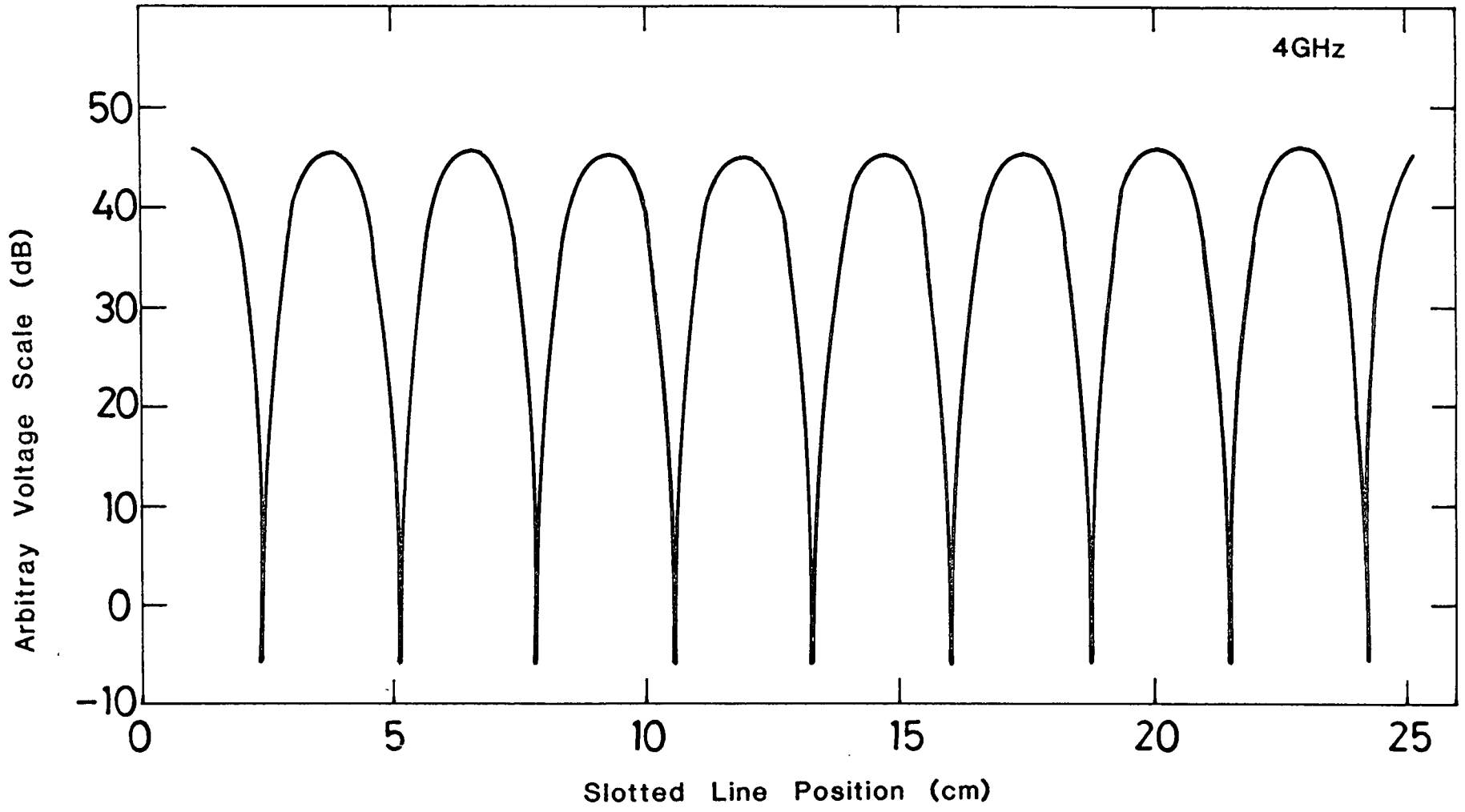

FIG. 33. Standing Wave Along the Open Circuited Slotted Line.

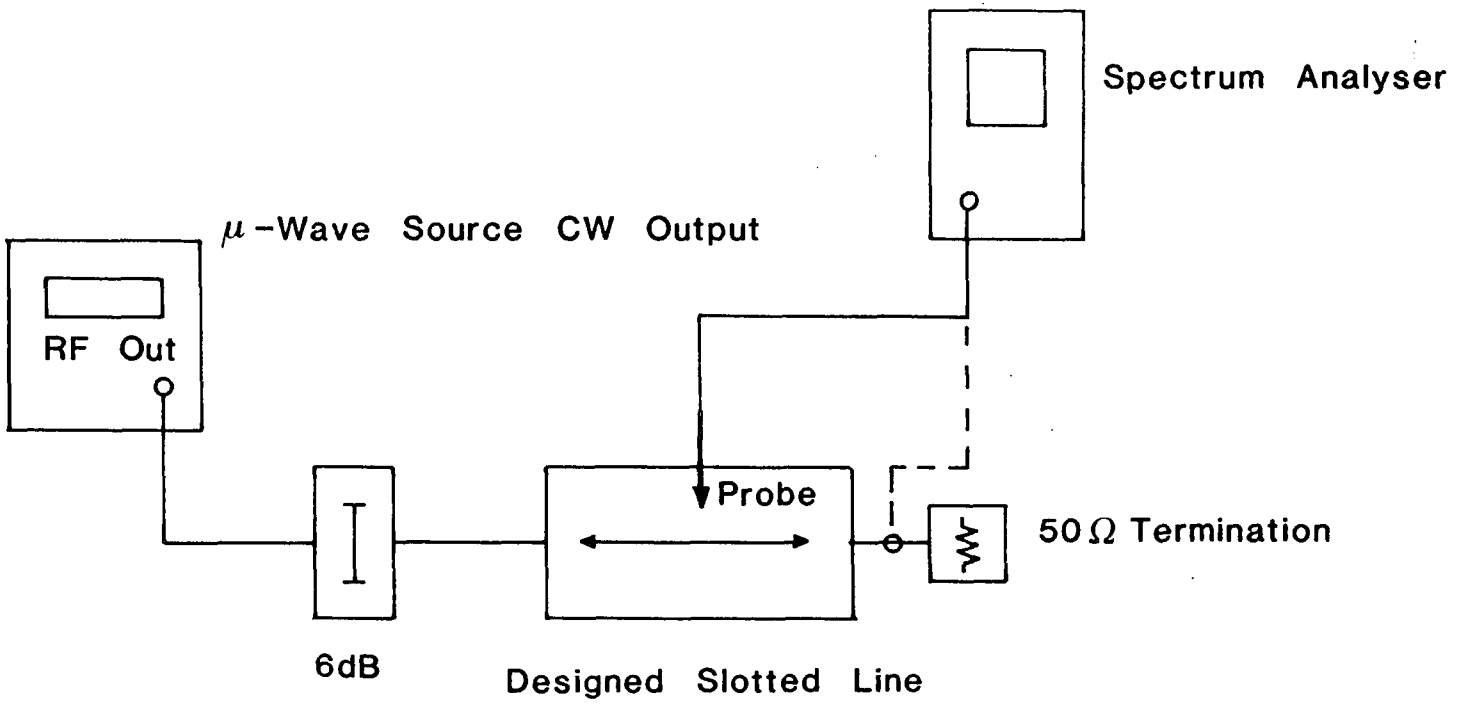

FIG. 34. Probe Coupling Coefficient (Kp) Measuring System.

where

k_P = probe coupling coefficient

P_P = power absorbed by the probe

P_L = power measured of the slotted line output

The power was measured with the aid of the spectrum analyser. The use of the power meter was avoided since it would not only measure the power at the desired frequency but also that contributed by the generators harmonics content. The procedure was carried out twice, before and after the modifications were made to the carriage and probe designs. Initially, the undercarriage dimensions and the probe assembly did not provide a 50 Ω impedance path. Furthermore, the probe line with some of the dielectric removed, presented a different impedance at the junction point where the output was taken from the carriage.

The variation of the probe coupling coefficient k_p with frequency is shown in Fig. 35. Three plots were drawn for maximum, medium and minimum probe depths with the 0 dB regarded as the reference. Although the coupling of the lower frequencies seems to be low, there is a great deal of similarity between the shapes of the three plots suggesting that no unwanted effects due to the probe depth seriously degraded the line performance.

As part of the modifications the probe dimensions were altered, by increasing its diameter from 0.25 mm to 0.35 mm, and by keeping the dielectric sleeve undisturbed. On examination it was found that the coupling had changed by as much as 7 - 8 dB for the low frequencies shown in Fig. 36, giving a more level response over the total frequency band up to 18 GHz.

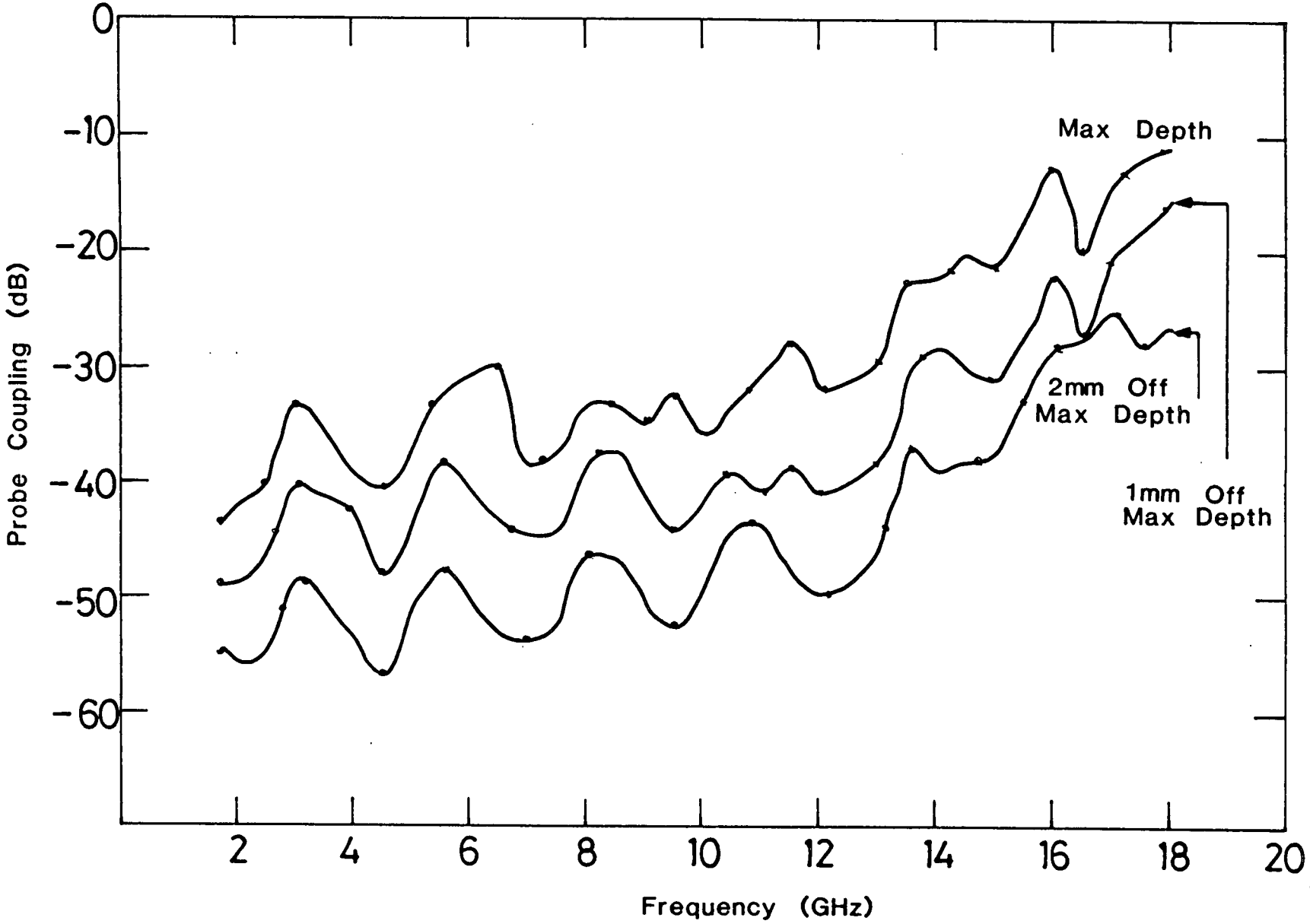

FIG. 35. Variations of Probe to Line Coupling with Frequency at Different Depths.

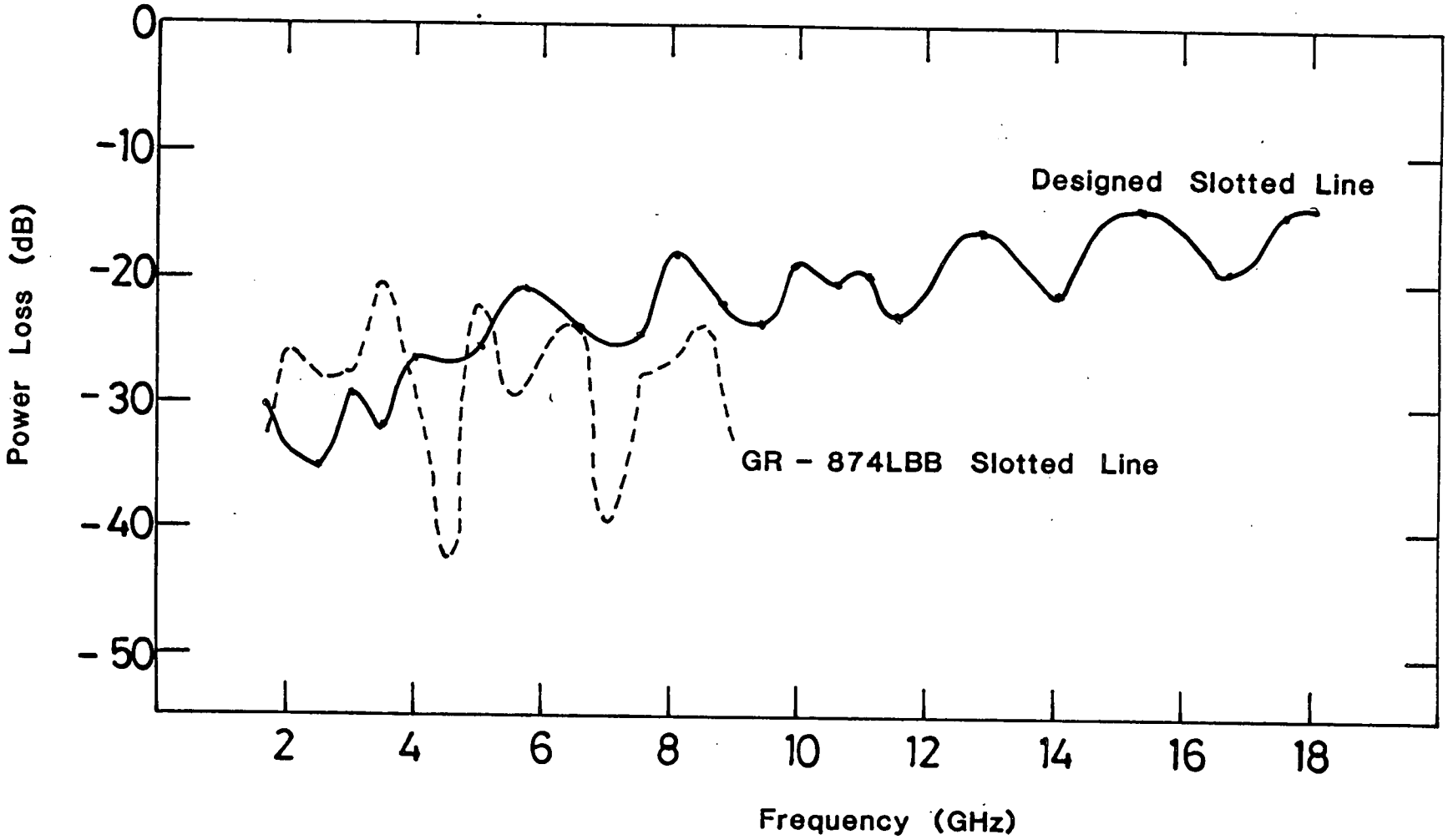

FIG. 36 Comparison Between the Project and Commercial Slotted Lines.

5.5 PROBE TUNING ASSEMBLY MEASUREMENTS

The "peaks" and "dips" on the graphs were accepted as being a direct consequence of the stub tuner. This was confirmed by investigating the response of a standard GR slotted line (see dotted line on graph) where similar variations although more prominent, were also encountered. The reason for this may be understood if the impedance of the probe end is considered as the load, and the length of the probe to its connector as the transmission line (Z_o = 50 Ω). By design the tuner was placed in shunt a distance from the fixed load. Theoretically, the load is matched to the line not only when the adjustable short is correctly tuned but also when the stub is placed at the correct distance from the load.

In assessing the required stub location, three quantities had to be evaluated. One was the standing wave ratio, the second the distance between the first voltage minimum and the termination, and the third was the wave length. Basic standing wave measurements and knowledge of the operating frequency were sufficient to calculate the desired values. Standard Smith chart techniques were employed to establish the required stub position w.r.t. the created standing wave pattern. [4]

$$\ell_2 = d_{(min)} + \ell_1 \qquad (5.17)$$

where

ℓ_1 = distance of stub from first voltage minimum (towards the load)

ℓ_2 = distance of stub from first voltage minimum (towards the generator)

d(min) = distance of first voltage minimum from the load

The test set-up shown in Fig. 37, consisted of a 2 - 12 GHz slotted line terminated with the probe of the designed line. The latter was in turn terminated at both ends by its characteristic impedance. The resulting VSWR was plotted against frequency and is shown in Fig.38 Unfortunately, it was not possible to cover the entire frequency range which would have allowed a complete evaluation of the stub tuner location to be made. (see table of Fig.39). An attempt was however made to estimate approximately the required position, bearing in mind that the stub does not necessarily have to be placed near the first minimum from the load but any number of half wavelengths away from the calculated distance. Similarly if the tuner was to be situated correctly at the lowest frequency then it is possible that it would be effective for the higher frequencies since the minima will repeat at much shorter intervals. Projecting the obtained results, yielded approximate maximum distances of $\ell_1 \simeq 37$ mm and $\ell_2 \simeq 50$ mm, assuming that the tuner will be effective within 5% of the desired distance.

It was felt that an estimate of optimum tuner location could not be obtained unless all the frequencies of interest were investigated.

The performance of the plungers was assessed by measuring their reflection coefficients. Each tuner was in turn used as an adjustable short circuit terminating either a GR or a Flann slotted line and the VSWR was measured, which was then converted to a reflection coefficient. It must be noted that the results did not truly represent

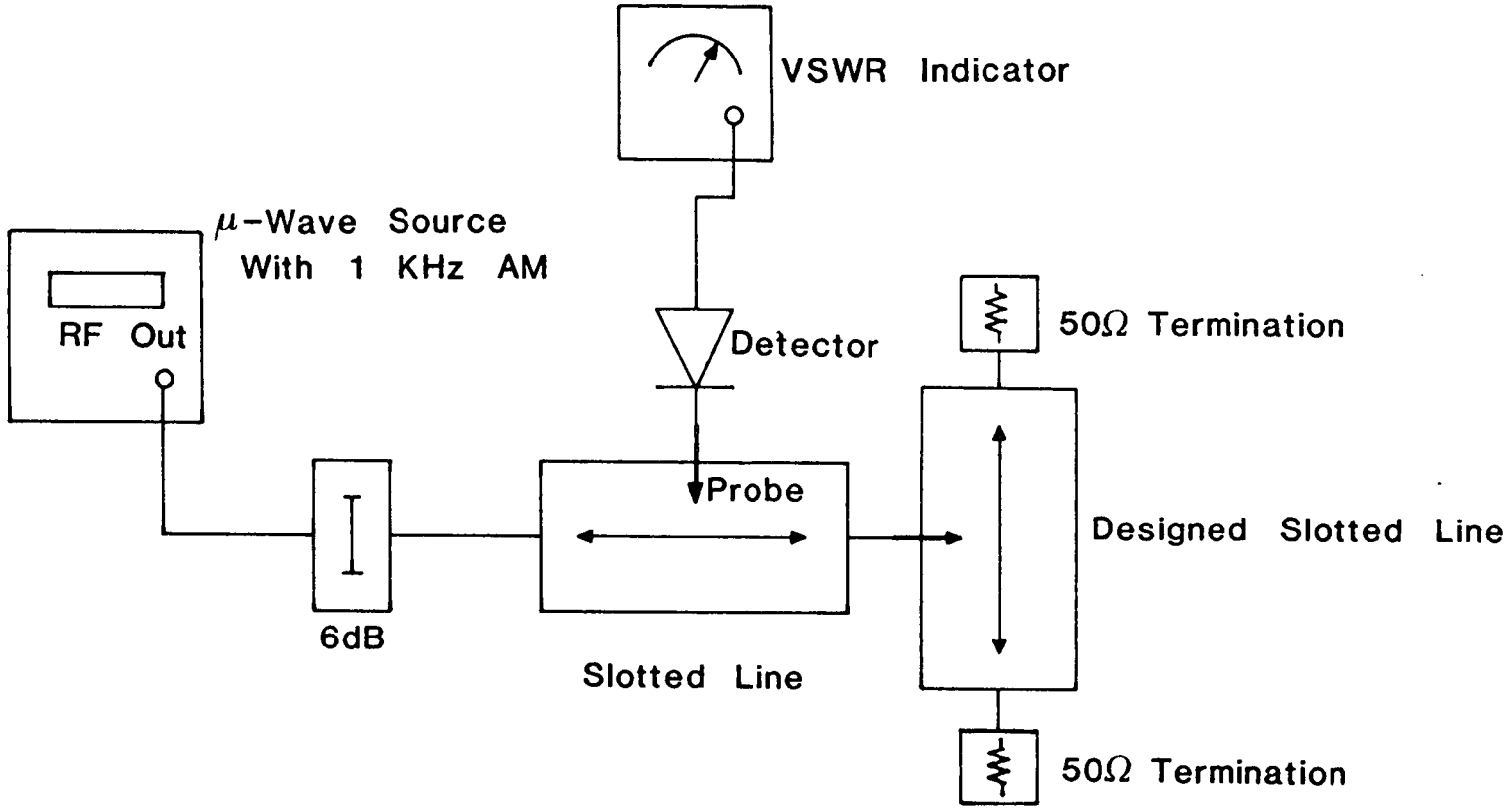

FIG. 37. Experimental Setup for the Measurement of the Probe Standing Wave Ratio (S_V)

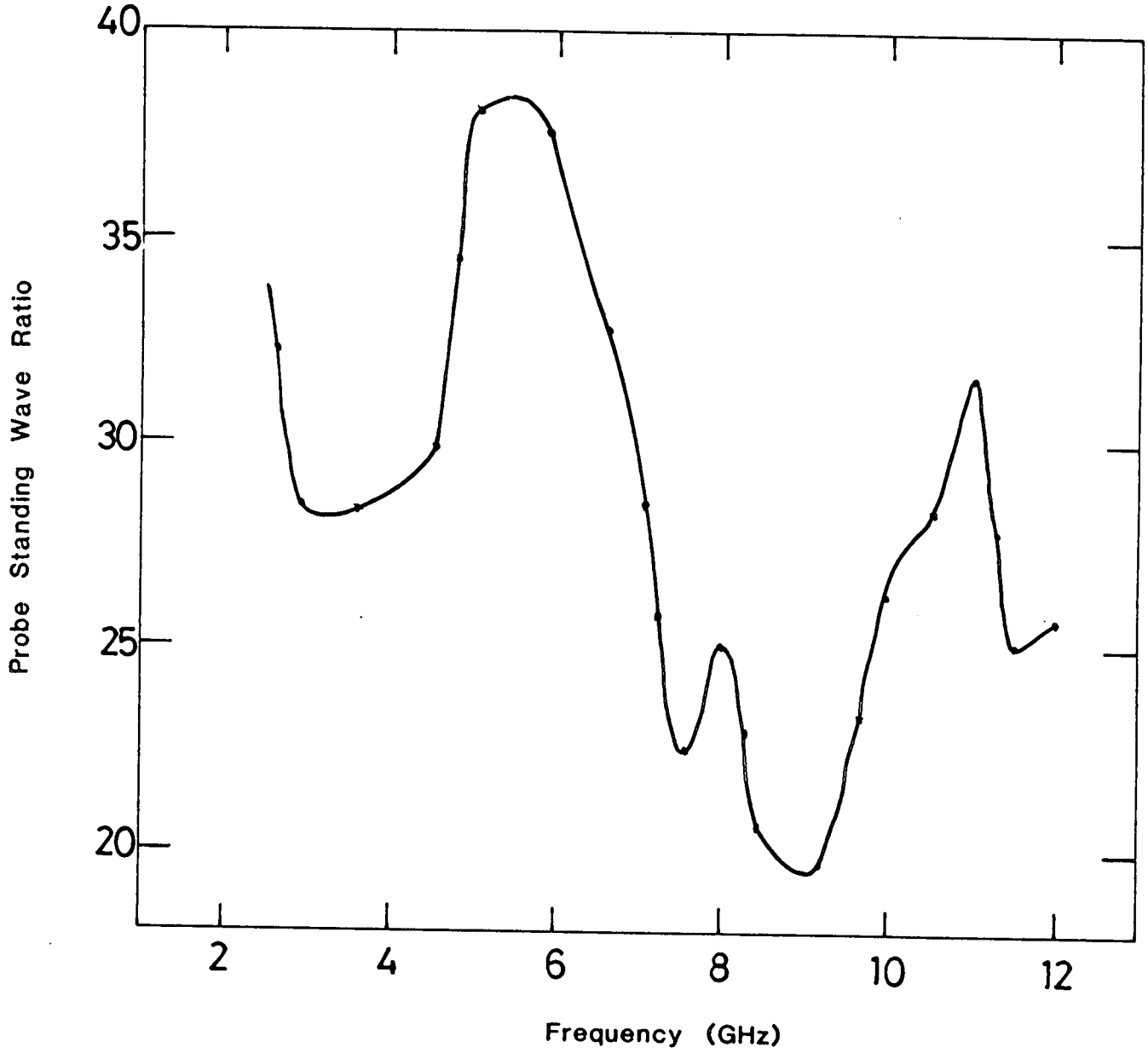

FIG. 38. Probe VSWR (S_V) Variations with Frequency.

Frequency (GHz)	Distance of 1st Min from Probe Tip (mm)	Tuner Location w.r.t. 1st min	
		Towards Probe End (mm)	Towards Generator (mm)
2.5	25.63	22.39	28.87
3.0	20.55	18.00	23.01
3.5	16.83	14.64	19.02
4.0	14.15	12.24	16.06
4.5	12.69	11.02	14.36
5.0	10.59	9.16	12.02
5.5	9.72	8.42	11.02
6.5	6.97	5.72	8.22
7.0	5.07	3.89	6.25
7.5	5.41	4.09	6.73
8.0	4.60	3.48	5.73
8.5	5.71	4.49	6.93
9.0	3.00	1.85	4.15
9.5	2.26	1.22	3.30
10.0	1.81	0.94	2.68
10.5	2.33	1.60	3.06
11.0	1.92	1.24	2.60
11.5	8.13	7.35	8.91
12.0	1.01	0.26	1.76

FIG. 39. The Relationship Between Stub Tuner Location and the First Minimum From the Probe at Different Frequencies.

the quality of the reflecting short circuit. This was because the use of GR - SMA and N type - SMA adaptors respectively, as well as the use of SMA connectors in the stubs introduced some resistance which reduced the amount of reflected power. This was made obvious by testing a fixed SMA short circuit using the same type of adaptors over the same frequency range (Fig.40). Even though a better quality of tuners might have been required if they had to be used as adjustable shorts, it was accepted that their performance was adequately satisfactory for the purpose of the intended matching and tuning.

5.6 DETECTOR CHARACTERISTICS

The detector module was finally examined for its modulation band width capability and power-current characteristics. Its response to varying modulating frequencies was assessed for the range of 0.1 - 100 KHz, monitoring the level of the output voltage while the input was maintained at a constant 1.32 V p-p. Level variations were plotted against frequency as shown in Fig. 41.

When a diode is used as an r-f detector an important relationship is between the input signal and rectified current. If a detector is to behave as a square-law device, under small signal conditions, the detected current should be proportional to the r-f power, since higher than the second order terms in the power series expansion may be neglected. The detector module was connected via a 10 dB attenuator to a single frequency generator and the diode output current was measured for varying power levels at three different frequencies. (Fig. 42).

From the shape of the calibration curves, it can be deduced that

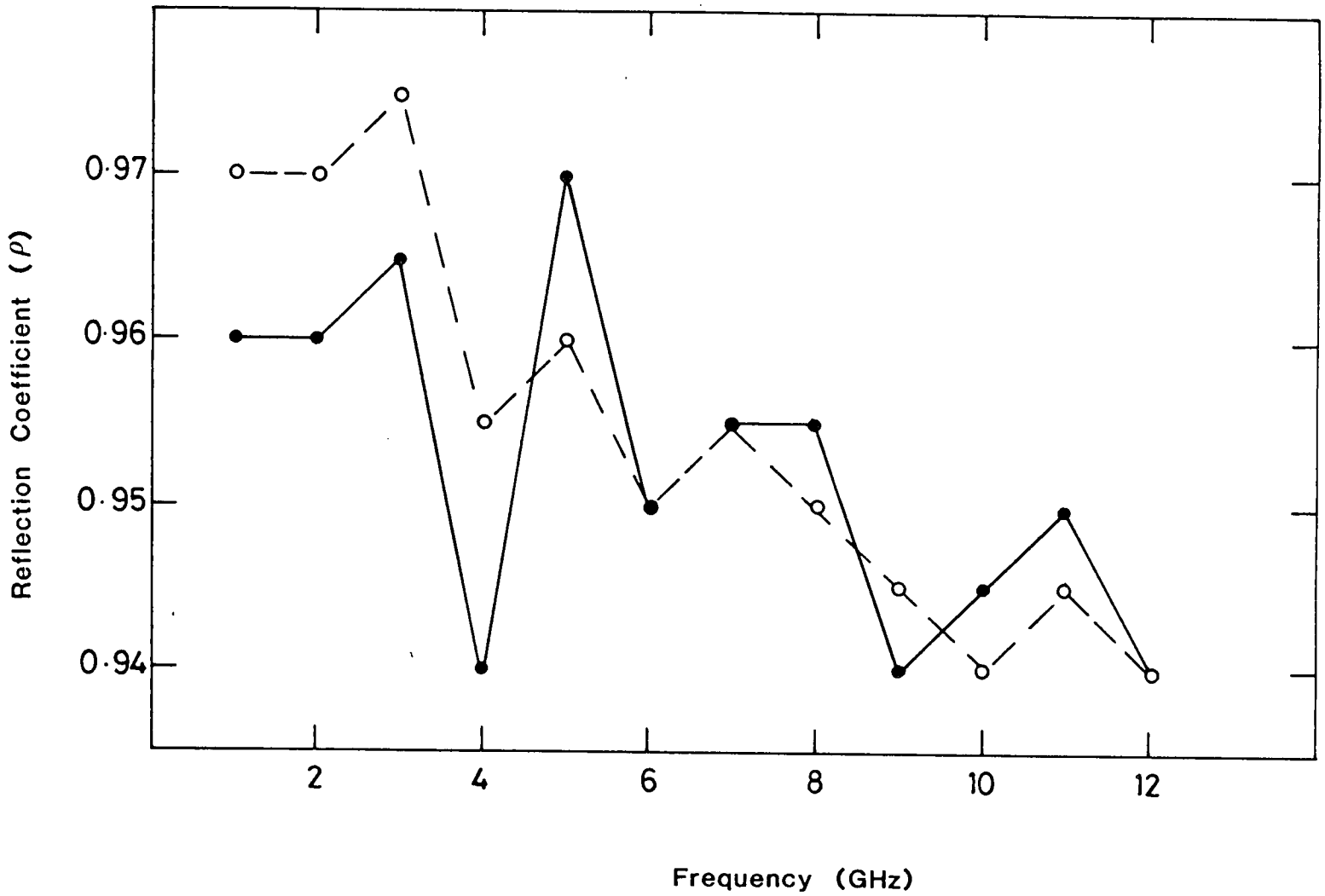

FIG. 40 Variation of the Reflection Coefficient (ρ) of the Tuner with Frequency [o--o—o Indicates the Responce of an SMA Fixed Short Circuit .]

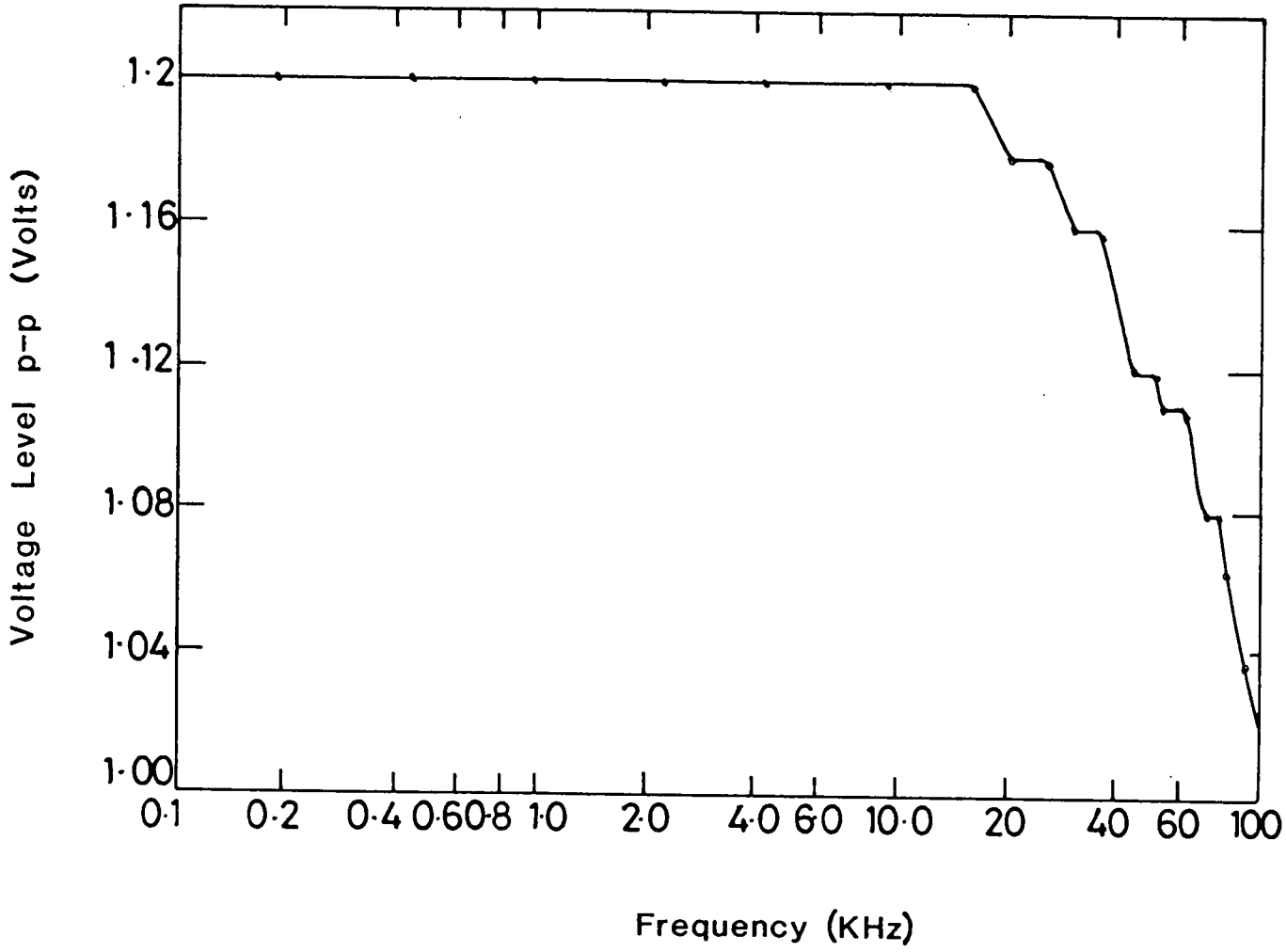

FIG.41. Voltage Variations of the Detector with Modulating Frequency.

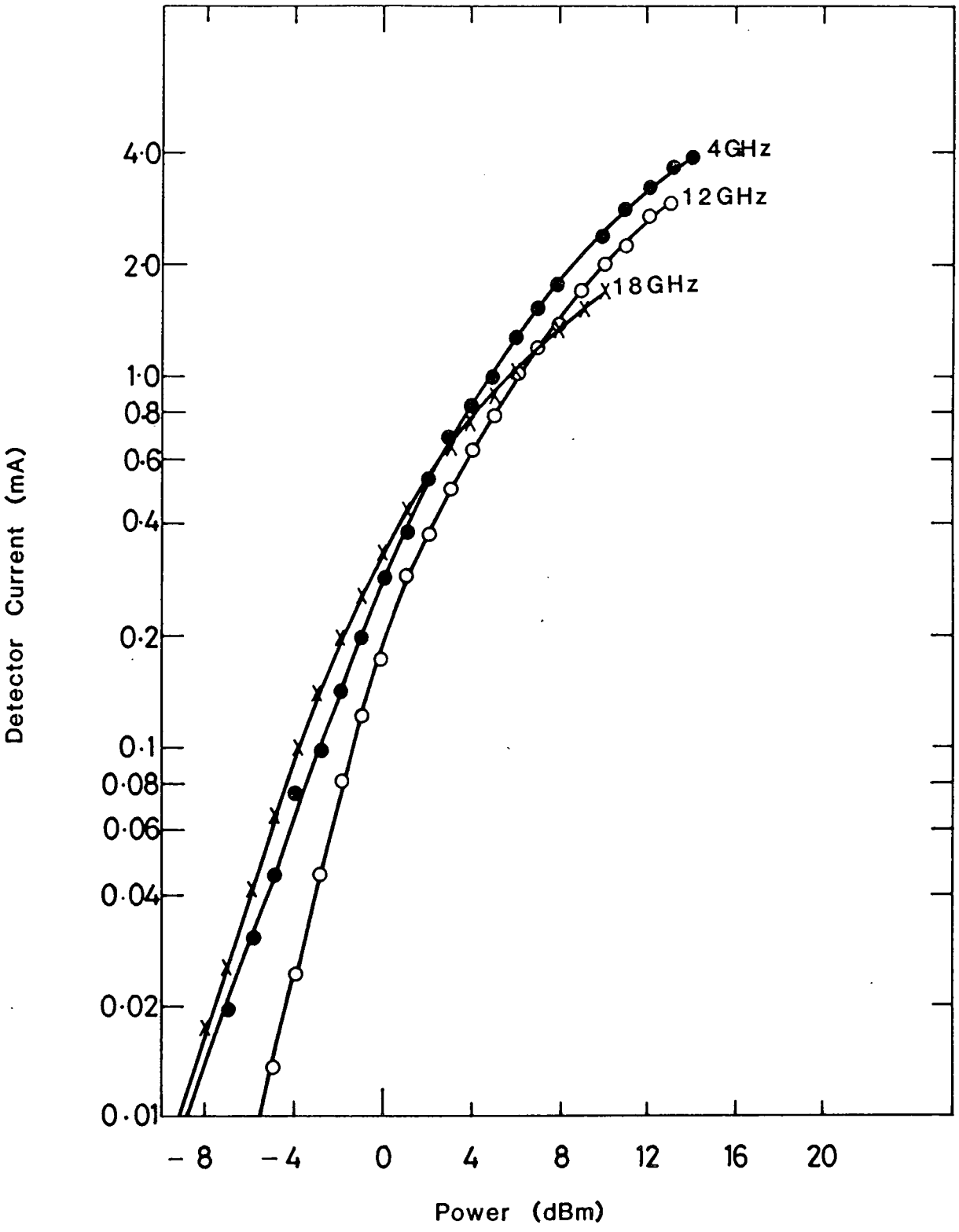

FIG. 42 Detector Current Variations with Input Power

the module behaves as a square law device for input power levels of up to about 0 dBm. This would suggest that for an average probe to line coupling of 20 dB, a slotted line input signal of more than 100 mW would be required to upset the square law relationship.

CHAPTER 6

COMMENTS AND CONCLUSIONS

6.1 PROJECT OBJECTIVES

This project was undertaken with two main objectives in mind. The first was to design and construct a low cost slotted line, the second to ensure that it was of sufficient accuracy to be used as an important and a necessary measuring aid in subsequent research applications. There are already coaxial slotted lines available on the market operating of frequencies up to 18 GHz.

What made this particular design interesting, if not unique, was that for the first time a coaxial cable with a dielectric medium other than air was used in its construction.

The benefits from such a substitution quickly became obvious. The cable may be obtained at low cost from manufacturers such as Radiall, Omni-Spectra, etc. and some of them for a small extra charge will sell straight lengths made to very close tolerances. Using a dielectric-filled cable, apart from reducing the overall length of the slotted line by a factor of $1/\sqrt{\varepsilon_r}$ also eliminates the difficulties that may be encountered in precision machining of air lines, reflected in the high cost of the product.

It became apparent from the beginning that a good, error free performance of such a slotted line will mainly depend on sound mechanical design and precise construction. Every available technique, based on microwave frequency principles, was adopted and incorporated

achieve the required electrical operation and still maintain low cost. Accordingly, a thorough understanding of transmission line theory and wave propagation is an essential study as a background for the successful design of the slotted line and its accessories. However, the aim and the emphasis was to translate the theory and resulting relationships into practical realisations.

6.2 RELEVANCE OF THE THEORY

In chapter 2 initially, wave transmission theory was briefly reviewed with attention paid to the manner how the power is attenuated in a transmission line. The attenuation constant α was expressed in terms of power as well as line parameters in high frequency applications. Similarly, equations for the evaluation of the signal phase velocity for various media were restated.

A section of coaxial line was represented by an equivalent circuit containing lumped elements of resistance, inductance, conductance and capacitance per unit length. R, L, G and C were used in the derivation of secondary parameters, propagation constant γ and characteristic impedance Z_o. The complex expressions one obtains for the attenuation α , phase shift β , and characteristic impedance Z_o, simplify for lossless and low loss cases.

An important equation of practical use is the one for the characteristic impedance of the line derived from E and H field distributions within the coaxial line, in terms of the inner end outer conductor dimensions. This formula was applied continually in the design of the slotted line and its accessories, to maintain a characteristic impedance of 50 Ω.

Finally, the behaviour of an electromagnetic wave propagating along a line was examined for different loads under mis-matched conditions. The subsequent formation of standing waves was discussed and formulae developed interelating the load Z_L, to reflection coefficient ρ_v and S_v. These proved to be extremely useful relationships and were extensively used in the calculations and testing of the slotted line.

Chapter 3 dealt with the requirements for the electrical performance of each individual part of the design. The importance of conductor concentricity and uniformity was highlighted, needed for accurate measurements of the electric field intensity. The effect of the slot size on the cable was discussed in terms of the reduced capacitance resulting in characteristic impedance changes and possible formation of additional standing waves. These factors were of primary consideration in deciding the slot width.

Like the slot width the electric probe needed to be of small dimensions, even at 18 GHz its diameter should be a fraction of the wavelength. If the dimensions are large it would cause reflections and introduce errors in VSWR readings. The analysis of the effect due to power absorption by the probe was considered by assuming it to be an admittance shunting the transmission line. The equations for the conductive and susceptive components were given, and used for calibration purposes. In addition shifts of the standing wave maxima, and to a lesser extent minima, caused by the probe, were discussed, and equations found relating the true and the measured VSWRs.

The schematic representation of the probe and its equivalent circuit which included the inductance introduced by the short-circuiting plunger was of particular importance. It indicated that

for maximum output, the tuned circuit of C_2, L, and R should be resonant, and this can only be satisfactorily achieved if the capacitance C_2 between the probe and the slot is kept constant, otherwise tuning would be made redundant. Requirements of this nature were continually taken into consideration, and influencing the mechanical aspects of the design.

6.3 ELECTRICAL REQUIREMENTS AND MECHANICAL CONSTRUCTION

The construction of the slotted line components was described in chapter 4. Whenever appropriate attempts were made to justify construction procedures by referring to relevant microwave design principles. When planning the clamp, the main objective was to provide a means for mounting the probe carriage assembly and enabling it to travel the slotted cable length, while maintaining perfect symmetry with its surroundings. This required precision machining, and special gauges were used to achieve milling tolerances of less than 0.01 mm. Both halves of the clamp were simultaneously machined to the specified dimensions, so that they were identical; they were also dowelled to allow complete realignment in the event of being dismantled.

The semi-rigid cable was slotted after it was placed in the clamp for two reasons. Firstly, this ensured that the slot ran symmetrically between the clamp walls, placing the probe centrally within the slot.

Secondly, suspecting that the two conductors may not be absolutely concentric, it was decided that a reference plane was needed, of known distance from the inner conductor was needed. Having made the assumption that this was by far the straightest of the two conductors, it was decided that it was more important to maintain a uniform distance

between the probe and the inner conductor, than to maintain constant penetration.

Therefore the slot depth was determined more in terms of clearance between the slot bed and the inner conductor, rather than distance from the cable surface to the dielectric forming the slot bed.

The cable was slotted by inserting a circular cutter through the clamp slot until the predetermined depth was achieved. It is worth noting at this point that a number of small copper particles could be embedded in the soft PTFE sleeving of the cable, and if so they should be carefully removed.

Initially, the clamp slot was decided to be 6.35 mm wide. The choice of this particular dimension was simply based on the fact that the probe PTFE sleeve was 4.1 mm in diameter and therefore a large enough slot had to be provided to allow the probe skirt to reach the slotted semi-rigid cable. During the course of testing however, this was found to create excessive radiation leakages to the extent that above 13 - 14 GHz there were detectable effects caused by a mere movement of one's hand over the clamp slot.

Radiation of this type can only be eliminated theoretically if the outer conductor wall is infinitely thick. Practically this can be simulated by making the clamp slot as wide as the cable slot itself, so that its slot walls would seem to be a natural extension of the cable slot walls, providing the outer conductor with sufficient thickness. This was not however mechanically possible since the cable slot was only 1.27 mm wide, making it difficult to create a clamp extension of similar dimension within which the probe and skirt had to be accommodated. The smallest obtainable width was that of 2.3 mm which resulted in the leakages being minimised to an acceptable

level inherent to all slotted lines.

Apart from the changes in the undercarriage skirt design, a number of modifications were carried out, concerning the opening in which the probe was placed, as well as the junction leading to the connector for the detector module. As it was previously discussed a small ring of the dielectric sleeving was initially removed from the probe; a junction was made and the absorbed power was delivered to a connection at the back of the carriage. Initial calculations did not account for uniform, matched transmission from the probe tip to the junction, or to the connector leading to the tuner. This led to varying amounts of power being delivered to the output depending on the operating frequency, while maximum tuning could only be achieved for specific distances.

After ensuring that a 50 Ω path was created for the probe, by altering its dimensions, it was decided to remove the junction and simply take the output from the carriage top through a standard SMA tee. The alterations proved successful in that more constant coupling was achieved and satisfactory tuning was provided even though the tuner was not located at the optimum position.

The use of adjustable pads proved quite useful, in that "play" caused by material wear as well as small misalignments could be corrected by simply adjusting the tensions on the screws behind the pads. Another minor problem that was encountered concerned the probe depth mechanism and in particular the locking nut. Having been made from duralumin, it proved too soft, causing the thread to "stretch" after only a few locking operations. This was overcome by making the mechanism from stainless steel which is much tougher and resilient. A cylindrical, threaded insert was also fitted in the top surface of the

carriage assuring lasting, trouble-free operation.

6.4 ELECTRICAL PERFORMANCE

The performance of the slotted line with its accessories was examined in chapter 5. Quantities such as wave length, power loss and coupling between the line and the probe were measured so that an overall assessment of the line's quality could be made.

It was interesting to note that the wavelength was neither that of free space, nor was it reduced to that of a PTFE filled transmission line. In fact with the line being partially filled with dielectric, a correction factor had to be introduced if the relationship $f = c/(\lambda\sqrt{\varepsilon_r})$ was to remain valid. Having taken this into consideration the measurement of frequency could be accurately obtained using the slotted line.

Although the residual VSWR was not very easy to determine, the indicating variations from 1.02 to 1.25 were deemed acceptable when considering that the VSWR's of the lines connectors as well as those of the tuners and terminations were also included.

Similarly slotting a small diameter cable, such as the one used, was bound to create more accute impedance changes which were enhanced when part of the dielectric was removed.

Another contributing factor was of course the effect of the slotting process. There was no way of ensuring that the slot bed and sides would be smooth, and that no copper fillings from the outer conductor would have been embedded in the dielectric.

Examining the variations of power loss of the line with frequency, it was found that it exhibited very little loss even at very high

frequencies. The results compared well with the manufacturer's specifications, taking into account that the connectors and the slot contributed small amounts of extra loss.

Similarly, the attenuation constant α behaved in much the same way, indicating an increase with frequency.

From observing the maxima and minima of the standing waves produced by either a short circuit, an open circuit or a characteristic impedance termination, the conclusion is that no apparent irregularities are present in the line. In the case of the matched termination (Fig. 28 - Fig 30) one must allow for the fluctuations as being the result of the effect of the probe when measuring very low VSWRs. As mentioned previously in the case of a low VSWR the location of the maxima as well as that of the minima is affected by the probe. This is not however the case in the short/open circuit condition. Here, the minima are not affected by the presence of the probe (Fig.31 Fig.33) resulting in more uniform patterns. As it is seen from the graphs, the levels of the maxima and minima are consistent and varying very little for the entire length of the line of different frequencies. These variations could be explained partly as being the result of instrument drifting e.g. the VSWR indicator, or inconsistency of power output from the generator.

The amount of power absorbed by the probe was considerably improved as a result of the modifications outlined in chapter 5. As seen from Fig. 36 the coupling is not constant but instead it varies with frequency. One explanation for this, could be that at some frequencies the tuning is more efficient than at some others. This might be the result of the short circuits being more effective at certain positions in the tuners, thus reflecting more of the input signal

power. Another explanation is that the stub being at a fixed distance from the probe is more effective for frequencies whose wavelengths happen to be the correct fraction of that distance. An attempt was made to calculate the required stub location unsuccessfully since not all the frequencies of interest could be considered.

Similarly the detector module was found to have an input VSWR of approximately 3:1, which would suggest that depending on frequency a varying amount of power would reach the diode thus creating an inconsistant coupling. However, these variations seem acceptable in view of the fact that slotted lines like the GR-874LBB produced similar results. A coupling from -35 dB to -14 dB, of maximum probe depth, can still provide sufficient power for measurements using sensitive apparatus, like the spectrum analyser and the VSWR indicator.

6.5 FUTURE WORK AND RECOMMENDATIONS

Overall, the design may be considered successful in that it may be used as a general purpose slotted line. However, with some improvements it can be used in specific applications where a high degree of accuracy is essential.

Precision connectors such as the APC-7 type would greatly improve the performance of the slotted line in terms of power loss and residual VSWR reduction. The SMA type connector used, although adequate, proved troublesome, inconsistent, and not mechanically robust enough, for the numerous matings that slotted line connectors have to undergo.

As mentioned before the innovation in this particular design was the use of semi-rigid dielectric filled cable. Therefore, one is advised to choose one of high quality and approach manufacturers

that supply lengths produced specifically within very close tolerances for conductor concentricity and straightness. Although they do charge extra for it, the advantages more than balance the cost.

Discussing the carriage in section 4.2 it was mentioned that it was made from duralumin, a choice based purely on machinability, durability and the fact that being a light metal would not contribute added weight to the slotted line. Theoretically, however, duralumin is not a very good conductor and this affected the amount of power transferred from the probe tip to the detector. A brass, or steel carriage with the probe path silver plated would be more acceptable and in addition it would provide the added strength to withstand the tension from the tightening of the locking nut on the probe depth adjustor.

The coupling could be further improved by incorporating some kind of double tuning system. This would require not only the plunger in the tuner to be movable but the detector module as well. This means that for any frequency the diode should be "tuned" in terms of distance from the probe so that maximum power transfer is achieved.

This could be done by replacing the probe unit with a length of semi-rigid cable similar to that used in the slotted section of the line. This would then be shaped at one end, so that the inner conductor was exposed, and protruded through the undercarriage to act as the probe. The other end would be extended through the adjustor mechanism and fitted with an appropriate connector, to which the tuner would be attached. The section of cable between the carriage top and the tuner would then be slotted exposing the inner conductor onto which a connector of the extended receptacle type could be attached, to provide the output to the defector. The whole arrangement could

be encased in an appropriate metal sleeving to eliminate possible radiation leakages; this offers the added advantage of replacing the SMA probe unit with cable capable of operating at high frequencies with minimal exhibition of loss.

Following these modifications a slotted line of excellent performance could be produced, for all types of research applications, being fairly easy to construct and inexpensive enough to satisfy the aims of the project.

REFERENCES

1 BLAKE, L. V. Transmission Lines and Waveguides, John Willey & Sons, 1969.

2 CHIPMAN, R.A. Theory and Problems of Transmission Lines, Schaum's Outline Series, McGraw-Hill, 1968.

3 Compiled by the Staff of the Radio Research Laboratory, Harvard University, Very High Frequency Techniques Vols. I & II, McGraw-Hill, 1947.

4 EVERITT, W.L.& ANNER, G. E. Communications Engineering McGraw-Hill, 1956.

5 GENERAL RADIO, Instruction Manual for Type 874-LBB Slotted Line, G R Company, 1966.

6 GINZTON, E.L. Microwave Measurements, McGraw-Hill, 1957.

7 GLAZIER, E.V.D.& LAMONT, H.R.L. Transmission and Propagation, Vol.5, Her Majesty's Stationery Office, 1958.

8 HARVEY, A.F. Microwave Engineering, Academic Press, 1963.

9 HUGGINS, W.H. Broad-Band Non-Contacting Short Circuits for Coaxial Lines, Proc. Inst. Radio Eng. Sept. 1946.

10 LANCE, A.L. Introduction to Microwave Theory and Measurements, McGraw-Hill, 1964.

11 LAVERGHETTA, T.S. Microwave Measurements and Techniques, Artech House, 1981.

12 MONTGOMERY, C.G. Technique of Microwave Measurements, McGraw-Hill, 1947.

13 MONTGOMERY, C. G.& DICKE, R.H.& PURCELL, E.M. Principles of Microwave Circuits, Dover Publications, 1965.

14 MORENO,T. Microwave Transmission Design Data, Dover Publications, 1958.

15 RAGAN,G.L. Microwave Transmission Circuits, Dover Publications 1965.

16 SINNEMA,W. Electronic Transmission Technology, Prentice-Hall, 1979.

17 SUCHER, M.& FOX,J. Handbook of Microwave Measurements, Vols I & III, Polytechnic Press of the Polytechnic Institute of Brooklyn, 1963.